University of Nottingham
UK | CHINA | MALAYSIA

# Experimental and numerical evaluation of novel dual-channel windcatchers for energy-saving technology integrations

Thesis submitted to the University of Nottingham for the degree of

**Doctor of Philosophy, August 2023**


**Jiaxiang Li**

**16521936**

Supervised by

**John Calautit**

**Saffa Riffat**


Signature 

Date 08 / 31 / 2023

The candidate confirms that the work submitted is his/her own, except where work which has formed part of jointly-authored publications has been included. The contribution of the candidate and the other authors to this work has been explicitly indicated below (page iii). The candidate confirms that appropriate credit has been given within the thesis where reference has been made to the work of others.

## Jointly-authored Publications

**Journal paper:**

**Title of publication no.1:** Experimental and numerical evaluation of a novel dual-channel windcatcher with a rotary scoop for energy-saving technology integration.

**Authors:** Jiaxiang Li, John Calautit, Carlos Jimenez-Bescos and Saffa Riffat

**Journal:** Building and Environment

**Year:** 2023

**Volume:**230

**Contributions:** I conceptualised the idea, developed the experimental setup, conducted CFD simulation and validation and wrote the manuscript.

**Title of publication no.2:** Evaluating the energy-saving potential of earth-air heat exchanger (EAHX) for Passivhaus standard buildings in different climates in China.

**Authors:** Jiaxiang Li, Carlos Jimenez-Bescos, John Calautit and Jiawei Yao

**Journal:** Energy and Buildings

**Year:** 2023

**Volume:** 288

**Contributions:** I conceptualised the idea, conducted the IES-VE simulation, PHPP calculation, validation of the research model and wrote the manuscript.

**Title of publication no.3:** Experiment and numerical investigation of a novel flap fin louver windcatcher for multi-directional natural ventilation and passive technology integration.

**Authors:** Jiaxiang Li, John Calautit and Carlos Jimenez-Bescos

**Journal:** Building and Environment

**Year:** 2023

**Volume:** 242

**Contributions:** I conceptualised the idea, developed the experimental setup, conducted CFD simulation and validation and wrote the manuscript.

**Conference paper:**

1. **Jiaxiang Li, Carlos Jimenez-Bescos, John Kaiser Calautit.** 2021. "Evaluating the energy-saving potential of Earth-Air Heat Exchanger in Passive Houses in different regions in China." In Applied Energy Symposium 2021: Low carbon cities and urban energy systems. Tokyo, Japan.
2. **Jiaxiang Li, Carlos Jimenez-Bescos, John Kaiser Calautit.** 2021. "Ventilation and dehumidification performance of a novel multi-channel windcatcher system with passive dehumidification for reducing the energy demand in buildings." In 16th Conference on sustainable development of energy, water and environment system. Dubrovnik.
3. **Jiaxiang Li, John Calautit, Carlos Jimenez-Bescos.** 2022. "A multidirectional windcatcher for passive technology integration under variable wind directions." In Applied Energy Symposium 2022: Clean Energy towards Carbon Neutrality. Applied Energy Symposium 2022: Clean Energy towards Carbon Neutrality.
4. **Jiaxiang Li, John Calautit, Carlos Jimenez-Bescos**. 2021. "Ventilation and dehumidification performance of a novel multi-channel windcatcher system with passive dehumidification for reducing the energy demand in buildings." In 16th Conference on sustainable development of energy, water and environment system. Dubrovnik.

# Acknowledgements

This thesis was completed with the support of a number of important individuals and organisations to whom I am very thankful. First of all, I would like to thank my supervisors, Dr. John Calautit, Prof. Saffa Riffat and Dr. Carlos Jimenez-Bescos for their constant support, guidance and encouragement throughout these years of study, not to mention their advice and unsurpassed scientific insights for which I am extremely grateful. Thank you for giving me the opportunity to work with you on this research project.

I would like to thank my parents for their support in both financial and emotional ways. I would also like to thank my uncle and aunt for their support in the manufacturing of the experimental prototype and materials.

I would like to acknowledge all the support and encouragement I have received from my friends during the whole study. Special thanks must go to my friend Han Wang and Haodong Zhu for their friendship and support in the research.

Finally, I would also like to acknowledge the academic and technical support of the University of Nottingham and its staff for providing the facilities and academic support I required.

# Abstract

Windcatchers are utilized in building design as natural ventilation devices, providing fresh air supply and thermal comfort under suitable outdoor conditions. However, their performance is often constrained by environmental factors such as outdoor temperature, wind speed and direction. While passive heating, cooling, and heat recovery devices have been integrated into conventional windcatcher designs, the impact of changing wind conditions, which can render the windcatcher ineffective, is often not considered. Addressing this gap, this research builds upon two novel dual-channel windcatcher systems to provide a fresh air supply irrespective of the wind direction and allow for passive/low-energy technology integration.

The first proposed design is a rotary scoop windcatcher consisting of a rotary wind scoop and a chimney. In this design, the positions of the supply and return duct are “fixed” or would not change under changing wind directions to ensure a consistent fresh air supply, irrespective of wind direction and facilitate the integration of passive/low-energy technologies. An open wind tunnel and test room were employed to experimentally evaluate the ventilation performance of the proposed windcatcher prototype. A Computational Fluid Dynamic (CFD) model was developed and validated to further evaluate the system's ventilation performance. The results confirmed that the system could supply sufficient fresh air and exhaust stale air under changing wind directions. The validated CFD model was enhanced in the simulations, incorporating technologies such as an anti-short-circuit device, wing walls, wind scoop area, and wind cowl design, to increase the pressure difference between the inlet and outlet and reduce the system friction. The modified windcatcher achieved a 28% improvement in ventilation rate and outperformed a conventional four-sided windcatcher of the same size by up to 58%. Furthermore, the full-scale simulations of the building and windcatcher of varying heights were conducted using an atmospheric boundary layer wind flow to better capture the true nature of the wind flow that the building will encounter in real-world conditions to provide a more realistic assessment of the windcatcher's performance.

The second design is a windcatcher with inlet openings equipped with flap fins and a chimney in the middle. As this flap fins louver windcatcher is developed from the rotary scoop

windcatcher, the dual-channel design remains for the fixed supply and return duct position for passive/low-energy technology integration. Inspired by the check valve device, the flap fin mechanism allows wind to flow only one way into the windcatcher's supply channel which creates a substitution for the wind scoop. The lightweight flap fin operates via gravity and takes advantage of the wind pressure around the openings to control the airflow. The wind tunnel experiment and CFD simulation model were developed to evaluate the ventilation performance of the proposed windcatcher prototype and investigate the impact of each parameter like the thickness, length, layout of the fins and wind directions. The field test of the flap fins louver windcatcher was also tested in this research. The results showed that the ventilation performance of the flap fin louver windcatcher was independent of the wind direction in the field test and wind tunnel experiment, and the use of lighter and longer fins would enhance the ventilation rate. The current scaled experiment model with a diameter of 20cm could provide about 10L/s fresh air supply at 2m/s environment wind speed with an air change rate over 27 $h^{-1}$.

Overall, this research contributes to the development of more efficient windcatcher systems for further passive technology integrations, enhancing their viability as sustainable ventilation solutions. Two novel windcatchers were proposed in this research and the ventilation performance of the windcatchers was independent of the environmental wind direction. Passive technologies such as passive heat recovery were integrated into the windcatchers to provide indoor thermal comfort. The ventilation efficiency of the two windcatchers was also higher than the traditional conventional windcatchers.

# Table of contents

# List of Figures

# List of Tables

# Preface

The work presented in this thesis was carried out between October 2020 and August 2023 in the Department of Architecture and Built Environment, University of Nottingham. As an outcome of this study, the following peer-reviewed journal and conference papers have been published:

**Peer-reviewed journals:**

- Li, J., et al., *Experimental and numerical evaluation of a novel dual-channel windcatcher with a* rotary *scoop for energy-saving technology integration.* Building and Environment, 2023: p. 110018.
- Li, J., J. Calautit, and C. Jimenez-Bescos, *Experiment and numerical investigation of a novel flap fin louver windcatcher for multi-directional natural ventilation and passive technology integration.* Building and Environment, 2023: p. 110429.

**Conference paper:**

- Jiaxiang Li, Carlos Jimenez-Bescos, John Kaiser Calautit. 2021. "*Ventilation and dehumidification performance of a novel multi-channel windcatcher system with passive dehumidification for reducing the energy demand in buildings*." In 16th Conference on sustainable development of energy, water and environment system. Dubrovnik.
- Jiaxiang Li, John Calautit, Carlos Jimenez-Bescos. 2021. "*Ventilation and dehumidification performance of a novel multi-channel windcatcher system with passive dehumidification for reducing the energy demand in buildings.*" In 16th Conference on sustainable development of energy, water and environment system. Dubrovnik.
- Jiaxiang Li, John Calautit, Carlos Jimenez-Bescos. 2022. "*A multidirectional windcatcher for passive technology integration under variable wind directions.*" In Applied Energy Symposium 2022: Clean Energy towards Carbon Neutrality. Applied Energy Symposium 2022: Clean Energy towards Carbon Neutrality.

# Patent

Six patents were achieved in China including about the windcatchers and the passive technologies in this research. The patents are owned by the authors: Jiaxiang Li, John Calautit and Carlos Jimenez-Bescos.

1. Flap fins louver windcatcher was designed in the research which overcame some limitations of the traditional windcatcher.
   Patent number: 2022228239367
2. Using the flap fins louver windcatcher designed and heat pipes to achieve a high-efficiency heat recovery with low system friction.
   Patent number: 2023201447657
3. Using the rotary scoop windcatcher designed and different passive technologies to achieve passive heating and cooling via the windcatcher system.
   Patent number: 2023201446809
4. Using the flap fins louver windcatcher designed and evaporative cooling to achieve a stable passive cooling in the supply air.
   Patent number: 2023201448221
5. Using the flap fins louver windcatcher designed and solar heating to achieve stable passive heating in the supply air.
   Patent number: 202320144858X
6. Using the flap fins louver windcatcher designed and stove to increase the heating efficiency of the stove and provide fresh air for combusting safely.
   Patent number: 2023201447445

# Nomenclature

| Symbol | Physical meaning |
|---|---|
| A | Area of the return duct ($m^2$) |
| D | Hydraulic diameter (m) |
| $F_{wind}$ | Force generated by the wind pressure ($N$) |
| $I$ | Turbulence intensities, |
| $M_{friction}$ | Friction torque at the connection of the flap fins and windcatcher wall ($Nm$) |
| P | Pressure (Pa) |
| Q | Ventilation rate (L/s) |
| R | Radius of the return duct (m) |
| $R^2$ | Determination coefficient |
| T | Air temperature (K) |
| $T_k/L/W$ | Thickness/ length/ width of the flap fins (m) |
| t | Time (s) |
| g | Gravitational acceleration ($m/s^2$) |
| u | Velocity (m/s) |
| $u_i$ | Velocity at the measurement point (m/s) |
| $U_{average}$ | Average velocity in the measurements (m/s) |
| ρ | Density ($kg/m^3$) |
| $\theta$ | Open angle of the flap fin (°) |
| $\tau_t$ | Stress tensor ($N/m^2$) |
| μ | Molecular dynamic viscosity (Pa s) |
| $\Delta P$ | Pressure difference between the two sides of the fins ($Pa$) |

# Chapter 1 Introduction

## 1.1 Research background

With the development of the economy and living standards, the demand for indoor air quality in buildings has increased, and researchers are exploring new solutions to reduce energy consumption in the building sector due to rising energy prices and concerns about global warming [1]. The built environment is seen as one of the key sectors that can significantly contribute to achieving a sustainable energy economy. The construction and built environment industries are responsible for over 40% of the direct and indirect global carbon emissions [2]. Over half of the energy consumption in the building comes from the usage of heating, ventilation and air-conditioning (HVAC) systems [3, 4]. Air-conditioning is one of the fastest growing energy use in the built environment and places enormous strain on the electricity grid in many parts of the world. In 2016 about 10% of the global electricity was used for cooling [5], and in cities like Shanghai with hot climates, the cooling consumption could reach up to 40% of the total energy load [6]. People spend over 80% of their time inside the building and sufficient ventilation for occupants is vital to work and living. The importance of ventilation keeps increasing as people are spending more time in buildings [3, 7]. Thus, an effective cooling solution with low energy consumption needs to be investigated for low-carbon development [8].

Researchers are looking for sustainable and economical solutions to provide building occupants with good indoor thermal comfort and air quality while minimizing the use of air-conditioners [9]. While there are many technology options for enhancing the building's performance, natural ventilation is an attractive solution and has been the focus of many research studies. This is due to its capability to provide a fresh air supply and heat, moisture and pollutants removal from the building by using only the natural forces of the wind and thermal buoyancy [10]. However, natural ventilation is typically insufficient to provide the required indoor thermal comfort in unfavourable hot and cold climatic conditions. For example, in hot and humid climates, the

high outdoor temperature and humidity in both daytime and nighttime could further cause thermal discomfort to the occupants [11, 12]. This has led researchers to investigate alternative solutions, such as combining natural ventilation with other passive/low-energy strategies, including solar heating, heat recovery, cooling and dehumidification to provide indoor thermal comfort and air quality and minimize the use of air-conditioners [9, 13, 14].

Windcatchers, as natural ventilation devices, offer better energy efficiency and enhance the well-being of occupants compared to mechanical ventilation devices [15]. Windcatchers can be applied on the roof to capture the wind above the building and bring in fresh air supply while extracting polluted air using the wind pressure [16, 17]. The high outdoor humidity and temperature in both daytime and nighttime would cause thermal discomfort [12]. Thus, combining passive technologies and the windcatcher has become a popular research direction in natural ventilation to provide heating, cooling and dehumidification [13, 14]. Various passive technologies have been integrated into the windcatcher system, such as evaporative cooling in hot and dry climates [18-20], heat transfer coil for passive heat recovery [15, 21] and Earth-Air Heat Exchanger to precool the supply air [22].

## 1.2 Research problem and question

Traditional natural ventilation devices, such as windcatchers, rely heavily on outdoor wind and climate conditions for the ventilation performance of windcatchers and the thermal performance of passive technologies [23-25]. The impact of environmental conditions on windcatchers is especially relevant in terms of wind direction, as confirmed by field tests conducted on windcatchers with passive heat recovery [26]. Actual wind conditions are variable, and windcatchers cannot operate under a stable wind as assumed in the wind tunnel and Computational Fluid Dynamics (CFD) simulations [27]. A slight change in wind direction always affects the ventilation performance of the traditional windcatcher, which in turn, affects the effectiveness of passive technologies [28-31]. When the wind direction frequently deviates from the design wind direction, providing stable ventilation and passive heating and cooling is almost impossible. The limitations of unstable windcatcher performance in the application are especially impactful in multi-opening/sided windcatchers. The supply and return airflow

direction within the windcatcher channels will vary as the wind direction changes. This variation could influence the ventilation rate and the performance of the integrated low-energy or passive technologies, as shown in Figure 1.1 [16, 32]. Three operation conditions are presented in Figure 1.1 including the passive cooling device installed on the windward side, leeward side and both sides. If the passive cooling device was installed on the windward side, as presented in the first figure in Figure 1.1, the passive cooling system would be effective if the wind came from the side with the passive cooling device. However, if the wind direction was changed and only one passive cooling device was installed, the hot supply air can not be cooled in the windcatcher and the waste return air takes away the energy from the passive cooling device. This issue can be solved by installing the passive cooling device on both sides of the windcatcher but the energy efficiency is poor as the return air would always waste energy.

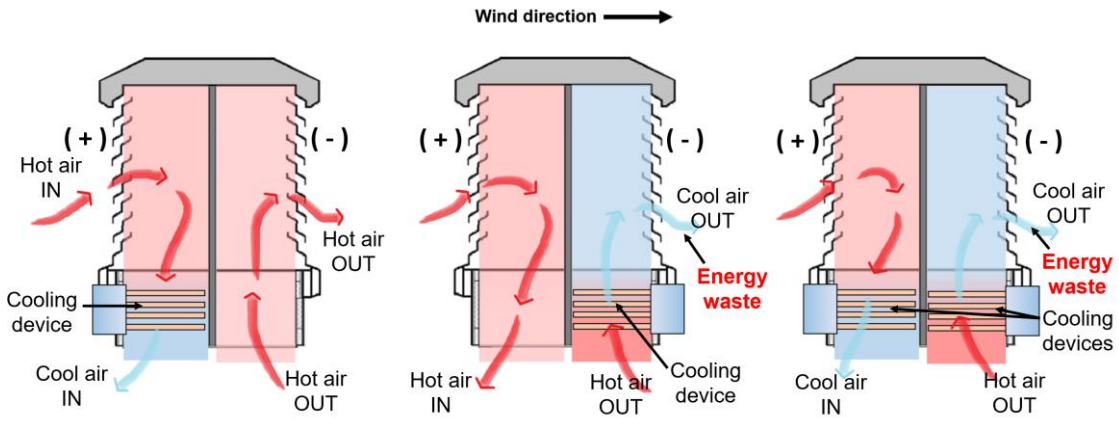


Figure 1.1 Limitation of the passive cooling device integration in traditional four-sided windcatcher

The efficiency of passive technologies integrated into the windcatcher would also be affected by inappropriate wind directions. For example, some previous studies investigated the heat recovery in a conventional four-sided windcatcher, the heat recovery efficiency was affected by the frequent switching of inlet and outlet [29, 33]. In most of the previous research, the impact of the changing wind direction was not considered and the experiments on windcatcher performance were finished under a fixed wind direction [23, 34]. Several studies have examined the effectiveness of incorporating passive cooling and heat recovery technologies into the windcatcher [33, 35-37]. However, the emphasis has primarily been on the windcatcher's capability to cool or heat the incoming airflow, with little attention given to its performance

under varying wind directions. This is noteworthy because the stable operation of the system under different wind directions was crucial for the building [29]. Moreover, as an effective and low-cost cooling method, the evaporative cooling system in a windcatcher achieved a good performance in some greenhouse cooling studies but the research was delivered under a fixed wind direction without considering the influence of the varying wind direction [19, 38]. An evaporative cooling system was applied in a single-side windcatcher assisted with the solar wall but the varying wind directions would not only decrease the ventilation efficiency but also cause thermal discomfort with the reverse flow of the solar-heated air [18].

Installing the passive heating and cooling technologies or heat recovery devices in the current windcatchers can provide thermal comfort but the applications are limited due to the constraints of multidirectional or fixed windcatchers. Windcatchers with more openings were less sensitive to the varying wind directions with a better overall ventilation efficiency than windcatchers with one or two openings despite the windcatchers with one or two openings had a higher peak ventilation rate under the designed wind direction [39]. However, none of the current technology or research has been able to achieve good ventilation performance independent of changing wind directions while simultaneously achieving a high-efficiency passive technology integration solution. Moreover, to maintain a stable fresh air supply at low wind speeds, additional fans may be required, which compromises the zero energy consumption and cost-effectiveness of the windcatcher system [40].

## 1.3 Research aim and objectives

This research aims to develop and evaluate novel dual-channel windcatcher systems using the rotary scoop windcatcher and flap fins windcatcher for multidirectional ventilation.

The research incorporates a dual-channel design for further integration of passive heating, cooling, dehumidification and heat recovery technologies. Several objectives of this windcatcher evaluation were achieved, including:

(1) Providing a comprehensive review of the literature on the windcatcher and passive technologies in building technologies and windcatcher technologies;

(2) Designing the novel windcatchers including the rotary scoop windcatcher and flap fins

windcatcher to overcome the research gap achieved from the literature review;

(3) Developing the windcatcher prototypes and conducting the experimental testing using a wind tunnel (Both types of windcatcher tested) and field test (Only flap fins windcatcher tested) to prove that the ventilation performance of the windcatcher is independent of the environmental wind direction;

(4) Conducting the numerical CFD modelling according to the prototype and validation of the windcatchers to provide a more comprehensive understanding of the windcatcher evaluation;

(5) Conducting the parametric analysis of the validated rotary scoop windcatcher system for better ventilation efficiency and comparing its performance against current commercial systems and building regulations.

## 1.4 Novelty of research

To address the challenges posed by unstable windcatcher performance under varying wind directions and the limitations of passive technologies in conventional windcatchers, two novel dual-channel windcatchers, rotary scoop windcatcher and flap fins louver windcatcher, are proposed to provide wind-driven natural ventilation independent of the wind direction and suitable for passive technology integrations.

The rotary scoop windcatcher includes two concentric ducts with the outer duct incorporating a rotary wind scoop with a central aperture through which the return duct passes. A vertical tail fin positioned at the back generates torque to rotate the wind scoop, ensuring the fin aligns with the incoming wind. Consequently, the outer duct consistently serves as the supply duct, benefiting from the positive pressure generated by the wind scoop, enabling seamless integration with passive technologies. Simultaneously, the central chimney extracts stale air from the building, designating the inner duct as the constant return duct.

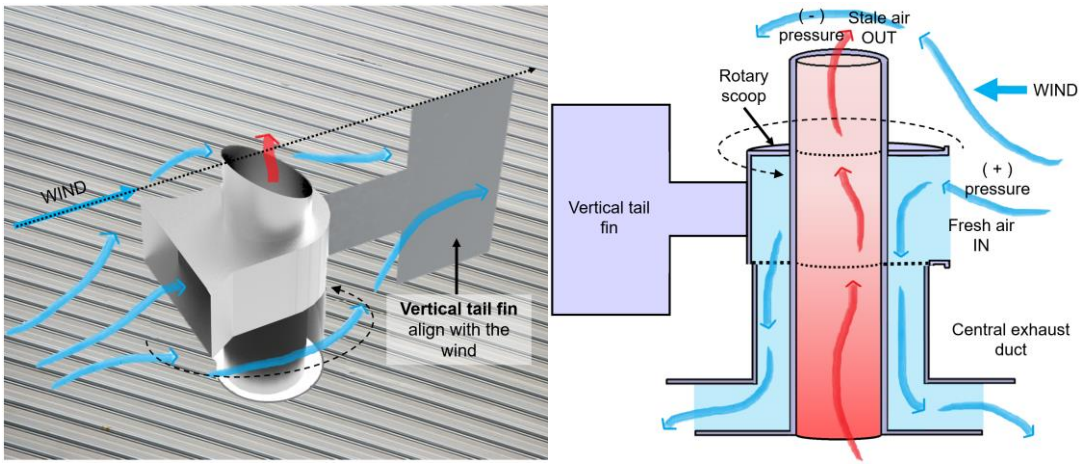


Figure 1.2 Proposed rotary scoop windcatcher with dual channels for supply and exhaust streams

A flap fin louver windcatcher designed based on the conventional 8-side windcatcher was proposed in this research, and the flap fins were applied at each opening to control the airflow supply based on the check valve strategy. The flap fin louver windcatcher, as shown in Figure 1.3, uses the pressure differential at the openings to control the opening and closing of the flap fin automatically. The fins are lightweight, which allows for a self-opening and -closing mechanism. As the wind blows from the windward side, the flap fin on this side will open, allowing the air to enter the windcatcher into the room below. If the pressure outside of the openings were lower than the inside, the pressure difference would force the flap fins to be attached to the windcatcher wall and block the opening, which is slightly smaller than the flap fin, to avoid air leaving the windcatcher. This effectively shuts the flap fins on the leeward side

openings of the windcatcher, which are in the negative pressure region.

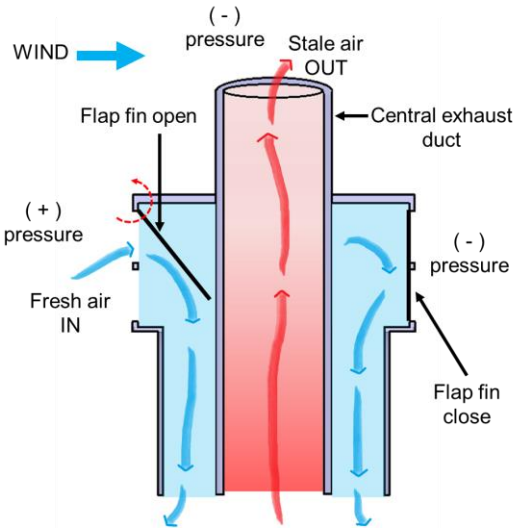


Figure 1.3 Airflow diagram of the flap fins windcatcher

In the flap fin louver windcatcher design, the air would always enter the supply channel from the windward side openings without leaving the windcatcher channel on the leeward side as the flap fins will be closed. The stale air is extracted via the central return duct, which works as a chimney and prevents the mixing of the supply and exhaust air channels. With the combination of chimney and flap fin design, the airflow supply and exhaust direction inside the natural ventilation system will be fixed regardless of the wind direction. Hence, the adjacent concentric circular channels allow for the installation of passive or low-energy technologies to address the issues in this research.

## 1.5 Thesis outline

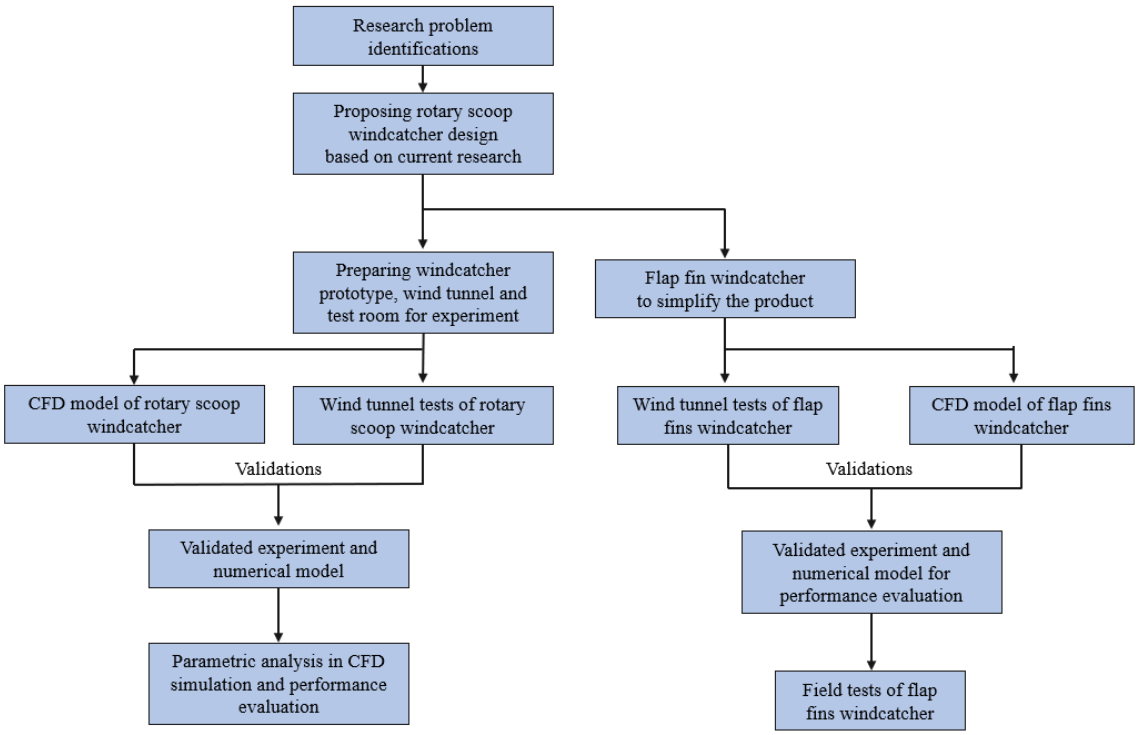


Figure 1.4 Flow diagram of this research

The flow diagram of this research is presented in Figure 1.4 and this thesis is separated into 7 chapters and the summary of each chapter is listed below.

Chapter 1 is the introduction which provides a background of the research and introduces the structure of the research. The research problem and question are contained in this chapter and the aim and objectives are stated in this chapter with the novelty of the research.

Chapter 2 is the literature review which reviews the current windcatchers and passive technologies in the windcatcher system to identify the limitations of current research and applications. The proportion of the current windcatchers and passive technologies in windcatchers is reviewed in this chapter and the limitations of the current windcatcher product and research are discussed to analyse the research gap.

Chapter 3 is the experiment section which presents the development of the wind tunnel, test room and the prototypes of two windcatchers. The designs and dimensions of the wind tunnel and test room are presented in detail and the development of the rotary scoop windcatcher and

flap fins louver windcatcher are presented. The measurements in the wind tunnel experiment and field study are also presented in this chapter.

Chapter 4 is the numerical method section employed in the research covering the theory of the CFD, mesh generation, boundary conditions, solving and validations of the windcatcher model. The parametric analysis of the rotary scoop windcatcher is also evaluated in this chapter.

Chapter 5 presents the results of the experiment of the wind tunnel and test room evaluation. The wind tunnel test results of the rotary scoop windcatcher system are presented for validation and evaluation. The wind tunnel test and the field study results of the flap fins windcatcher are also presented for validation and the evaluation of different parameters of the windcatcher.

Chapter 6 contains the validated simulation results of two windcatchers, full-scale simulation and the parametric analysis of the rotary scoop windcatcher.

Chapter 7 concludes the research in this thesis and discusses the limitations of current prototypes. The possible developments of the windcatchers in this research are also discussed in the future work section in this chapter and the contributions of this research to the knowledge are concluded.

# Chapter 2 Literature Review

## 2.1 Introduction

In this chapter, a systematic review of the windcatcher and passive technologies in the windcatcher system to provide natural ventilation and indoor thermal comfort was conducted. This chapter aims to demonstrate the research gap using a comprehensive literature review. With the literature review of the current research on windcatchers and passive technologies, the proportion of the current windcatchers was achieved and the passive technologies suitable for windcatchers in different regions were presented to explore the limitations and potential of the development of the multidirectional windcatchers for more regions with different demands.

## 2.2 Traditional Windcatcher

A windcatcher is a natural ventilation device integrated with the rooftop design to capture the wind from higher levels and bring in fresh air supply while extracting polluted air similar to that of a mechanical ventilation system [16, 17]. Wind, as an important renewable energy, is a major driving force in building natural ventilation for indoor thermal comfort and indoor air quality [1]. The windcatcher takes advantage of the natural wind forces surrounding it. The positive pressure at the windward side of the windcatcher drives the supply airflow. While the negative pressure at the leeward side and sides of the windcatcher extracts the polluted air out of the building [9]. Windcatchers, also named wind towers, as natural ventilation devices, offer better energy efficiency and enhance the well-being of occupants compared to mechanical ventilation devices [15].

Windcatcher has been applied commercially in the UK, as shown in Figure 2.1 (a), for over 30 years [41]. However, studies believe that the origin of windcatchers is Iran, as shown in Figure 2.1(b), with many complex and high applications for thousands of years [42]. One of the earliest traditional windcatcher applications was recorded in the 1970s in Tappeh Chackmaq, Shahrood City in Iran [43, 44]. In terms of modern windcatchers, hundreds of commercial windcatchers have been applied in the UK in different buildings such as public buildings, schools and

shopping malls [45, 46].

Figure 2.1 Photo of roof top windcatcher applications (a) in the UK [47] and (b) in Iran [48]

Windcatchers play a significant role in modern climate-adaptive architecture by providing natural ventilation and passive cooling which aligns with the need for sustainable cooling solutions in the era of climate change. In tropical and hot regions, mechanical ventilation and cooling contribute to most of the energy consumption in the building industry which generates the second largest carbon footprint after the heavy industry which can be reduced by an appropriate natural ventilation system [42].

Natural ventilation can remove heat and indoor pollutants, thereby providing good indoor thermal comfort and air quality. However, natural ventilation may not always be suitable due to unfavourable outdoor temperatures and humidity [13]. The high outdoor humidity and temperature in both daytime and nighttime would cause thermal discomfort [12].

To enhance thermal performance, low-energy and passive technologies were incorporated with windcatchers, such as evaporative cooling, heat pipes and thermal mass. In desert areas with hot and dry summers, evaporative cooling was established to be an effective passive cooling method, but water resources should also be considered [18-20]. The windcatcher can also be combined with a solar wall to achieve better ventilation performance [37]. Evaporative cooling and humidification were also applied in a natural ventilation system using a solar-wall-assisted windcatcher [49]. Some of the research also investigated the performance of applying an earth-air heat exchanger (EAHE) [22] in a windcatcher system or a heat transfer coil connected to a low-temperature thermal mass in the building [15].

Thus, combining passive technologies and the windcatcher has become a popular research direction in natural ventilation to provide heating, cooling and dehumidification [13, 14]. To

enhance thermal performance, low-energy and passive technologies were incorporated with windcatchers, such as evaporative cooling, heat pipes and thermal mass. In desert areas with hot and dry summers, evaporative cooling was established to be an effective passive cooling method, but water resources should also be considered [18-20]. The windcatcher can also be combined with a solar wall to achieve better ventilation performance [37]. Evaporative cooling and humidification were also applied in a natural ventilation system using a solar-wall-assisted windcatcher [49]. Some of the research also investigated the performance of applying an earth-air heat exchanger (EAHE) [22] in a windcatcher system or a heat transfer coil connected to a low-temperature thermal mass in the building [15, 21].

This literature review focused on windcatcher technologies in different climate conditions with passive heating and cooling technologies and evaluated the potential of using windcatchers to provide indoor thermal comfort under different climate conditions.

The reveal gaps between the research and the demand of the building industry need to be investigated and the criteria of paper selection (inclusion and exclusion) are listed:

- The research can be found in Scopus (www.scopus.com);
- The key word ‘Wind catcher’ & ‘Windcatcher’ were used to provide a range of research;
- The research needs to focus on the building's natural ventilation;
- The research published after 2000 (2000-2023);
- Only the peer-review works in English were selected.

As the literature review focused on the building ventilation performance, some of the research focusing on other regions that occurred in the search was not covered, such as water desalination. Moreover, in order to evaluate the research methodology of the latest applications of the windcatcher, only the research after 2000 was selected. Even though some of the fundamental research about windcatchers in the very early stage was not included, the selection of the research could provide a clear understanding of the regions and investigation methods of the windcatcher by the current researchers.

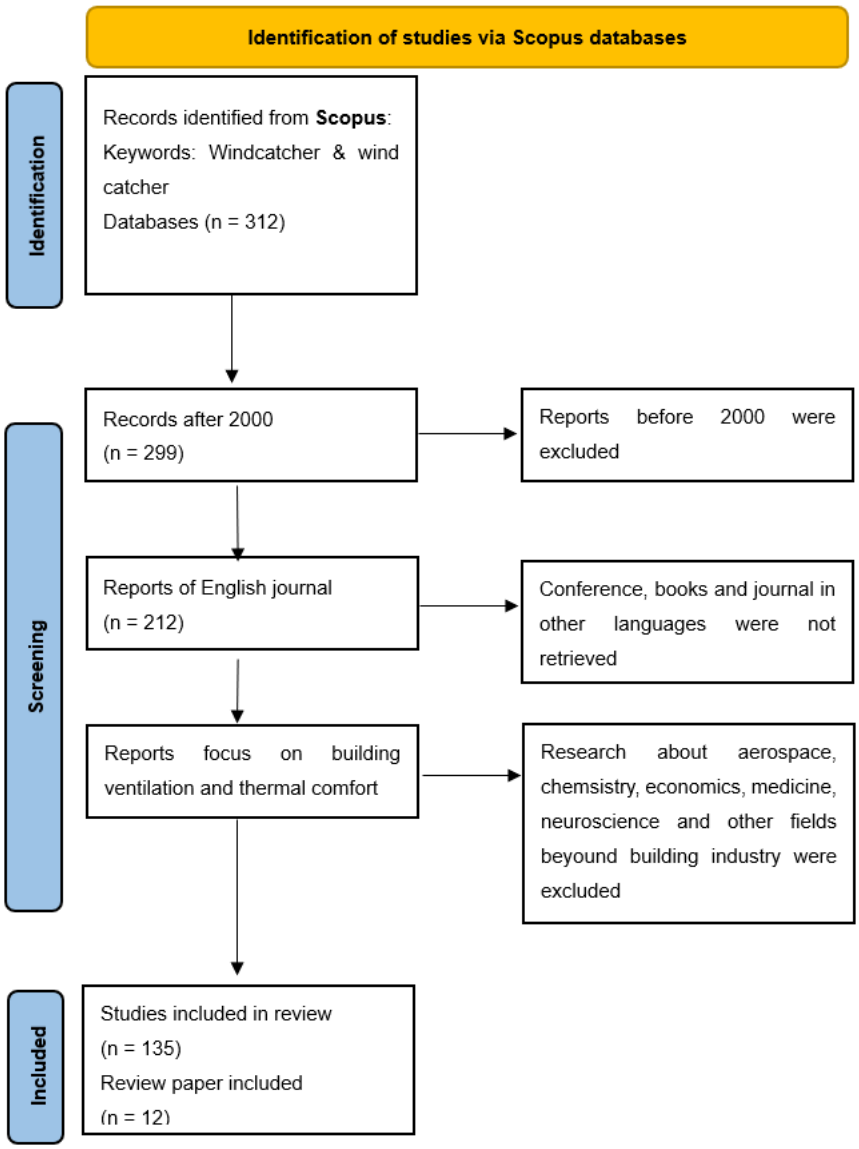


Figure 2.2 PRISMA Chart of the review

### 2.2.1 The proportion of windcatcher types

The geometry of the windcatcher was not limited to a specific shape which can be diverse with different cross-section shapes, opening numbers and heights in different locations, building types and wind conditions [50, 51]. The proportion of the windcatcher research is presented in Figure 2.3.

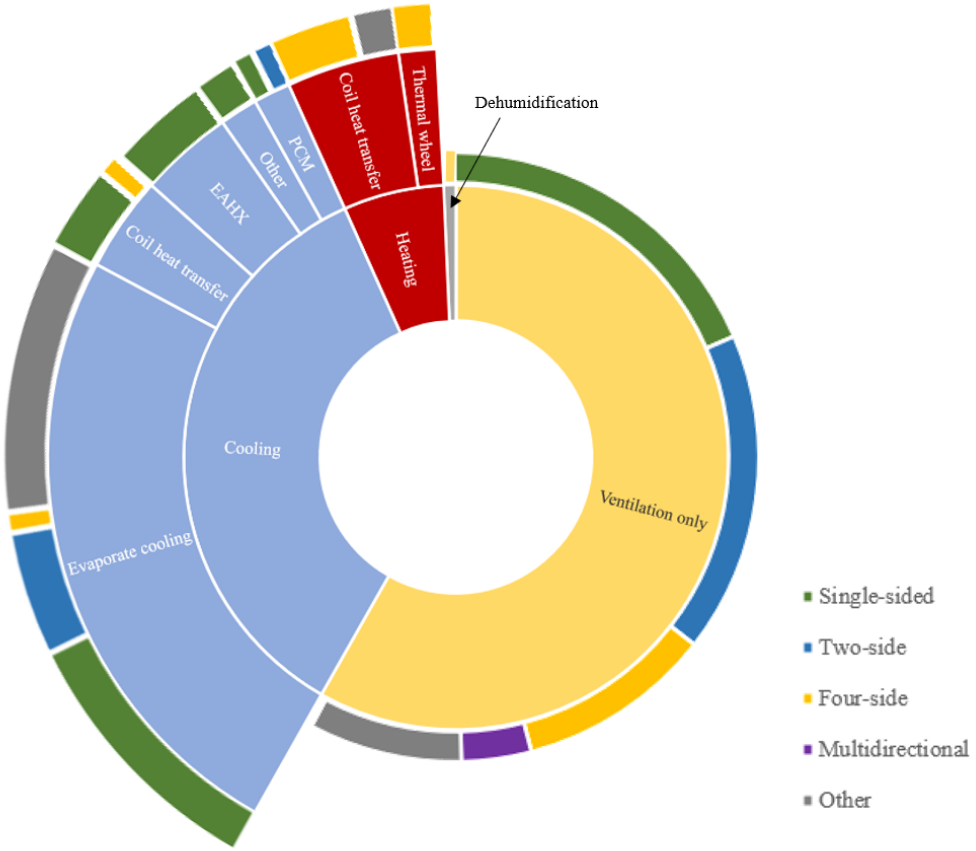


Figure 2.3 The classification of windcatchers investigated in the review by the number of openings and research topic

Passive technologies in windcatchers for ventilation, heating, cooling and dehumidification in this review are shown in Figure 2.3. Over half of the research focused on the ventilation performance of windcatchers due to the fundamental purpose of windcatchers being to facilitate natural ventilation as an alternative to mechanical ventilation systems. The heating and cooling functionalities of windcatchers have also been investigated in the research studies, with 8 and 48 studies respectively. The significant difference in the numbers suggests that cooling is a more critical aspect of windcatchers in the regions with the demand for windcatchers. Moreover, providing free cooling using a water spray system in a current windcatcher is much easier than utilizing any free heat source to provide heating. And the only research was found on dehumidification [52]. As most of the research on windcatchers was delivered in regions with hot and arid conditions, the demand for the windcatcher dehumidification is limited and the difficulty of removing the moisture without increasing the indoor air temperature dramatically

is also a challenge for application. Overall, the research distribution reflects the multifunctionality of windcatchers and underscores the need for further exploration and enhancement of their heating and dehumidification capabilities, while continuing to advance their primary role in natural ventilation and cooling.

Some traditional windcatchers only have one opening for fresh air supply, and the system has to operate with windows or other openings as an outlet [53]. While the multiple-opening windcatchers are more efficient as they can capture wind flow from different wind directions [54]. The windcatcher takes advantage of the natural wind forces surrounding it. The positive pressure at the windward side of the windcatcher drives the supply airflow. While the negative pressure at the leeward side and sides of the windcatcher extracts the polluted air out of the building [9]. By maximizing the pressure difference between the inlet and outlet openings, the efficiency of the windcatcher ventilation system was improved for better indoor air quality [55, 56].

About 40% of the research investigates the single-side windcatcher and the passive technology integrated into a single-side windcatcher, as shown in Figure 2.4. The single-side windcatcher is the simplest windcatcher with only one opening to capture or extract the airflow which decreases the complexity and difficulty of the research model. For example, a single-side windcatcher system integrated with an evaporative cooling system was investigated and all the supply air can be precooled by the water spray system to provide a low indoor air temperature [57].

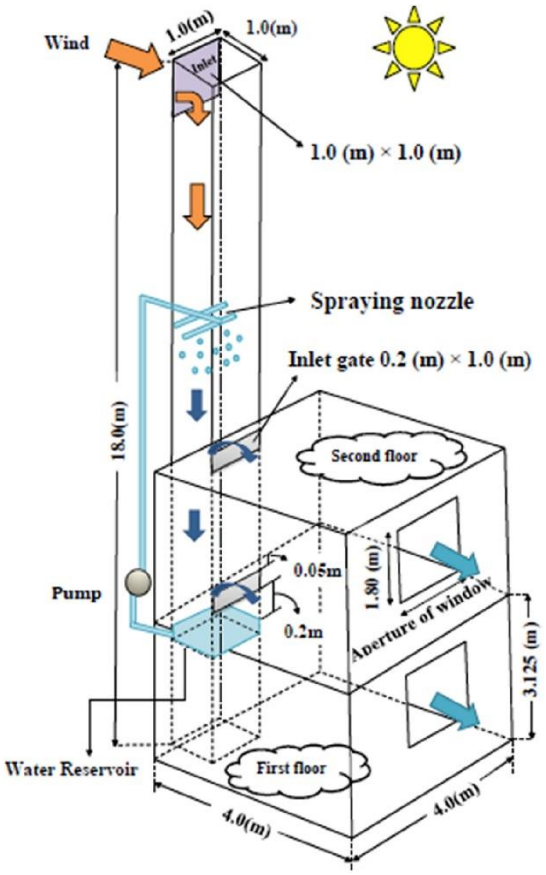


Figure 2.4 Single-side windcatcher system [58]

About 28% of the research investigated the two-side windcatcher which also had a simple design to allow passive technology integrations such as an evaporative cooling system. Although different two-side windcatchers always have two openings to capture the wind and extract the air separately, different designs were applied with different ventilation strategies. Some of the models used separated inlet and outlet channels to provide the cross flow, as shown in Figure 2.5 [59]. Another type of the model was not that effective in ventilating the room which placed the inlet and outlet together and some of the supply air would be extracted by the outlet directly without circulating inside the room, as shown in Figure 2.5 [60]. The performance of this type of two-side windcatcher is similar to a single-side windcatcher and additional openings like the window are necessary for this type of ventilation system. The evaporative cooling system can still be applied to these two types of ventilation systems. In most of the research about two-side windcatchers, the supply and return openings were adjacent and placed in the middle of the room to allow the supply air to circulate inside the room and leave the building after circulation [61]. An anti-short circuit device (ASCD) was necessary for

this type of two-side windcatcher to improve the airflow distribution for better air circulation [62].

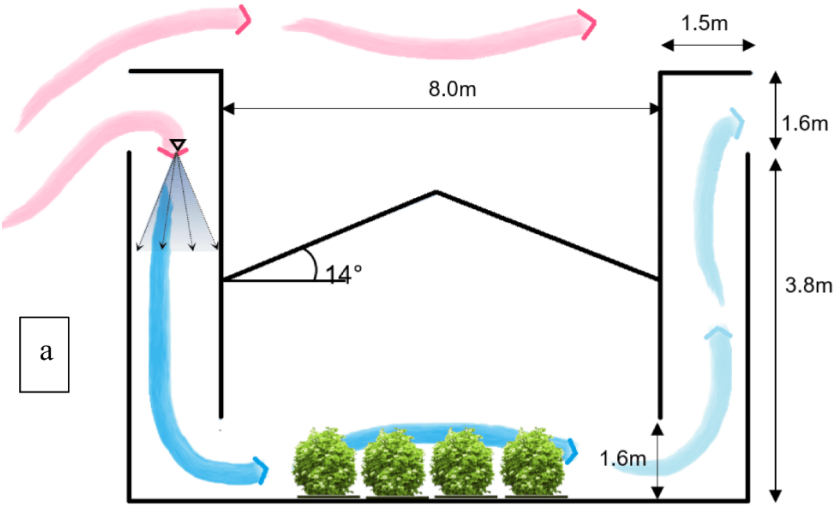


a

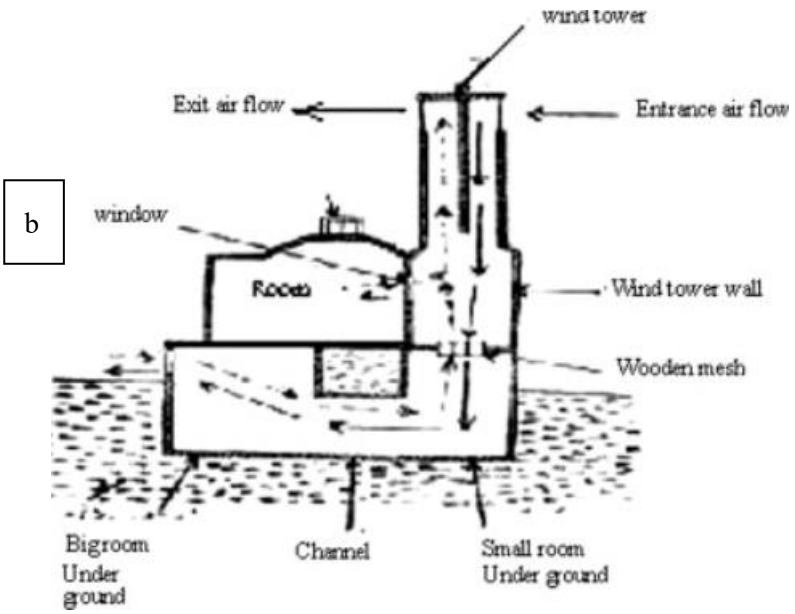


b

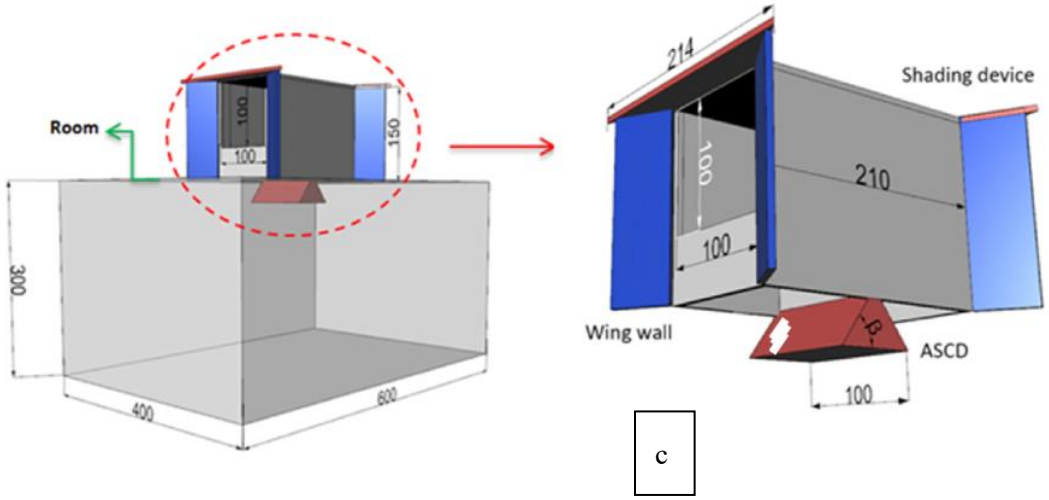


Figure 2.5 Schematic diagram of two-sided windcatchers (a) windcatcher with separate inlet and outlet channels [59], (b) with adjacent openings and channels combined in a single windcatcher [60] (c) with cross flow function [62]

Only two research in this review investigated the performance of a three-side windcatcher and the evaporative cooling performance in the system including a field test case study in Madrid [63] and a CFD simulation model [64].

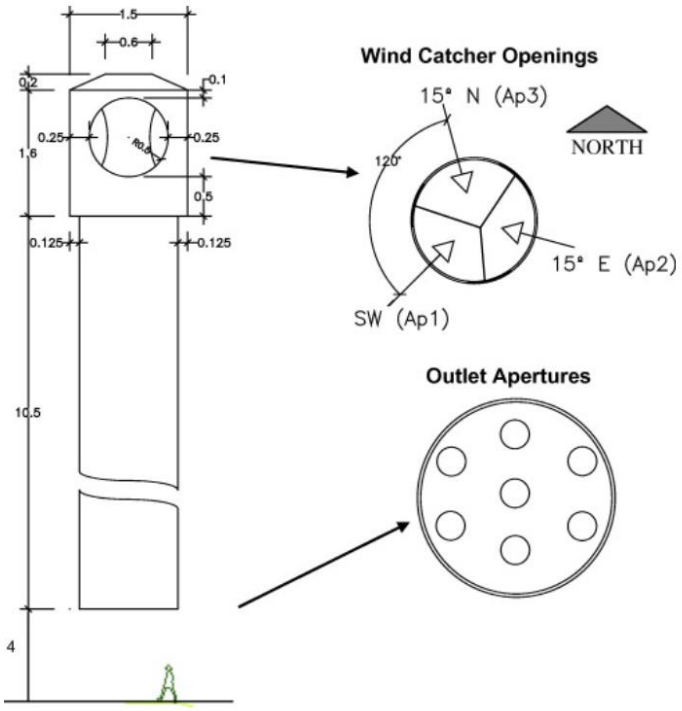


Figure 2.6 Three-side windcatcher with evaporative cooling system [63]

About 16% of the research investigated the ventilation and passive technologies in four-side windcatchers, as shown in Figure 2.7. With the increasing opening numbers, the sensitivity of

ventilation performance to the wind directions was decreased but the wind direction still had an impact on the ventilation efficiency of the four-side windcatchers. Moreover, the maximum ventilation efficiency of a four-side windcatcher is smaller than a two-side windcatcher with the same opening area and the maximum ventilation efficiency of a windcatcher with six or more openings is also smaller than windcatcher with fewer openings [39]. In other words, under the same environmental wind speed and the suitable wind direction, the ventilation rate of a windcatcher with fewer openings is higher than that of a windcatcher with more openings.

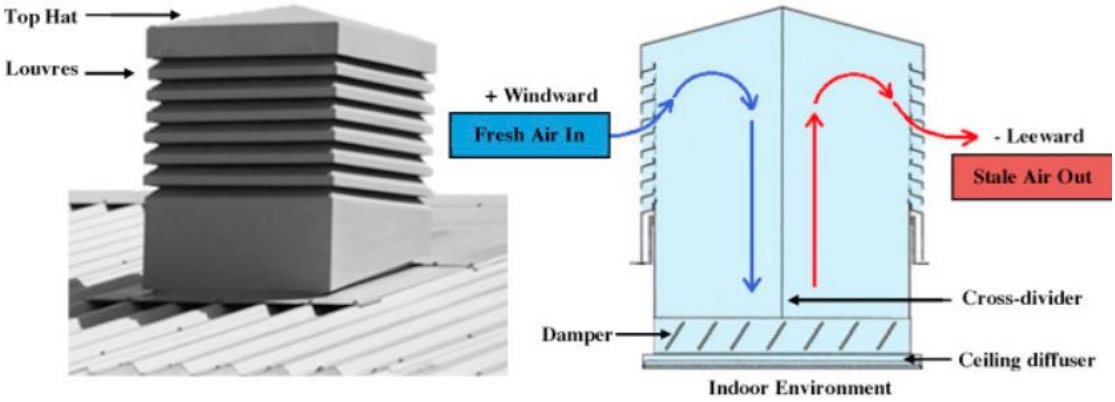


Figure 2.7 Four-side windcatcher for natural ventilation [65]

With the increasing opening numbers, the difficulty of passive technology integration also increased as the supply and return channels kept changing during the operation. In this review, 22/8/2/1 research investigated passive cooling technology in the single-side/ two-side/four-side/multidirectional windcatchers respectively. The models got complex and the performance of passive technologies became unstable with the increase of the windcatcher opening numbers. Thus, most of the recent research and applications focused on ventilation and evaporative cooling to provide passive cooling and the integrations of the heat recovery unit, EAHE system and PCM were very limited because of the unstable performance of the windcatcher system. The lack of a multidirectional windcatcher system resulted in difficulties in applying those passive technologies based on the local climate conditions and limited the applications of windcatcher systems in different regions.

### 2.2.2 Proportion of research methodologies

The proportion investigation methods in different research in the review are shown in Figure

2.8. Over half of the research selected CFD to investigate and present the performance of windcatchers and parts of the research used more than one method such as using both of the Computational Fluid Dynamic (CFD) simulation and experiment testing. A comprehensive understanding of complex fluid flow and heat transfer can be presented and visualized in the CFD results which were hard to be monitored in detail in an experimental prototype. The visualisation of airflow patterns and other details provides invaluable support for the windcatcher system optimization design and performance predictions under various environmental conditions. Moreover, investigating the windcatcher performance in CFD enables the consideration of various design scenarios and boundary conditions at a fraction of the cost and time compared to physical prototyping and experimentation and the research process can be accelerated significantly with optimized solutions [66]. Finally, by using a CFD model validated by the experiment measurements, the accuracy and reliability of the CFD simulation were proved. Controlling the environmental parameters in the CFD simulation is much easier than the experiment which could provide wind conditions more uniform with a wider range of wind speeds than a wind tunnel [28].

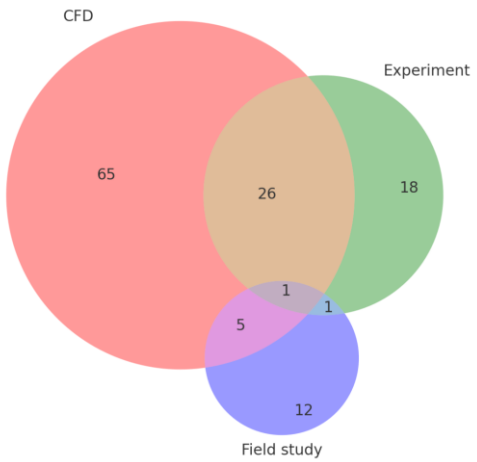


Figure 2.8 Research method proportion contained in the literature review

### 2.2.3 Windcatcher experiment design

This chapter reviews experimental works related to windcatchers, focusing on the scaling-up process, the impact of various wind directions, and material choices in prototype construction. Such a review helps identify the discrepancies between small-scale experiments and real-world

applications, informing the design decisions made in this thesis.

Most of the researchers used transparent Plexiglas to achieve high model accuracy and model visualization, as shown in Table 2.1, and the range of scaling up was between 1:10 to 1:50 depending on the size of the wind tunnel and windcatcher. As the airflow in the windcatcher wind tunnel test was always turbulent, achieving the identical Reynolds number to the real environment in the scaled model by high wind speed is not necessary [53].

Some research at the University of Auckland used an atmospheric boundary layer (ABL) wind tunnel to achieve a wind speed profile close to the actual environment around the building for a higher experiment accuracy [67, 68].

Table 2.1 Windcatcher experiment design in the literature review

| Research | Year | Scaling Up | Wind Directions | Materials |
|---|---|---|---|---|
| [53] | 2008 | 1:40 | 0° to 180° (15° interval) | Wood |
| [25] | 2010 | 1:40 | 0° to 90° (15° interval) | Wood |
| [69] | 2012 | 1:40 | 0°, 30°, 60° | Plexiglas |
| [24] | 2016 | 1:50 | 0° to 90° (15° interval) | Plexiglas |
| [61] | 2016 | 1:10 | Fixed at 0° | Plexiglas |
| [24] | 2016 | 1:50 | 0° to 90° (15° interval) | Transparent material |
| [70] | 2017 | 1:25 | Fixed at 0° | Plexiglas |
| [71] | 2019 | 1:25 | 0° to 90° (15° interval) | Plexiglas |
| [72] | 2019 | 1:30 | 0° to 45° (22.5° interval) | Plexiglas |
| [68] | 2021 | 1:12 | Fixed at 0° | Plexiglas |
| [67] | 2022 | 1:12 | 0°,40°,90°,140°,180° | Transparent material |

## 2.3 Windcatcher Technology: An Overview

Passive technologies integrated within windcatchers have seen considerable exploration in academia due to their potential to significantly enhance the energy efficiency and sustainability of built environments. One such technology is the solar wall, which uses the sun's radiation to

heat the air in a contained space, creating a buoyancy-driven airflow that enhances the natural ventilation facilitated by the windcatcher [37]. Another passive strategy employed in windcatchers is evaporative cooling. This process lowers air temperature by using the heat in the air to evaporate water, hence effectively providing cooling in hot, dry climates [49]. The Earth-Air Heat Exchanger (EAHE) is another passive system that can be used in tandem with a windcatcher [8]. EAHE uses the thermal stability of the earth to precondition the air, thus providing passive heating or cooling to the building. Moreover, heat recovery using heat pipes or thermal wheels can efficiently transfer heat between supply and return air, potentially offering a mechanism for enhancing the energy efficiency of windcatchers [15]. Lastly, Phase-Change Materials (PCMs) can be integrated into windcatchers to enhance their thermal performance and energy efficiency. The use of PCMs in a windcatcher effectively decouples the ventilation and cooling cycles, allowing each to be managed according to the building's needs and the external conditions to improve indoor thermal comforts.

The combination of these passive technologies within windcatchers presents a compelling approach for harnessing natural forces to create comfortable and sustainable indoor environments.

### 2.3.1 Solar wall

A solar chimney is a passive solar ventilation system that capitalizes on the convection of heated air to generate airflow within a building. Solar chimneys typically consist of a vertical shaft with black internal surfaces to absorb solar radiation and heat the air within. Efficient natural ventilation is then forced by the buoyancy from the heated air and the cooler air from lower openings in the building. The solar chimney has better ventilation efficiency in the building with large glazing on the south and sufficient solar radiation [73]. With appropriate control strategies of a solar chimney system, the heated air in the chimney leave the building to generate ventilation in summer and enter the room in winter to provide space heating [37]. However, if the wind direction was against the design direction of the passive system, for example from the right to the left in Figure 2.9, the wind pressure will blow the heated air from the solar chimney to the room resulting in thermal discomfort.

The windcatcher can also be combined with a solar chimney to achieve better ventilation performance [37]. When the environment's wind speed was too low to generate sufficient fresh air supply, the solar chimney would take the role to force the airflow which overcomes the limitation of the windcatcher at low wind speed conditions [18].

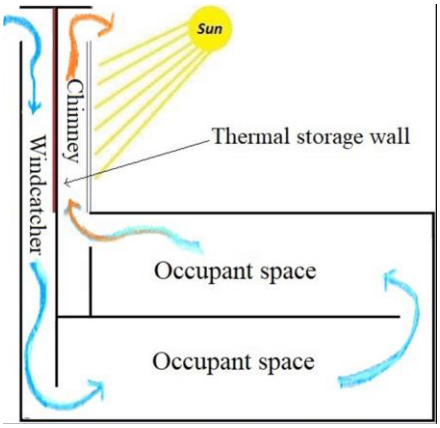


Figure 2.9 A combination of windcatcher and solar chimney in the ventilation system [37]

### 2.3.2 Evaporative cooling

An evaporative cooling system is often employed in building design using the evaporation of water to reduce ambient temperature. The system operates by passing hot, dry air over a wet surface, typically a wetted column [74] or water spray [37], which causes the water to evaporate and absorb heat from the air to create a supply of air with a lower temperature than the outdoor environment temperature. The efficiency of the evaporative cooling system is much higher than the traditional air conditioning systems and the humidification process is also beneficial to the occupants in arid climates. Evaporative cooling and humidification can be applied in a natural ventilation system using a windcatcher [49]. By combining the solar chimney and evaporative cooling system in a windcatcher system, over 70% of the summer operational cost can be saved in a classroom in a hot and arid climate [40].

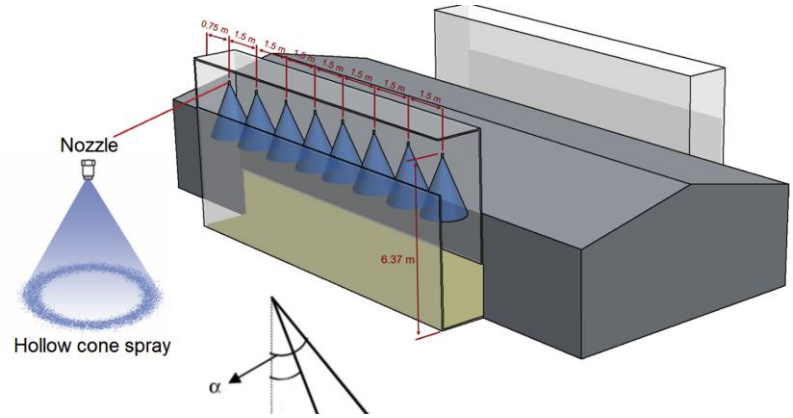


Figure 2.10 Windcatcher with water spray evaporative cooling system [19]

### 2.3.3 Earth-air heat exchanger

Earth-Air Heat Exchangers (EAHE) are a competitive energy-saving technology in buildings that can be applied in various climate conditions [8]. The EAHE system was widely used to utilize the thermal mass of soil to provide precooling and preheating to the supply air [75]. The soil temperature at the level of a few meters below the ground is almost constant over the whole year, while the ambient air temperature fluctuates throughout the year and a day [76].

The combination of a windcatcher with an EAHE can further enhance the efficiency and sustainability of a building's ventilation and climate control system and the performance of applying an earth-air heat exchanger (EAHE) in a windcatcher system was investigated [22]. A windcatcher aids in driving air circulation by using wind forces [35] and buoyancy forces, such as the chimney in Figure 2.11 [77] to draw air into or out of the building. When air passes through the EAHE before entering the building, the air is preconditioned - cooled in the summer and heated in the winter - which significantly reduces the energy load on any additional HVAC systems. Additionally, the windcatcher can also function during periods of low or no wind, using buoyancy effects, to ensure the continuous operation of the EAHE. This integration presents an excellent solution to achieve a high level of thermal comfort in buildings while promoting energy efficiency and sustainability [78].

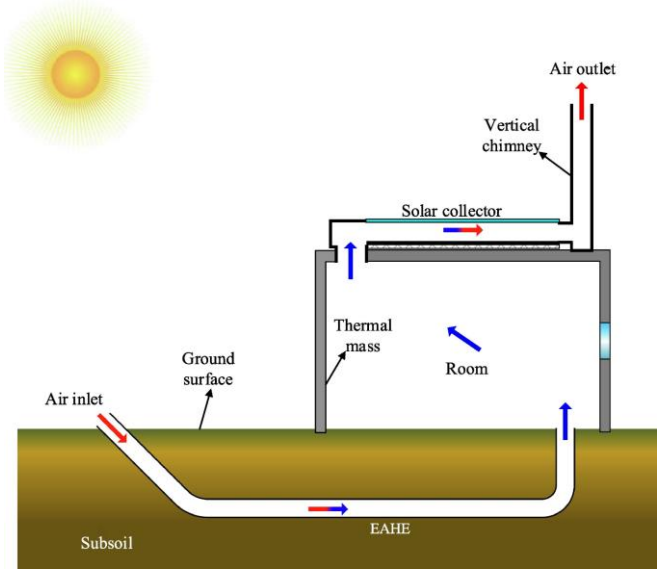


Figure 2.11 Solar-assisted EAHE system integrated into a building [77]

### 2.3.4 Heat recovery

Heat recovery systems in buildings serve a crucial role in energy conservation by capturing and reusing waste heat that would otherwise be lost to improve the building's thermal efficiency. The energy consumption of the building can be dramatically decreased by the heat recovery system [79]. A case study in the UK showed that applying heat recovery in natural ventilation was effective in providing a fresh air supply with low energy consumption [26]. Common types of heat recovery systems in natural ventilation systems include heat pipes [29, 33, 80] and thermal wheels [79, 81]. Heat recovery systems using heat pipes are typically suitable for natural ventilation systems with low system resistance and the airflow can be forced by wind source [82].

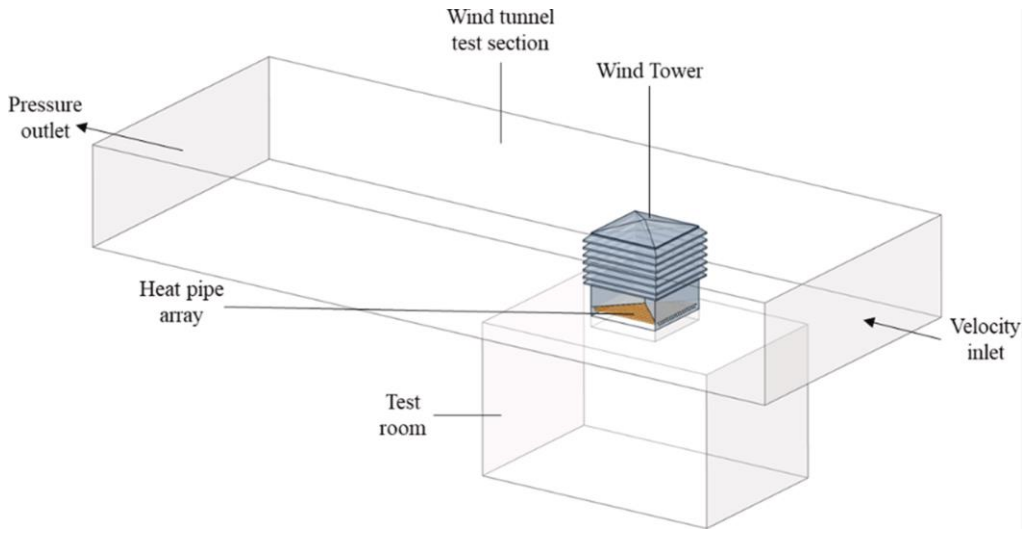


Figure 2.12 Windcatcher heat recovery system with heat pipes [29]

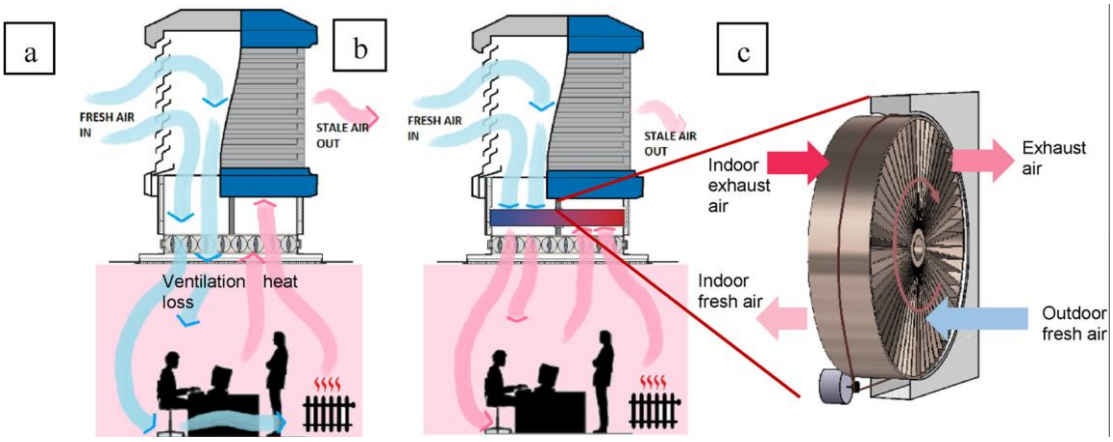


Figure 2.13 Windcatcher heat recovery system with rotary wheel [79]

### 2.3.5 Phase change materials

The PCM can store or release large amounts of energy when they transition between solid and liquid phases which could provide sufficient thermal mass without taking too much space in the building [83]. PCM can be integrated into the building structure to absorb excess heat during the day with high external temperature by the melting process which could provide a lower indoor air temperature. Conversely, during the night or when the external temperature drops, the stored heat is released as the PCMs solidify, pre-warming the cooler incoming air. Installing PCM in the inlet channel of the windcatcher is effective in reducing the indoor air temperature [84]. The integration of PCM in windcatchers could potentially pre-condition the supply air in

the regions with high-temperature fluctuations in a day to improve indoor thermal comfort and reduce the reliance on mechanical HVAC systems [85].

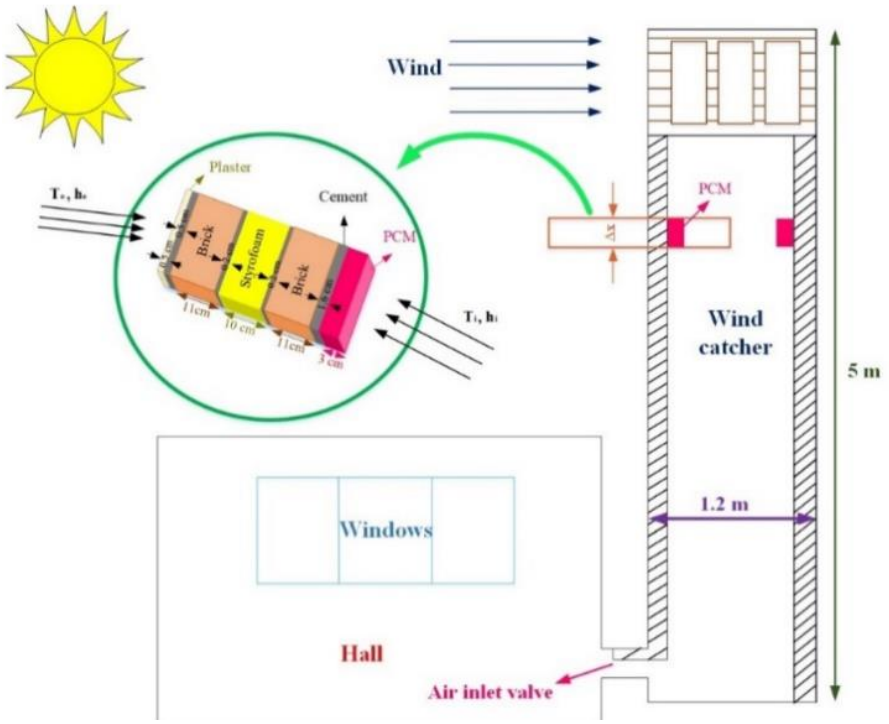


Figure 2.14 Windcatcher with PCM integration [85]

### 2.3.6 Summary

A comparison of conventional natural ventilation windcatchers is shown in Table 2.2. The ventilation performance, passive/low-energy technology integration and cost of the windcatchers were compared. The appropriate passive technologies and windcatchers need to be selected based on the demand of occupants and the local climate, including the air temperature, humidity and wind conditions during the whole year.

Table 2.2 Comparison of conventional windcatchers for natural ventilation

| Windcatcher type | Sensitivity to wind direction | Passive or low-energy technology integration | Advantages | Disadvantages |
|---|---|---|---|---|

| | | | | |
|---|---|---|---|---|
| Single-sided windcatcher /Wind tower [53] | High | • Earth-air heat exchanger [35]<br>• Evaporative cooling [36]<br>• PCM [85] | Low cost | Sensitive to wind directions |
| Two-sided windcatcher [24] | High | • Evaporative cooling spray or cloth [37] | High ventilation rate at design wind direction | Sensitive to wind directions |
| Four-sided windcatcher [41, 86] | Middle | • Heat pipe for cooling and heat recovery [29, 33, 80]<br>• Thermal wheel [79] | Good ventilation performance<br>Passive technologies applied | Passive technologies are sensitive to wind direction |
| Eight-sided or more openings windcatcher [39] | Low | None | Insensitive to wind direction | Low ventilation rate<br>No appropriate passive technologies |
| Flap fin louver windcatcher [87] | None | • Heat pipe heat recovery<br>• Evaporative cooling | Insensitive to wind direction<br>Passive technologies and heat recovery<br>Low cost | Lower peak ventilation rate than traditional windcatcher<br>Need further investigation for commercial use |
| Wind scoop windcatcher [28] | None | • Heat pipe heat recovery<br>• Evaporative cooling | Insensitive to wind direction<br>Higher peak ventilation rate than traditional windcatcher | Need further investigation for commercial use |

## 2.4 Windcatcher and energy-saving technologies in different climates

### 2.4.1 Köppen-Geiger climate classification

Köppen-Geiger climate classification is applied in this literature review to classify the research and applications of windcatchers. Köppen climate classification is widely used in geography, ecology, and atmospheric science in the world [88]. The classification was determined by the

local climate and natural vegetation to provide a clear classification of weather conditions and physical meanings [89]. The detailed classification was listed in Table 2.3 and the ratio of each climate type is presented in Figure 2.16. Although the arid and tropical climates contribute to over half of the area in the world, the ratio of population is different. For example, India has the largest population in the world and the climate in India area tropical and arid. However, most of the population in China, which has a similar population to India, area living in the temperate and continental climate regions. The area of continental region is much larger than temperate but the population on the north of the earth is much smaller than the population on the south.

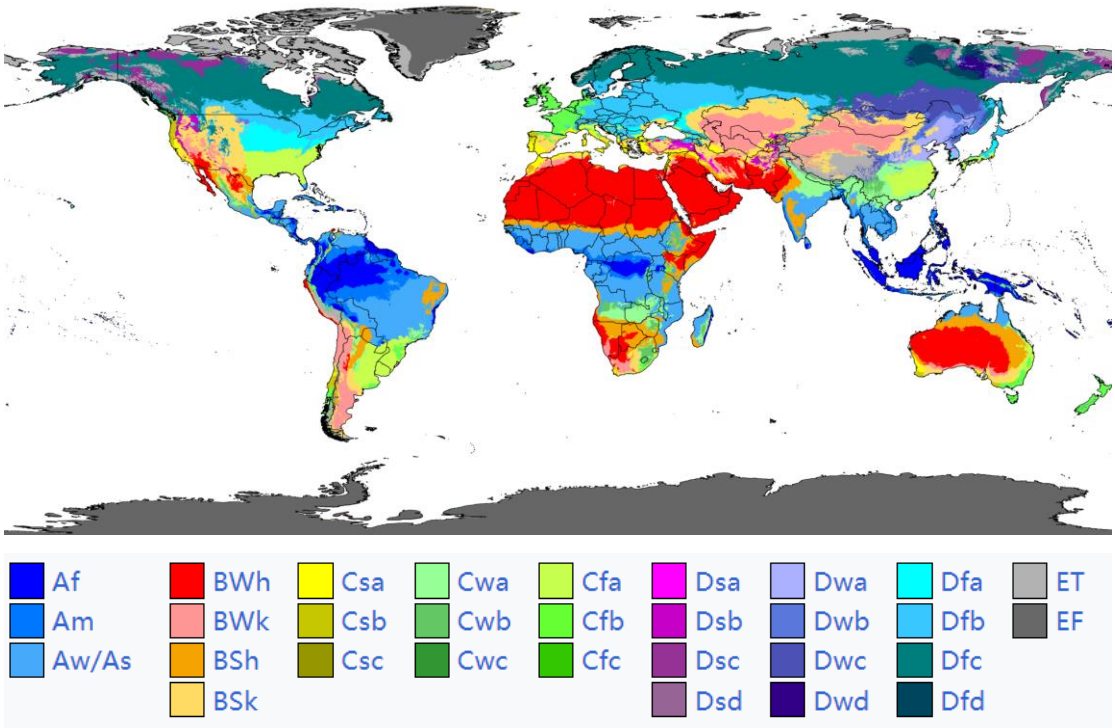


Figure 2.15 Köppen climate classification map of the world [90]

Table 2.3 Köppen climate classification scheme symbols description [90, 91]

| 1st letter | 2nd letter | 3rd letter |
|---|---|---|
| **A (Tropical)** | f (Rainforest)<br>m (Monsoon)<br>w (Savanna, dry winter)<br>s (Savanna, dry summer) | |

| | | |
|---|---|---|
| **B (Dry)** | W (Arid Desert)<br>S (Semi-Arid or steppe) | h (Hot)<br>k (Cold) |
| **C (Temperate)** | w (Dry winter)<br>f (No dry season)<br>s (Dry summer) | a (Hot summer)<br>b (Warm summer)<br>c (Cold summer) |
| **D (Continental)** | w (Dry winter)<br>f (No dry season)<br>s (Dry summer) | a (Hot summer)<br>b (Warm summer)<br>c (Cold summer)<br>d (Very cold winter) |
| **E (Polar)** | | T (Tundra)<br>F (Ice cap) |

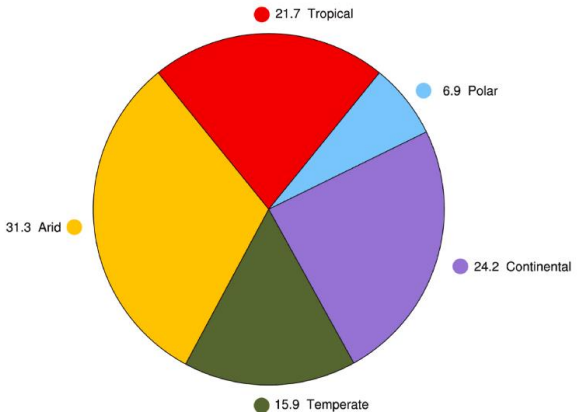


Figure 2.16 Area percentage of major climate type in classification [89]

### 2.4.2 Tropical climates

In hot and humid climates, a lower indoor air temperature compared to outdoor temperature is necessary and a suitable ventilation system design is vital [92, 93]. Most research on windcatchers in tropical climates has primarily concentrated on their ventilation performance. This focus has not been integrated with other passive technologies, due to the challenging climate conditions. Additionally, there is limited research on the application of windcatchers in extremely hot and humid conditions because researchers believe that windcatchers cannot provide adequate thermal comfort in tropical climates [1]. The low environmental wind speed in tropical regions also increased the difficulty of using natural ventilation to provide indoor

thermal comfort [94].

Using evaporative cooling is effective in a hot and arid region but achieving indoor thermal comfort in humid regions with evaporative cooling is challenging, as moisture is demanded in the indoor environment in hot and arid regions but unwanted in a humid region [95]. For example, research in Malaysia showed that evaporating cooling could decrease indoor temperature but the effectiveness of the evaporating cooling system is very limited and the high humidity is also a discomfort for the occupants [96]. Moreover, EAHE has high energy efficiency in a temperate region but applying the EAHE in a region in tropical climates would not provide any energy savings as the soil temperature in a tropical region was higher than the indoor thermal temperature setpoints in the whole year and no precooling can be provided by the EAHE system [8].

The performance of night-time ventilation with appropriate thermal mass in tropical climates is also limited as the outdoor temperature and humidity at night still exceed the temperature range for thermal comfort [97], such as in Shanghai with high humidity at night [98].

Even though using passive technologies to directly provide an indoor air temperature lower than the outdoor environment in tropical climates is challenging, a higher airflow speed around the occupants could benefit thermal comfort [99]. By minimizing and removing the heat inside the room using sufficient ventilation, the heat trap can be avoided with the support of a windcatcher and the occupants would feel less uncomfortable in the room [100]. The high wind speed above the building can be utilized by a windcatcher to provide a higher ventilation rate and airflow speed at the occupants' level, which is about 1.5m [101].

Much research about the windcatcher has focused on providing indoor thermal comfort in a tropical region. However, only a few research provided the location or the weather data of the research and the research with location is listed in Table 2.4.

Table 2.4 Windcatcher in hot and humid (tropical) region

| Passive technology | Research | Location/ weather data | Performance |
|---|---|---|---|
| External shading | [100] | Dala City, Yangon Township, Myanmar | Significantly reduces thermal discomfort hours |

| | | | |
|---|---|---|---|
| Ventilation only | [101] | Tangerang, Indonesia | 1.2 to 1.4 times ventilation rate increase |
| | [102] | Nagapattinam, Bengal | Indoor airflow around 0.1-1m/s reduced discomfort |
| | [103] | Rio de Janeiro City, Brazil | Air circulation increased from under 0.1m/s to about 0.25m/s in the room |

### 2.4.3 Hot and arid climates

Some studies consider that Iran is the origin of this technology as more complex and highly efficient windcatchers are being used there with hot and arid climate conditions [42]. As a technology widely used in the Middle East region's hot-arid climate, the number of windcatcher research in this region accounts for the largest proportion in this review and sufficient research of windcatchers integrated with passive technologies was also provided. The number of research in Iran accounts for the highest proportion in the list and the type of passive technology is also the highest.

Evaporative cooling is an effective and low-cost cooling method that has been applied in traditional windcatchers in hot and dry climates. In desert areas with hot and dry summers, evaporative cooling was established to be an effective passive cooling method, but the water resources should also be considered [18-20]. Using an evaporative cooling system is effective in reducing the air temperature in arid regions both two research in Yazd City, Iran [60] and Masdar Abu Dhabi [64] achieved an indoor temperature reduction of over 10℃. An evaporative cooling system assisted by a solar chimney in a three-floor building was evaluated in CFD simulation using the weather data in Yazd City, Iran and a total cooling capacity of 9kW was achieved [18].

EAHE is effective in providing cool air to the room in arid regions with lower soil temperatures in the ground a few meters deep. A 13℃ room air temperature reduction can be achieved in Baghdad, Iraq [78] and 15℃ in Yazd City, Iran [104]. A system cooling capacity of up to 30kW was achieved with a temperature reduction of up to 20℃ in Ouargla, Algeria [105].

Another research about the EAHE and evaporative cooling presented a system with a high cooling capacity of up to 10kW to provide passive cooling as shown in Figure 2.17 and the room temperature was decreased from 35℃ to 28.6℃ [35]. The location of weather data in this research is not provided but the combination of evaporative cooling and EAHE system is applied to provide indoor thermal comfort under hot and dry weather conditions. Thus, this research is classified as an application for windcatchers in hot and arid regions.

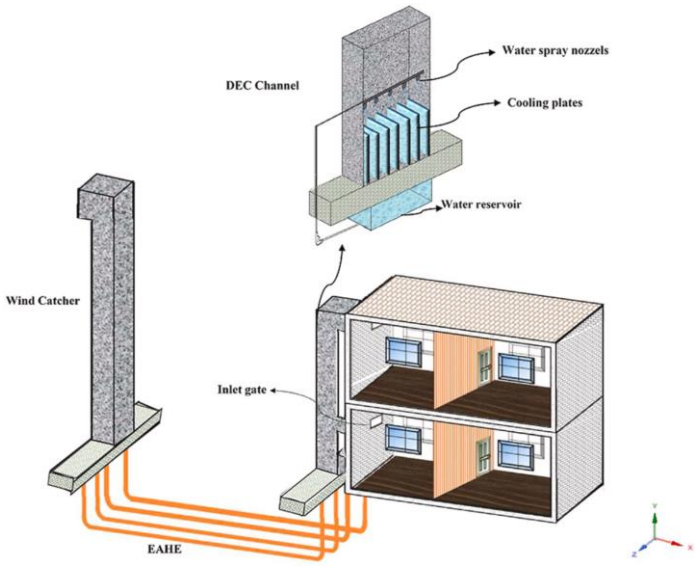


Figure 2.17 EAHE+ evaporative cooling in windcatcher system [35]

The low soil thermal inertia would result in a higher diurnal temperature in arid regions [106]. The high diurnal temperature range would cause a higher outdoor temperature in the daytime and a lower outdoor temperature at nighttime which can be utilized by installing PCM in a windcatcher system as the PCM can be recovered at night to make the passive cooling process recyclable which makes PCM a suitable solution for arid regions. A temperature reduction of up to 25℃ can be achieved in Iran by installing PCM in the windcatcher inlet [85].

The research about passive technology in windcatchers which provided location or weather data in hot and arid regions is listed in Table 2.5. Most of the research in arid regions achieved a good indoor air temperature reduction.

Table 2.5 Passive technology in windcatchers in hot and arid regions

| Passive technology | Research | Location/ weather data | Performance |
|---|---|---|---|

| | | | |
|---|---|---|---|
| Evaporative cooling + solar wall | [18] | Yazd City, Iran | 6-12℃ temperature reduction<br>Cooling capacity up to 9kW |
| Evaporative cooling | [57] | Kuwait | 52.4% of cooling energy reduction |
| | [60] | Yazd City, Iran | 10-15℃ temperature reduction |
| | [64] | Masdar Abu Dhabi | 10-12℃ temperature reduction |
| | [107] | Iran | 11.3-13.7℃ temperature reduction |
| | [108] | Kerman Iran | 10℃ temperature reduction |
| | [109] | Ouargla, Algeria | 18.6℃ temperature reduction |
| EAHE | [78] | Baghdad, Iraq | 13℃ temperature reduction |
| | [105] | Ouargla, Algeria | Cooling capacity up to 30kW<br>20℃ temperature reduction |
| | [104] | Yazd City, Iran | Reduce $T_{room}$ to 26.6℃ at 42℃ $T_{out}$ |
| PCM | [85] | Iran | 25℃ temperature reduction |

### 2.4.4 Temperate climates

Windcatcher is particularly used using natural ventilation itself or with the support of evaporative cooling to provide indoor thermal comfort to occupants in hot and arid regions. However, a large percentage of the world's population is living in regions with temperate climates. The climate conditions in a temperate climate are diverse and the issues for indoor thermal comfort are also diverse. For example, the summer in a temperate climate can be cold (Mediterranean), warm or extremely hot with both humid and dry conditions occurring. The

winter can be cold and warm with both humid and dry conditions occurring as well.

Providing indoor thermal comfort when the warm summer occurs is cost-effective. Natural ventilation is effective in saving energy from mechanical ventilation systems in temperate climate regions. For example, Denmark has a high latitude, and the outdoor air temperature in the summer in Denmark is not that unbearable even though overheating in the building would occur. Natural ventilation could replace mechanical ventilation in 90% of the operation time in a case study in Denmark [110]. However, if the outdoor temperature is extremely hot and humid, which is common in temperate regions, the cooling effect of the windcatcher will be limited, which is identical to the tropical climate. In the hot and humid summer with high outdoor temperatures for the whole day, the performance and possibility of using passive technology to provide indoor thermal comfort are also limited.

Moreover, both summer and winter ventilation needs to be considered, the demand is more diverse as the climate issues to be solved are diverse. In a mild or even cold winter, a high ventilation rate can cause thermal discomfort due to excessive heat loss. The passive designs for buildings against cold seasons mainly focused on minimizing heat loss and capturing more heat gains such as solar gains.

Under climate conditions with hot and arid summers, most of the passive technologies in hot and arid regions are still effective in providing indoor thermal comfort. As the summer in temperate regions may not be as hot and dry as those in arid regions, the passive cooling performance in temperate regions like Greece [111, 112] and Spain [37, 113] might be lower than in arid regions like Iran [107].

Under the climate conditions with hot and humid summers, the conditions in temperate regions are different to the tropical regions. The evaporative cooling is still ineffective but the EAHE is effective in temperate climates with hot and humid summers. Because of the colder winter in temperate regions, the soil temperature can be decreased in winter and the low-temperature thermal mass in the soil can be stored in summer to provide pre-cooling to the supply air. If the soil temperature is lower than the dew point temperature of the outdoor air, the moisture content in the supply air can also be decreased with the EAHE system [8]. Moreover, the preheating to the supply air in winter can also be provided by the EAHE system as the soil temperature in

winter is higher than the outdoor air temperature and the winter heating demand in a passive house with the EAHE system can be almost eliminated [8]. Thus, integrating the EAHE system into a windcatcher can be a suitable solution for indoor thermal comfort in temperate regions.

Moreover, most of Sweden has a temperate climate with a cold winter and the houses in Sweden are normally well-insulated without air conditioning. Thus, the overheating issue in buildings in the summer in Sweden is serious but integrating PCM inside the building could reduce the time of overheating in Sweden effectively [114]. However, the number of research on PCM in windcatchers in temperate regions is limited and the passive cooling potential of the windcatcher with PCM needs to be investigated in temperate regions or well-insulated buildings/ passive houses.

Many research studies have evaluated the passive heating performance of solar walls or Trombe walls. With the on/off control strategy, the solar wall could provide passive heating in winter and buoyancy-driven natural ventilation in summer. The windcatcher system can be combined with a solar wall system to heat the supply air and increase the indoor environment temperature [49]. However, a windcatcher is normally placed at a place higher than the building and induces the air downside to the buildings. The buoyancy effect created by the solar-heated air would force the air to flow towards the higher opening which is against the direction of wind-driven ventilation. Thus, the applications of the windcatcher and solar wall heating need to be further investigated to utilise the advantages of both windcatcher and solar wall heating.

The heat recovery system is normally used in mechanical ventilation systems because overcoming the high-pressure loss in the natural ventilation system is challenging. Thus, to apply heat recovery in the windcatcher system. Heat recovery techniques with low system pressure loss were proposed such as heat pipes [80] and thermal wheels [81]. However, balancing the cost, ventilation rate, and heat recovery efficiency is still a challenge and further research to lower the cost and improve the ventilation rate with high heat recovery efficiency is necessary.

The research about passive technology in windcatchers which provided location or weather data in hot and arid regions is listed in Table 2.6. The quality of passive design strongly depends on how the occupants use the building system [115]. The passive ventilation system designed for

summer might not be suitable for winter operation and separate systems might be necessary for buildings in temperate regions with multiple demands in different seasons.

Table 2.6 Passive technology in windcatcher in a temperate region

| Passive technology | Research | Location/ weather data | Performance |
|---|---|---|---|
| Cooling | | | |
| Solar chimney+ evaporative cooling | [37] | Tehran, Iran | 4℃ temperature reduction |
| Evaporative cooling | [63] | Madrid, Spain | 6-8℃ temperature reduction |
| | [111] | Athens Greece | 4℃ temperature reduction |
| | [112] | Greece | 2℃ temperature reduction |
| | [116] | Cuernavaca city, Mexico | Predicted percentage of dissatisfied less than 10% |
| | [113] | Seville, Spain | 6℃ temperature reduction |
| Heating | | | |
| Solar heating | [49] | Northern Mexico | 40℃ solar wall improved thermal comfort |
| Coaxial heat exchanger | [26] | London, UK | Indoor temperatures fell within BB101 recommended limits for 90% of all occupied hours |
| Heat pipe heat recovery | [80] | UK | 4.5℃ temperature increasing |
| Thermal wheel heat recovery | [81] | UK | 1-4℃ temperature increasing |

### 2.4.5 Summary

In the cold winter, the occupant did not have sufficient ventilation up to 79% of the time [117]. However, a sufficient fresh air supply would result in high energy consumption. Most of the research of windcatcher focuses on the regions in Groups A, B and C with hot summers and winters which is not extremely cold. In regions Groups D and E, the utilization of windcatchers is very limited as a huge amount of energy is wasted in heating the supply air. However, with the development of the building industry in those regions, the building airtightness keeps improving and the fresh air demand in the room can not be eliminated. Thus, developing further research using windcatchers for high-efficiency heat recovery ventilation is necessary for occupants in cold regions.

## 2.5 Research gap of windcatchers

The examination of existing literature on windcatchers has unveiled significant research gaps, particularly in the context of changing wind directions and the system's adaptability across various climates.

Impact of Wind Direction Variability: The literature reveals a crucial gap in understanding the performance implications of variable wind directions on windcatcher systems. Notably, studies have shown that slight changes in wind direction can significantly affect the ventilation efficacy of traditional windcatchers and the performance of integrated passive technologies [28, 29]. However, the operation of these systems under fluctuating wind conditions remains insufficiently examined [34].

Integration and Evaluation of Passive Technologies: Research focusing on passive cooling and heat recovery technologies within windcatchers often does not account for the dynamic nature of wind direction [33, 35-37]. For instance, the effectiveness of evaporative cooling systems in windcatchers was assessed at a fixed wind direction, overlooking the potential impact of wind variability [19, 38]. Applying heat recovery in a traditional windcatcher system using the heat pipes [29, 33, 80] and the thermal wheels [79] was effective in providing a fresh air supply with low energy consumption, but the system was sensitive to the changing wind direction [26]. This

oversight suggests a gap in evaluating these integrations under a wider range of environmental conditions, which is critical for ensuring consistent system performance.

Adaptation to Diverse Climatic Conditions: The predominant focus on arid and hot climates in windcatcher research neglects the potential applicability and necessary adaptations for temperate and continental climates, where demands for passive heating and cooling are both prevalent [118]. With the ongoing shifts in global climate patterns, including rising temperatures and humidity levels, the development of adaptable windcatcher systems for a broader range of climates is urgently needed. This includes considerations for passive cooling to mitigate increasing indoor temperatures during summers in regions previously characterized by milder conditions.

Overall, the increasing energy price and global warming issue result in the pressing demand for passive heating and cooling technologies in the passive ventilation system using the windcatcher system. A multi-directional natural ventilation device can be a solution for applications in various regions with complex local wind conditions. Passive/low-energy cooling and heating technology integrations for different climate conditions. Research about the passive heating, cooling and ventilation technologies also should be evaluated in field studies as well as in wind tunnel experiments and numerical simulations. This entails designing systems that can effectively address the increasing occurrences of extreme temperatures and humidity, thus supporting the development of the low-carbon building industry in a wider array of geographic and climatic contexts.

## 2.6 Summary

In summary, the literature review of windcatcher technologies and passive technologies in windcatchers to reduce building energy consumption was provided. The works in the literature review were classified based on the type of windcatcher, investigation method, passive technology and the climate of windcatcher applications. The importance of integrating passive technologies in windcatchers to provide indoor thermal comfort under different climate

conditions was emphasized in this review and the locations of windcatcher research with passive technology applications were listed in the review section. The research gap of multidirectional windcatchers with the potential for passive technology integration and the demand for windcatchers' passive technologies in more regions were also discussed in this section.

# Chapter 3 Experimental method

In this chapter, the experimental setups of the wind tunnel tests and the field tests were presented and the development of two novel windcatcher designs was explored. In the section on experiment setups, the dimensions and components of the wind tunnel and test rooms in the experiment were presented. The process and devices of measurement were also described in this section. In the section on the windcatcher prototype development, the design concept and the components of the rotary scoop windcatcher and flap fins louver windcatcher prototype were presented. The field test model and measurement device were also explored in this section.

## 3.1 Introduction

The experimental investigation is vital for research on windcatcher performance. First, a high-quality experimental method provides a robust and reliable method for other researchers and users to understand the real-world performance of windcatchers. The experimental method facilitates the replication of studies by providing detailed procedures and methodologies. Moreover, the results achieved in the experiment could validate the theoretical models in CFD simulation and use the computational method to provide valuable insights into the performance of windcatchers. The discovery of new phenomena or unexpected findings can also occur in the experiment which is difficult to consider or predict in the CFD simulations. Those unpredicted issues could include unanticipated effects of design modifications, environmental conditions, or interactions with other building systems which need to be solved in the research. Finally, the field test of a product provides a real-world assessment of windcatcher performance, unlike laboratory experiments or simulations. By testing windcatchers in the field, researchers can obtain a more accurate and comprehensive understanding of their performance under various conditions like wind speed and direction, temperature, humidity, and other atmospheric conditions.

Thus, in this research, an open wind tunnel was made to generate a stable wind condition for the experimental tests of different windcatcher prototypes and the windcatcher performance under different environment wind speeds. A scaled test room with an Anti-Short Circuit Device

(ASCD) was made as a building for the windcatcher performance evaluation. Different windcatcher prototypes were made for the wind tunnel tests to improve the windcatcher design and the performance of the windcatcher was tested in field tests to see whether the windcatcher achieved the design target.

## 3.2 Wind tunnel setups and testing

In this section, an open wind tunnel was made to generate a stable wind condition for the experimental tests of different windcatcher prototypes and the windcatcher performance under different environment wind speeds.

The overall wind generation system in Figure 3.1 contained: (1) A 720 W high-power industrial fan with a diameter of 700mm to generate the wind. (2) A soft plastic tube with a length of 3 meters and a diameter of 800mm to stabilise the wind. (3) A metal contraction was made of 1mm thick stainless steel to increase the wind speed at the outlet. (4) Two mesh screens with a diameter of 0.1 mm and a mesh gap of 0.3 mm to reduce the turbulence of the wind. (5) A 200 mm length wood honeycomb with straws with 10 mm diameter as flow conditioners to adjust the direction of winds to parallel. (6) A 400mm to 800mm insulation ring contraction increases the wind speed in the middle of the tunnel for a uniform airflow distribution. (7) A voltage controller was applied to control the voltage across the fan to control the fan power and the output wind speed. The dimensions of the wind tunnel and the location of the windcatcher are presented in Figure 3.2.

Figure 3.1 Wind generator photo

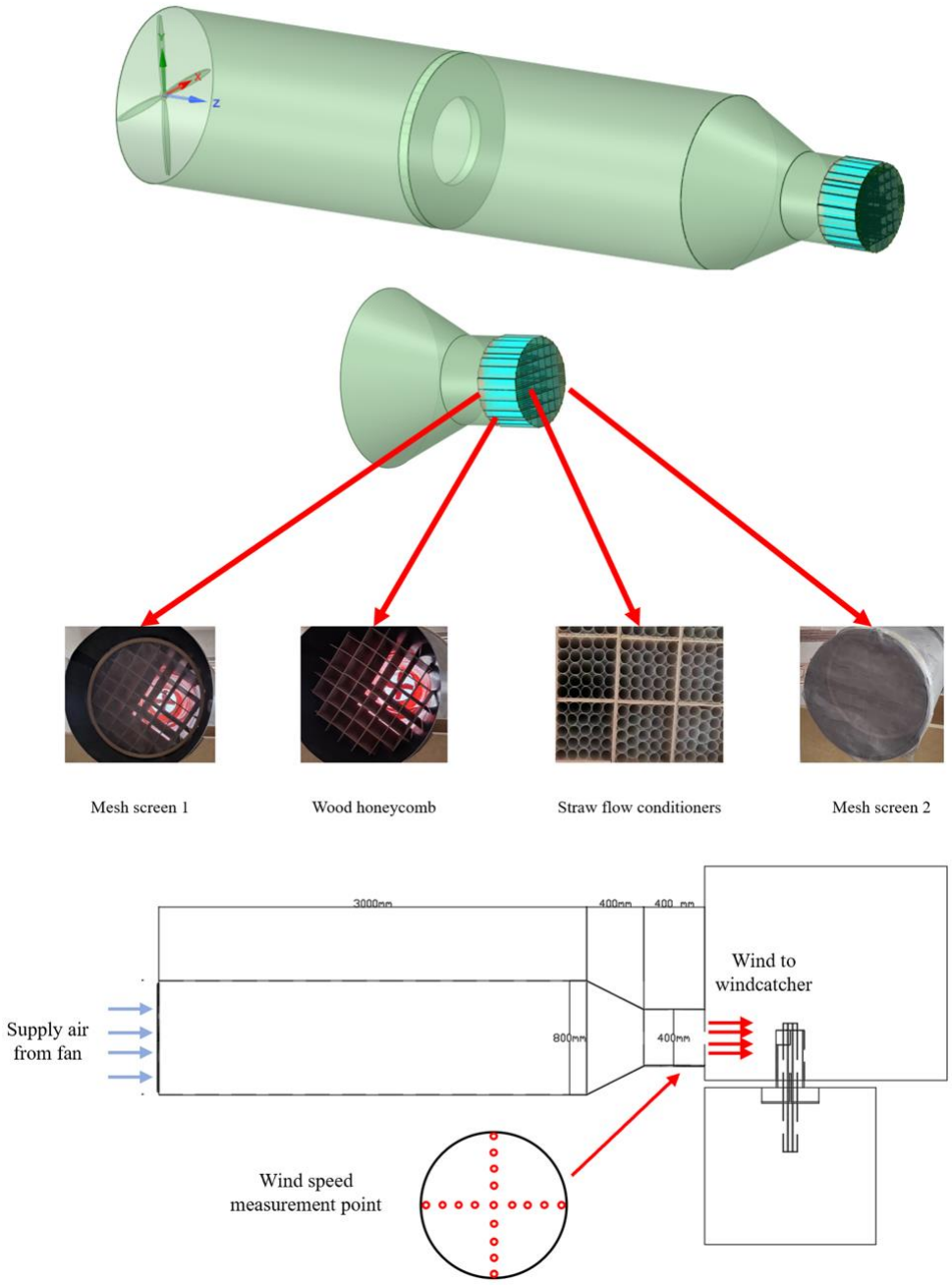


Figure 3.2 Open wind tunnel specification and wind catcher setup

Wind speeds were measured at 17 points at the open wind tunnel outlet, as shown in Figure 3.2, and the profile of wind speeds was used in the CFD model validation. Because the screen mesh and flow conditioner would increase the system's pressure loss, the maximum wind speed generated was 3 m/s. The average wind speed value of each point was obtained after the wind flow stabilised to eliminate the impact of instant wind speed fluctuation. The voltage of the fan was adjusted to change the wind speed and the wind speed profile in each test was measured to

achieve the actual wind speed profile under different average wind speeds. The Testo 405i anemometer, used in similar research for windcatcher airflow investigation [72] was used for wind speed measurement with an accuracy of $\pm(0.1 \pm 5\% \text{ of the readings})$ m/s. The wind speed fluctuation was minimized by the wind tunnel but it could not be eliminated in the experiment, taking the average value of the measurement was still necessary to avoid the error caused by the measurement.

Contraction is the most vital part of a wind tunnel to increase the speed of airflow [119]. Thus, the stainless-steel contraction was made first. The mesh screen and wood honeycomb were added into the contraction to stabilize the wind. Mesh screen distance was necessary for stabilizing the static pressure from perturbation and the mesh opening area range should be larger than 57% [119]. A long plastic was applied to stabilize the airflow after the fan before entering the contraction and straws were used to improve the honeycomb performance to eliminate the small-scale turbulence [119].

Initially, the insulation contraction in the middle of the plastic tube was not applied. Because of the difference between the wind generator system and the traditional open wind tunnel system, the fan was used to blow the wind to the windcatcher in the front rather than extract the air behind the windcatcher [120], and the wind speed profile at the outlet of the contraction was not uniform which was affected by the wind speed profile from the fan. The middle of the fan was blocked by the motor, as shown in Figure 3.3, and the airflow velocity in the middle was much lower than the on edge, as shown in Figure 3.4. Thus, a ring-shaped contraction was added in the front of the contraction to contract the airflow to the middle, and the performance was improved and the wind speed contour and turbulence contour with and without the ring-shaped contraction were shown in Figure 3.5 and Figure 3.6. Because of the low weight of insulation, it can be supported by a wood bar below, and the soft plastic tube rather than using a wood contraction and the difficulty of the experiment was decreased.

Figure 3.3 Fans of the wind tunnel

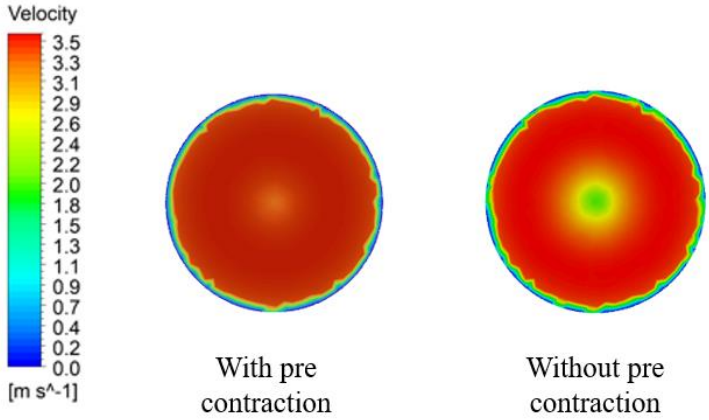


Figure 3.4 Airflow velocity profile example from the outlet (measured from the experiment and presented with the CFD plotting)

Because the wind from the wind generator was blown into open space around the windcatcher, the wind was diffused, and the wind speed was decreased to only half of the initial wind speed when it reached the windcatcher 0.5m away from the wind generator outlet. Thus, the ventilation performance of the windcatcher in this experiment would be smaller than using a uniform environment wind if the identical average wind speed was applied in the testing.

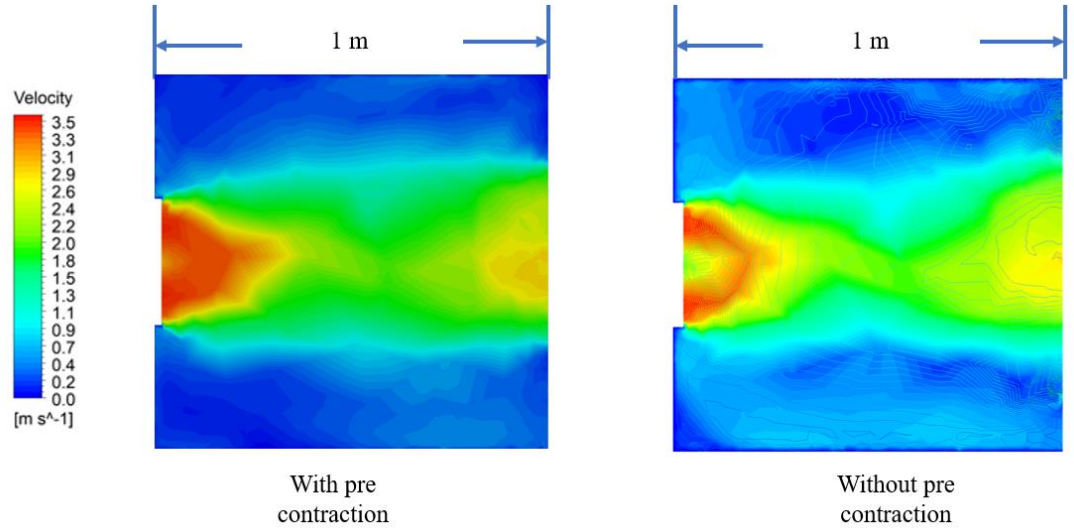


Figure 3.5 Wind velocity from the wind generator (Using the wind speed profile measured in the experiment)

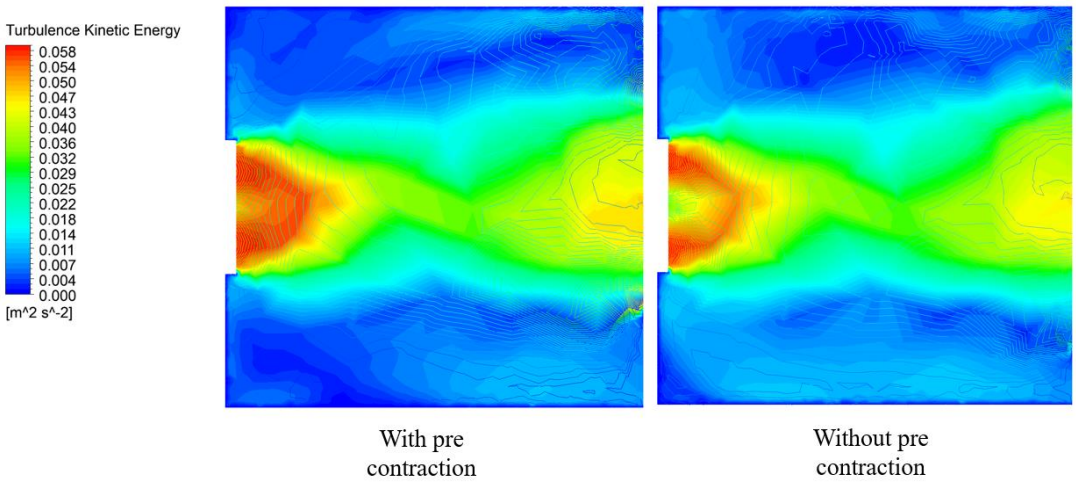


Figure 3.6 Turbulence Kinetic Energy from the wind generator (Using the wind speed profile measured in the experiment)

## 3.3 Test room setups and testing

In terms of evaluating the ventilation performance of a windcatcher, a test room was necessary to create a foundation for the windcatcher to evaluate the airflow entering the building. A wind tunnel was necessary to generate a stable wind output for the windcatcher ventilation experiment. In this research, a scaled test room was made to simulate the condition of a roof windcatcher installed in a building for ventilation evaluation.

The scaled test room contained several components including the insulation wall (Figure 3.9), the support beam (Figure 3.11), ventilation system ductwork (Figure 3.10) and an Anti-Short-Circuit-Device (ASCD) (Figure 3.12) to diffuse the supply air in the experiment.

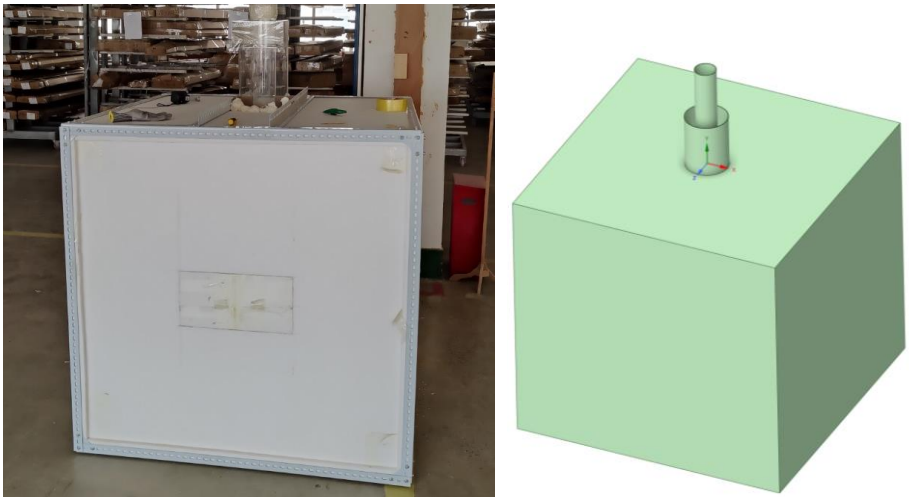

Figure 3.7 Test room photo and test room structure diagram

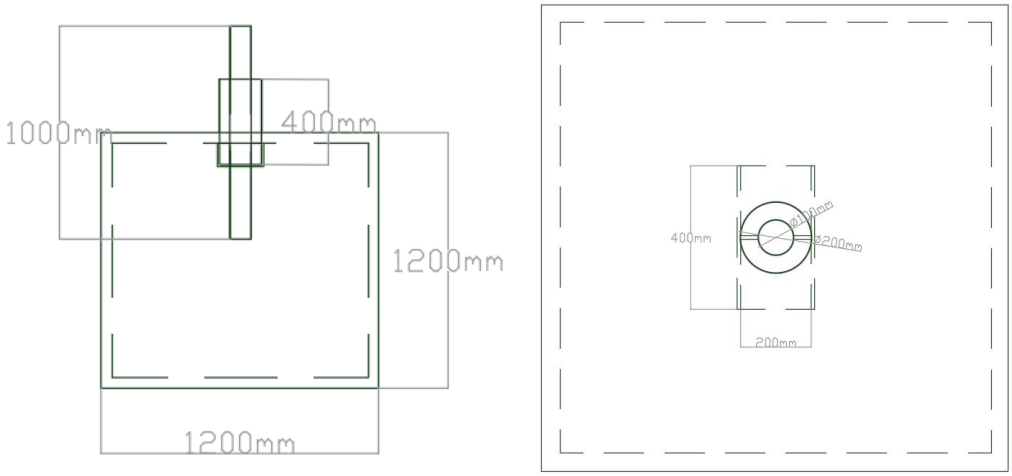


Figure 3.8 Test room front view and top view

A 1.2m length cube test room was made in this research using the insulation panel wall and steel beam structure, as shown in Figure 3.7. The diagram of the test room structure made in SpaceClaim was shown in Figure 3.7 and the dimensions of the test room were presented in Figure 3.8. Six 50mm thickness insulation broads in Figure 3.9 were used as a wall in the test room and the internal space was 1.331 $m^3$.

Figure 3.9 Insulation panel

Figure 3.10 Acrylic transparent tube

The steel beam, in Figure 3.11, was applied to constrain the insulation broad and support the weight of the windcatcher and ASCD. A 100mm diameter transparent acrylic tube was placed in the middle of the roof and a 200mm diameter transparent acrylic tube was placed coaxially outside the 100mm tube as the supply and return ductwork as shown in Figure 3.10.

Figure 3.11 L-shape steel structure

The air-short-circuiting was a problem in the natural ventilation system with the windcatcher in that the supply air entered the outlet duct directly without mixing the air inside the room [62]. A 400mm T-shape anti-short circuit device (ASCD) made by a 10mm thick wood broad was added to change the flow direction of supply air from vertical to horizontal. The extruded part on the top was connected to the steel beam above the insulation panel to support the weight of the acrylic tube and the wood structure itself. The bottom part was used to adjust the supply airflow direction to separate the inlet and outlet inside the room. The space between the ASCD and the insulation panel was filled with the foaming agent in Figure 3.12 to avoid air leakage. Two 400mm L-shape ASCD redirected the flow of supply air from vertical to horizontal. The ventilation performance of the windcatcher with and without ASCD was evaluated by CFD simulation. By using the CFD method discussed in Chapter 4, the ventilation performance of the windcatcher with and without the ASCD was evaluated. After applying the ASCD as shown in Figure 3.13, less than 1% of the air escaped the building without circulating inside the room while most of the air would leave the building directly if the ASCD was not applied. The airflow distribution in the building was more uniform after applying the ASCD, and the streamline was separated into different directions rather than flowing together.

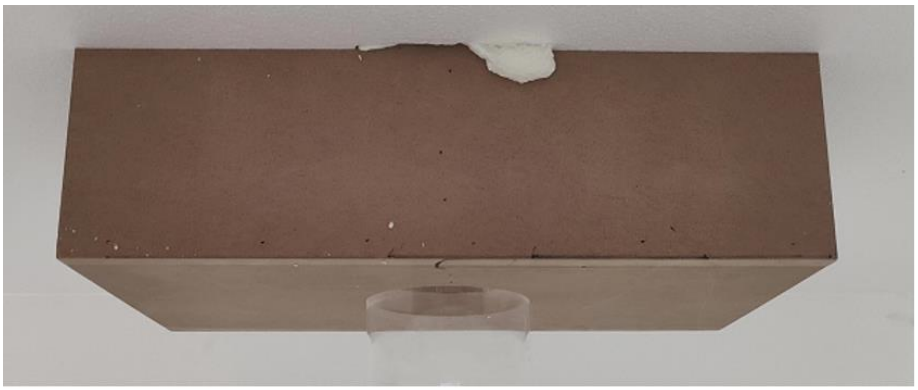

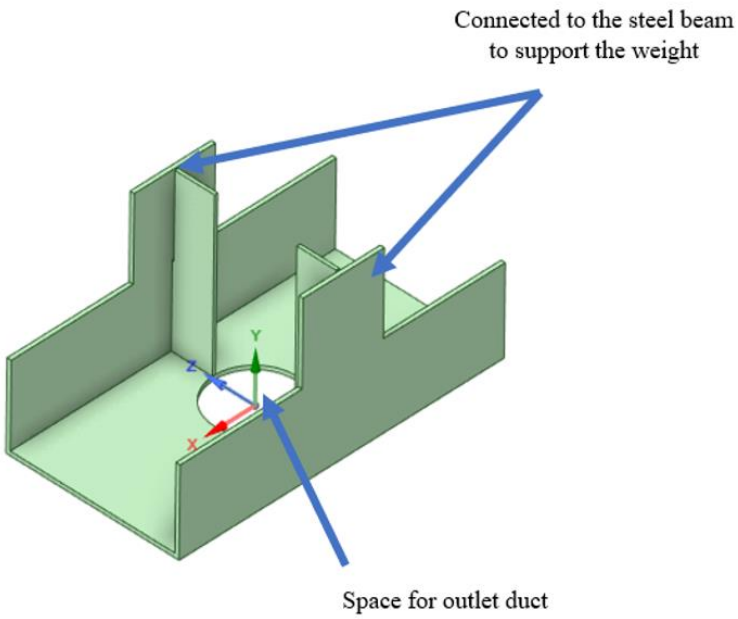


Figure 3.12 ASCD photo and structure

By using the CFD method discussed in Chapter 4, the ventilation performance of the windcatcher with and without the ASCD was evaluated. After applying the ASCD as shown in Figure 3.13, less than 1% of the air escaped the building without circulating inside the room while most of the air would leave the building directly if the ASCD was not applied. The airflow distribution in the building was more uniform after applying the ASCD, and the streamline was separated into different directions rather than flowing together.

The mass flow rate at 5m/s outdoor wind velocity in the model with and without ASCD was 0.1484 kg/s and 0.1496 kg/s, separately. Only a small decrease within 1% occurred after adding the ASCD. Thus, adding the ASCD was useful in providing better air circulation inside the room without significantly decreasing the ventilation performance of the windcatcher. The

ASCD would also benefit from the passive technologies in the windcatcher to avoid the cooled or dehumidified air leaving the building directly rather than circulating inside the room.

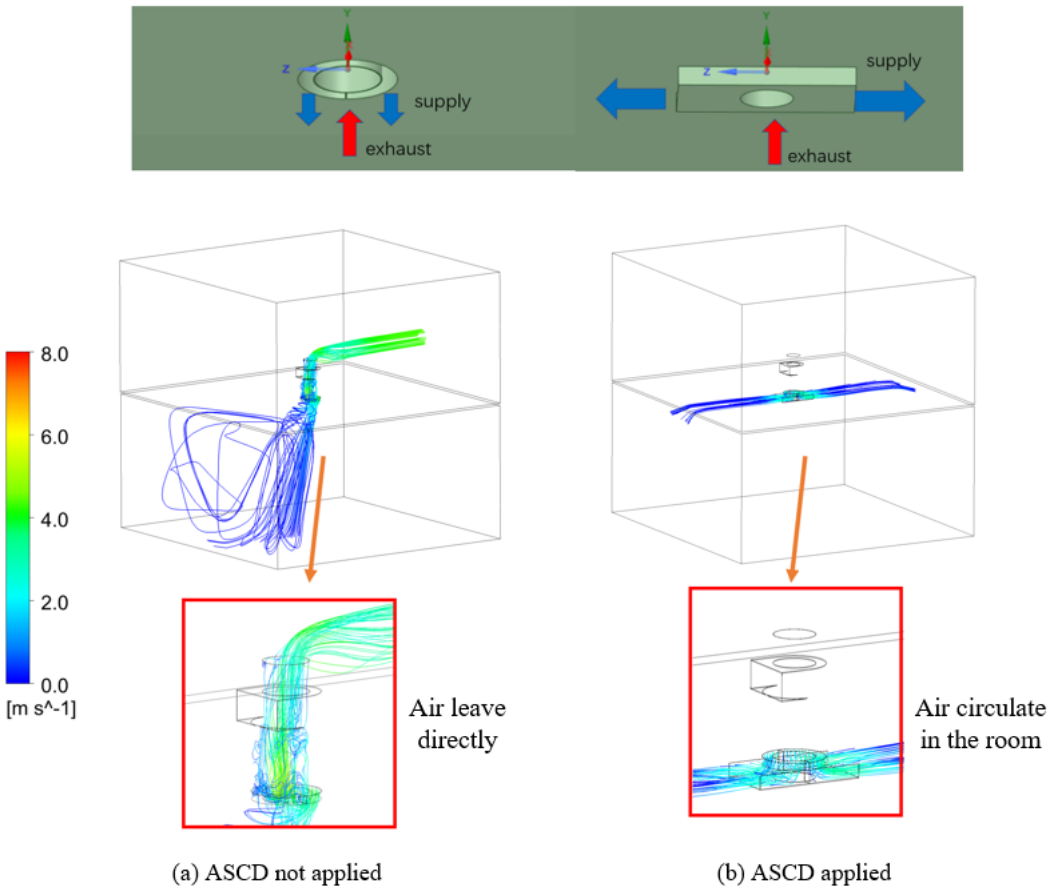


Figure 3.13 Anti-short circuit device impact on supply and exhaust airflow

All the edges of the insulation broad were cut at 45 degrees to increase the strength of the test room. With the constraint of the steel beam, an external force on the edge was provided on the edge to avoid disintegration. With the slope edge, the broad could support each other from the internal, or the broad will be deflected inside by external force by accident, which is hard to avoid in the experiment measurement. Overall, the test room was strong enough to support the windcatcher and do the experiment.

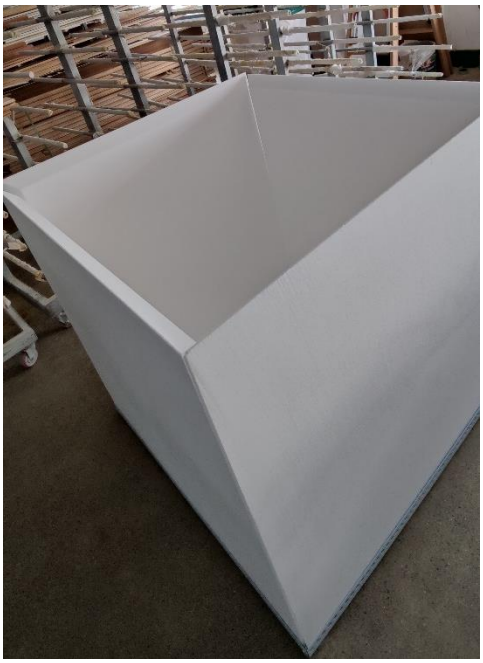

Figure 3.14 Insulation broad connection

The tracer-gas decay method was used to measure the airtightness of the sealed test room with low pollutants and environmental effects [121]. Carbon dioxide was selected as tracer gas because of its nontoxic physical properties, and the $CO_2$ concentration sensor (HTI HT2000) was used to measure the $CO_2$ concentration. The accuracy of concentration measurement at the condition below 5000 PPM was $\pm($ 50 PPM $\pm$ 5% of the readings). The carbon dioxide concentration measurement point is shown in Figure 3.22. As the carbon dioxide had a higher density than air, the carbon dioxide concentration at the bottom of the test room was higher than at the top, so the carbon dioxide sensor was placed in the middle of the test room. In the ventilation rate test, as the air was well circulated inside the test room with the help of the ASCD, the carbon dioxide concentration at the outlet can be used as the average concentration inside the room for air change rate calculation.

The air change rate of the test room was calculated by the CO2 concentration change rate using Equations (3.1) and (3.2) [122].

$$C(t) = \big(C(0) - C(e)\big) \times e^{-\mathrm{Qt/V}} + C(e) \tag{3.1}$$

$$n = Q/V \tag{3.2}$$

where $C(t)$ is the $CO_2$ concentration after t seconds in PPM;

$C(0)$ is the $CO_2$ concentration at the initial condition in PPM;

$C(e)$ is the $CO_2$ concentration of the environment in PPM;

Q is the supply air volume flow rate in $m^3/h$;

V is the internal volume of the test room in $m^3$;

$t$ is the time in s;

$n$ is the air change rate in $h^{-1}$.

In the airtightness measurement, after sufficient time to mix the $CO_2$ and the indoor air, the initial $CO_2$ concentration was 3350 PPM, and the final $CO_2$ concentration was 3200 PPM. The time of air exchange was 3050s and the environment $CO_2$ concentration was 500 PPM. The air change rate was 0.0625 $h^{-1}$ and the air leakage was 0.023L/s which was ignorable compared to the wind-forced ventilation. Thus, the test room can be treated as a full airtight box in the experiment.

## 3.4 Rotary scoop windcatcher prototype development

The wind scoop, which is also called the pressure cowl, has a rotary inlet opening which ensures that it faces the wind from all directions to make sure the ventilation performance would not be affected by the changing wind directions and it could be placed at higher locations to capture the wind with high wind speed, such as above the building [123]. An example of a wind cowl installed in 1991 in the ICI chemicals visitor centre in Runcorn, UK, was analyzed [30]. The ventilation performance of the traditional windcatcher decreased dramatically when the wind direction changed and the ventilation efficiency decreased by 50% in the two-side windcatcher and 40% in the three-side windcatcher [39]. Compared with the traditional windcatchers with multiple openings, the wind scoop could provide a stable fresh air supply for passive ventilation, cooling and heating technologies under changing wind directions.

This section aims to develop and evaluate the rotary scoop windcatcher design using experimental methods and the objectives contained the prototype making and the testing of ventilation rate and rotation.

The dual-channel wind scoop windcatcher was developed based on a displacement ventilation strategy with a pressure inlet to supply the air and a pressure outlet to extract the air from the room. The wind scoop windcatcher geometry with two concentric ducts and an airflow diagram

is shown in Figure 3.15. A rotary wind scoop was applied to the outer duct with a hole in the middle to allow the return duct to pass through. A vertical tail fin on the back generated the torque to rotate the wind scoop and face the wind. The outer duct will constantly be the supply duct with the positive pressure generated from the wind scoop for the passive technology integrations. The chimney in the middle would then extract the stale air from the building, making the inner duct the constant return duct. Overall, the supply and return positions were fixed and adjacent, no matter how the wind direction changed. On the contrary, the windward side in a traditional multiple openings windcatcher will be supplying the fresh air, and the rests would become return ducts which will change with the wind direction. As the supply and return duct were constantly adjacent to each other in the scoop windcatcher and the airflow direction would not change in operation, the energy can be recovered from the return air to the supply air stably and continuously in a passive heat recovery configuration such as heat pipes.

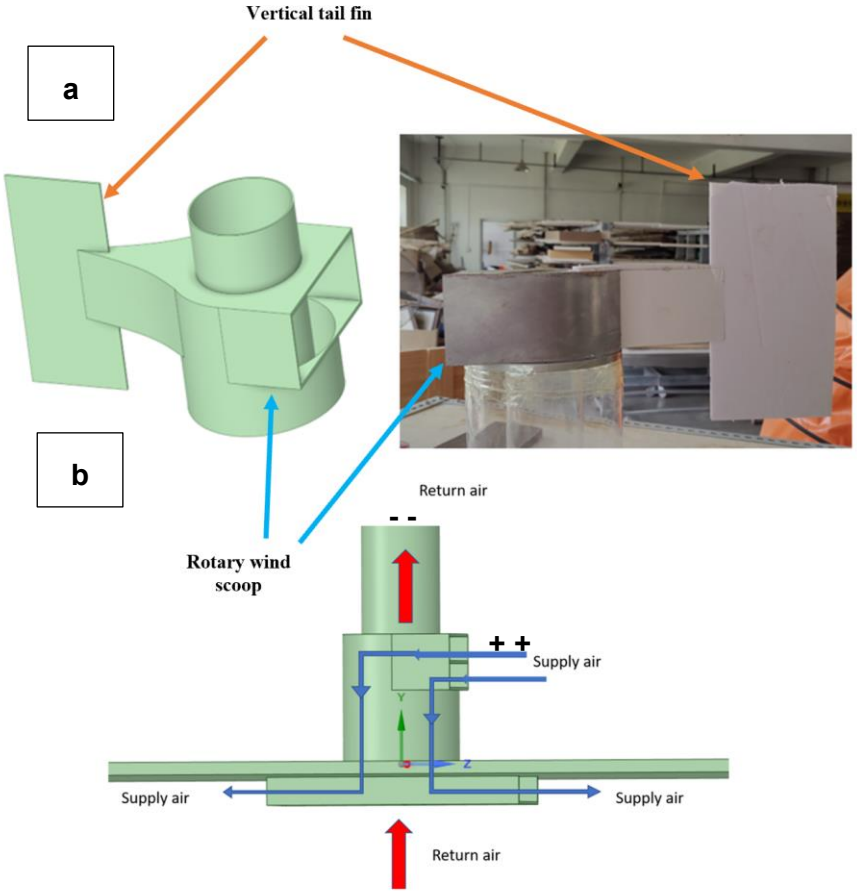


Figure 3.15 Diagram of proposed rotary windcatcher (a) components in the windcatcher, (b) supply and return airflow directions in the windcatcher and ventilated space.

The research flow diagram of the wind scoop windcatcher is summarized in Figure 3.16. A scaled experimental prototype was designed and constructed. The experiment evaluated the ventilation performance first, and the CFD validation was conducted after obtaining the experiment results. The full-scale CFD model was modified from the validated scaled model, and the ventilation performance was compared to the conventional windcatchers and building regulations.

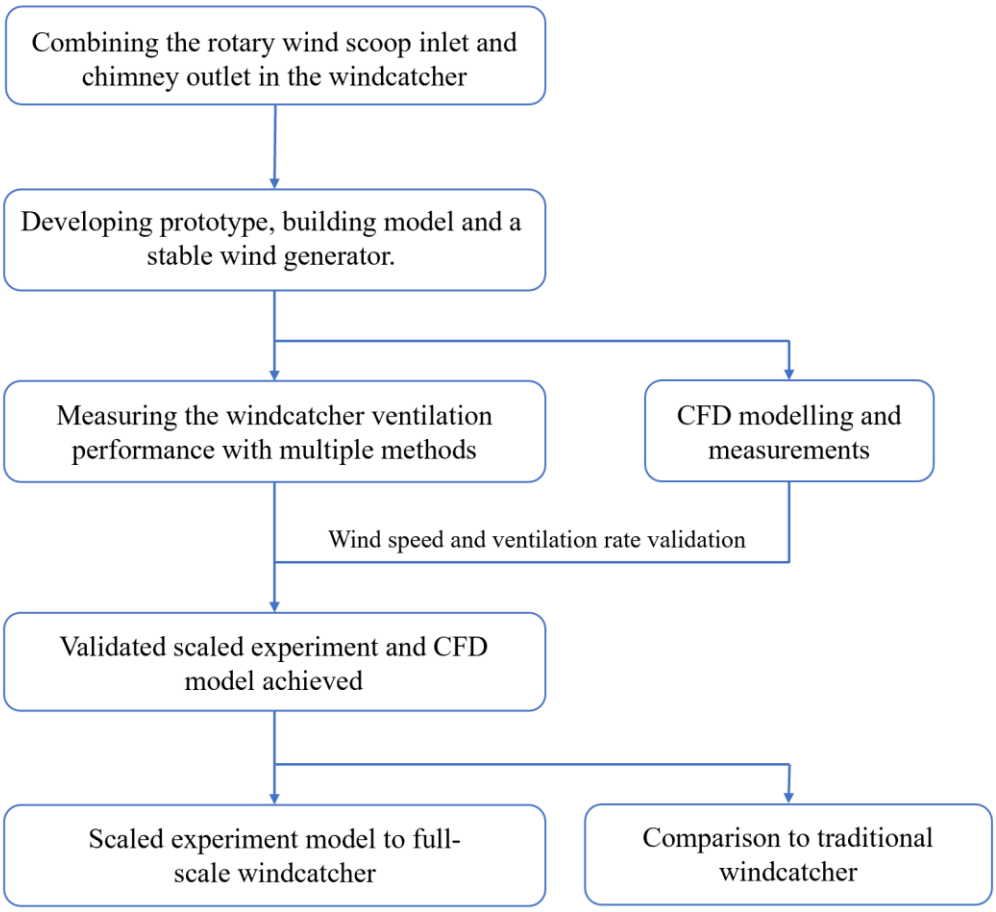


Figure 3.16 Research method for the development and evaluation of the dual-channel wind scoop windcatcher device

The prototype of this windcatcher contained the rotary wind scoop and ductwork. The rotary scoop was made of stainless steel, and the supply and return ducts were made of transparent acrylic tubes. The vertical tail fin was made of a wood bar and foam board. A ring-shaped bearing connected the rotary scoop and duct to let the supply air pass through the opening. The

wind scoop was supported by the ring-shaped bearing connected to the external tube for rotation. A 42cm high, 48cm long vertical tail fin was added to the back of the rotary wind scoop at a distance of 12 cm. The rotation performance of the windcatcher was tested at different wind speeds. A digital camera was used to record and evaluate the movement of the device. Because of the prototype manufacturing limitations, the windcatcher models for ventilation rate validation, in Figure 3.15, and the rotation test, in Figure 3.17, were slightly different. The extended part of the chimney was removed for the prototype used in the rotation test. It should be noted that the model for the ventilation rate validation was fixed and fully airtight with high friction between the wind scoop and chimney, which will prevent it from rotating. Thus, the chimney in the rotary test was slightly lower than the wind scoop to avoid friction and let the model rotate under the wind. This will be addressed in future works by using a different manufacturing technique to further optimize the prototype.

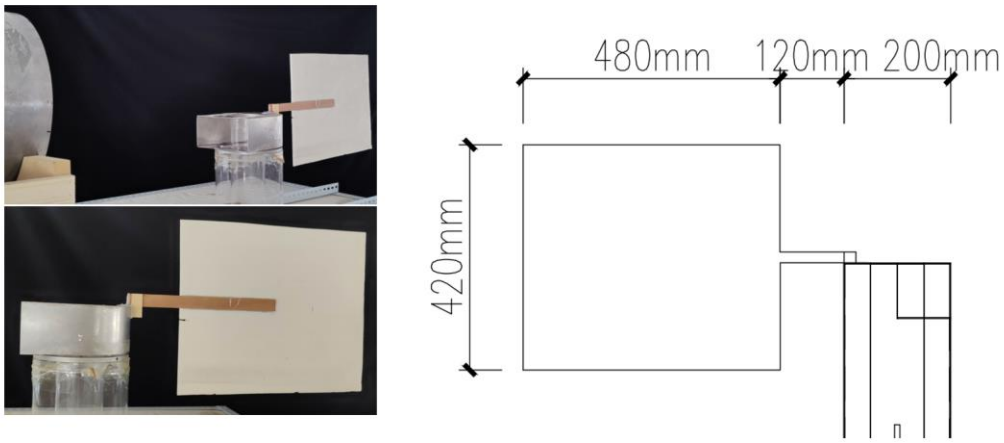


Figure 3.17 Windcatcher prototype model in the open wind tunnel testing

The dimensions of the windcatcher inlet were 10cm in height and 20cm in width determined by the reference value used in a previous research evaluating the ventilation performance of a windcatcher [61]. It should be noted that the current experiment prototype was not a fully airtight rotary windcatcher. Thus, in the research, the experiment model was simplified and adjusted by removing the ring-shaped bearing for the ventilation rate testing and removing the extended chimney for the rotation test. The geometry of this prototype and the components

inside need to be further optimized for both ventilation performance and rotation performance for further application.

## 3.5 Flap fins windcatcher prototype development

Currently, the research about integrating windcatchers and passive cooling or heating technologies to satisfy the thermal comfort, fresh air requirements and low carbon emissions for the building sector is insufficient, and an appropriate windcatcher needs to be developed. The rotary wind scoop can be used for multi-directional ventilation to supply air to the room [30, 124]. However, the high capital and maintenance cost of the rotary components not only limits the size of the natural ventilation but also increases the cost of the natural ventilation. Thus, providing a low-cost substitution for the rotary wind scoop would also benefit natural ventilation applications.

This section aims to develop and evaluate a novel dual-channel windcatcher with inlet openings equipped with flap fins and central stack exhaust for passive or low-energy technology integration with several functions similar to the rotary scoop windcatcher; (1) the airflow direction and ventilation rate inside the system are fixed regardless of wind direction, (2) the supply and return airflow channels are adjacent to allow heat transfer between them for example, for heat recovery, (3) the polluted air from the outlet would not contaminate the supply air, and (4) there will be no air-short circuiting. In this section, the experimental method was applied to evaluate the performance of the flap fins windcatcher and the impact of different parameters were evaluated including thickness, length and layout of the flap fins.

The design strategy is to create a component in the natural ventilation that only allows the air to enter the system in any wind direction without leaving the component. The complexity of the windcatcher needs to be lower than the rotary wind scoop to minimize the maintenance demand.

The flap fin louver windcatcher was designed based on the conventional 8-sided windcatcher, and the flap fins were applied at each opening to control the airflow supply based on the check valve strategy. A circular tube duct located centrally extracts the stale air out to the top of the windcatcher. The flap fin louver windcatcher, as shown in Figure 3.20, uses the pressure

differential at the openings to control the opening and closing of the flap fin automatically. The fins are lightweight, which allows for a self-opening and -closing mechanism. As the wind blows from the windward side, the flap fin on this side will open, allowing the air to enter the windcatcher into the room below. If the pressure outside of the openings were lower than the inside, the pressure difference would force the flap fins to be attached to the windcatcher wall and block the opening, which is slightly smaller than the flap fin, to avoid air leaving the windcatcher. This effectively shuts the flap fins on the leeward side openings of the windcatcher, which are in the negative pressure region. The dynamic process of opening and closing the flap fins at different sides works similarly to a wind scoop without the rotary components, which always have the opening facing the wind. The flap fin design creates a low-cost alternative to the rotary wind scoop and eliminates the rotating mechanism. The base windcatcher is 8-sided to avoid the blockage of the adjacent flap fins, as the flap fins design in the 4-sided windcatcher has poor performance. The open flap fin in the 4-sided windcatcher prototype blocked the adjacent flap fins which limited the open angle on the sides and the ventilation efficiency was also decreased.

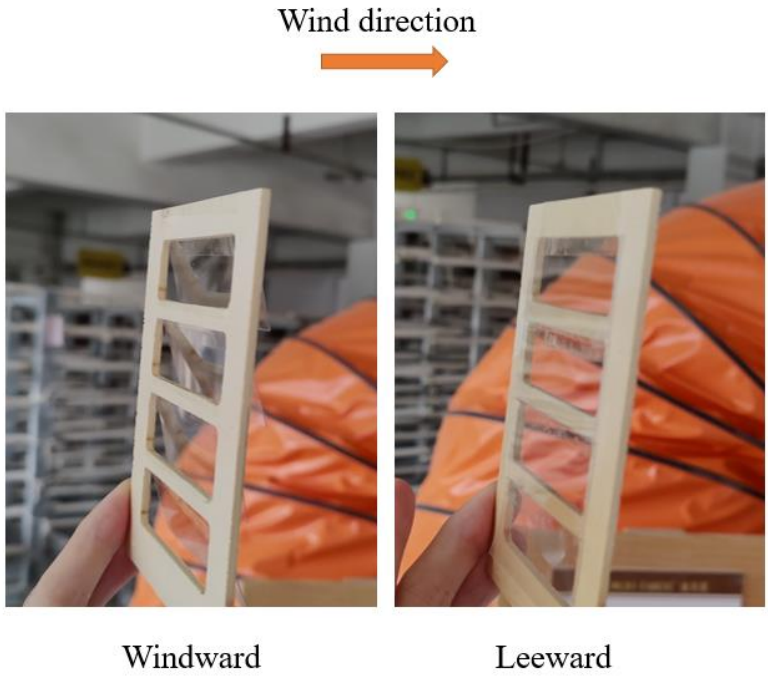


Figure 3.18 Plastic sheet on/off conditions

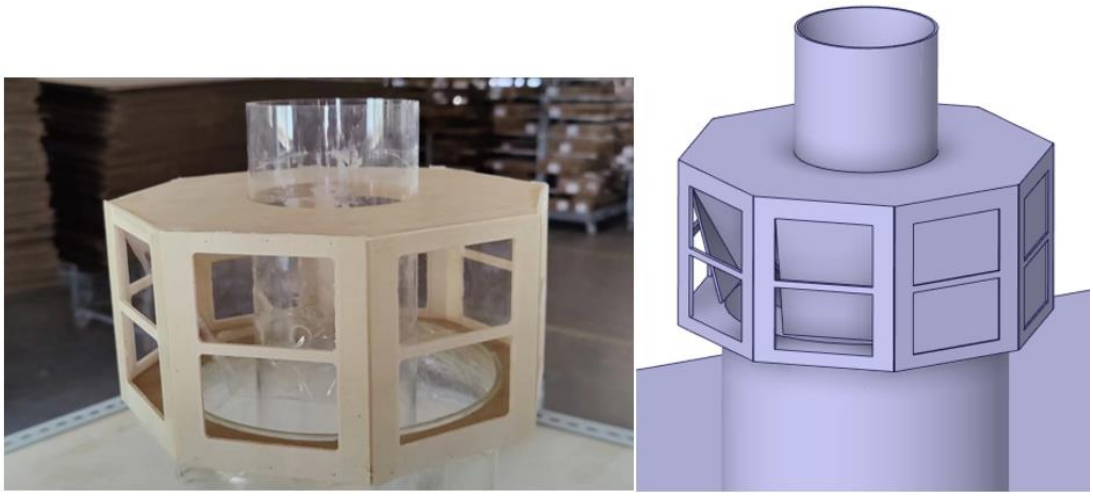

Figure 3.19 Figure Flap fins windcatcher initial prototype photo and SpaceClaim model

The flap fins were connected to the windcatcher frame by an adhesive film. During operation, the flap fins may become in contact with the adjacent fins (depending on the wind direction) and the internal tube; consequently, it will influence the open angle of the fins. The pressure distribution (at 2m/s wind speed) and the open/off condition around the flap fin louver windcatcher at 0º and 22.5º wind direction, obtained from the CFD model, are presented in the result section. It should be noted that when the approach wind is from 0º wind direction, the opening and closing of the flap fins at the oblique windward facade of the windcatcher were not similar in the windcatcher models with single height and double height.

The initial value of the flap fins inlet windcatcher height, 10cm, was determined by the previous research [61] and the initial height was set as a single height. The double height model was 20 cm in height two times the initial model's height. The flap fins were open in the single-height model but closed in the double-height model. While the rest of the flap fins opened/closed similarly.

In the proposed design, the air would always enter the supply channel from the windward side openings without leaving the windcatcher channel on the leeward side as the flap fins will be closed. The stale air is extracted via the central return duct, which works as a chimney and prevents the mixing of the supply and exhaust air channels. With the combination of chimney and flap fin design, the airflow supply and exhaust direction inside the natural ventilation system will be fixed regardless of the wind direction. Hence, the adjacent concentric circular

channels allow for the installation of passive or low-energy technologies.

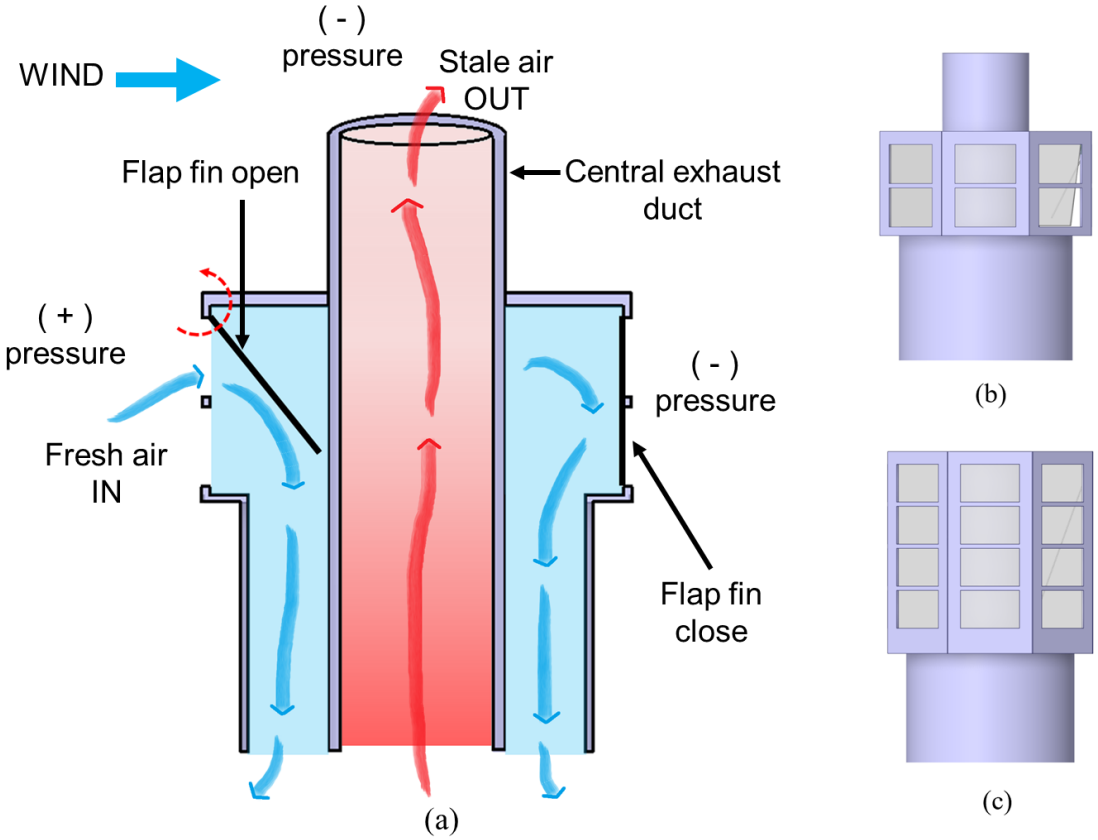


Figure 3.20 Flap fin louver windcatcher concept (a) airflow diagram (b) single height model (c) double height model

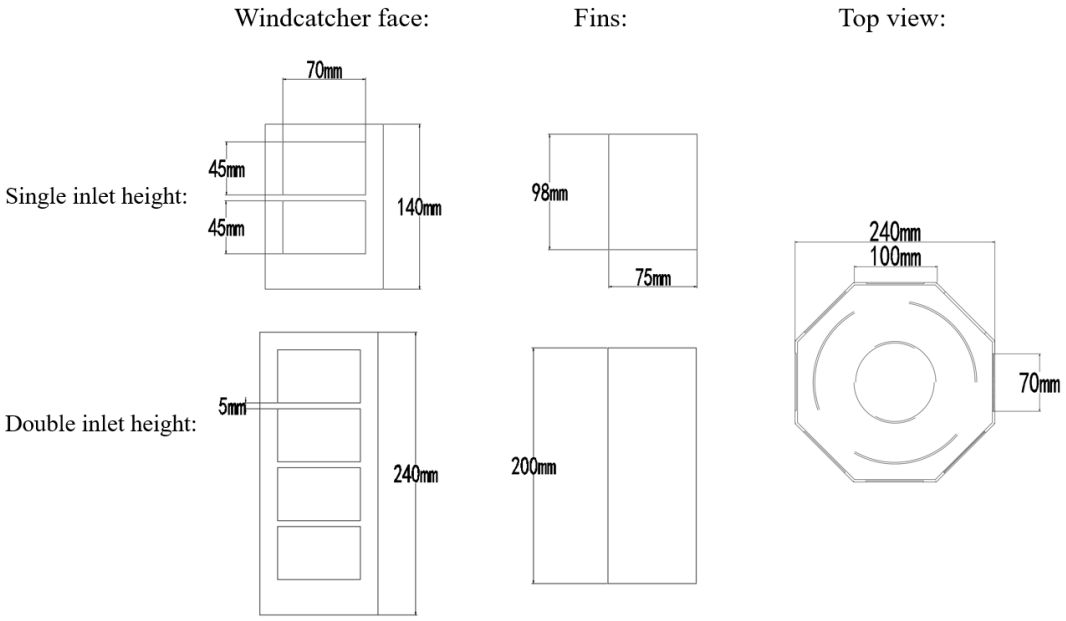


Figure 3.21 Windcatcher schematic and dimensions

The experimental model dimensions are detailed in Figure 3.21 and the rest part of the model was identical to the model used in the rotary scoop windcatcher evaluation, and this has been modelled in full scale in the numerical simulations. The inlet opening area in the double-height model was two times that of the opening area of the single-height model. The internal tube diameter was 100mm, and the external tube was 200mm. It should be noted that the supply and return channel areas were not balanced in the prototype, which would impact the total ventilation rate. This is because of the size of available products and the wind tunnel, which need to be optimized in future research. As the local workshop could manufacture wood products quickly with good accuracy, the windcatcher structure was made of wood, similar to the previous research [25, 53], and the flap fins were made of plastic sheets. The initial design of the proposed system/concept was selected based on the ease of manufacturing and limitations of prototyping equipment. In the experiment testing, the opening angle of the flap fins in the ventilation rate testing was recorded by taking the photo from the side and measuring the photo in the drawing software SpaceClaim.

## 3.6 Experiment measurements

The ventilation efficiency is the key factor of a windcatcher as it directly influences the performance of a windcatcher in improving indoor air quality and providing passive cooling. In the evaluation of windcatchers in this research, measuring the ventilation rate of the windcatcher under different environmental wind speeds and directions is vital for the research. In the experiment section, the speeds of airflow at different points were measured and the data were recorded to validate the simulation model. In the evaluation of the rotary scoop windcatcher and flap fin windcatcher, the wind speed measurement points were identical. The only difference between the two windcatchers was the ventilation rate of the flap fins windcatcher to different environments wind speeds had to be measured twice with the angle of different angles.

The wind measurement points and the wind speeds measured from the experiment and CFD simulation at these three different points in the test room, in the vertical plane in the middle of the model, were measured for the CFD model validation, as shown in Figure 3.22.

Validation point 1 was 1cm above the bottom of the ASCD and 20cm to the centre of the tubes. Validation point 2 was 5cm away from the wall and 55cm above the room's floor. The centre wind speed point was in the middle of the return duct, with a height of 5cm above the top surface of the test room.

As the air leakage of the test room is ignorable compared to the ventilation rate of the windcatcher at all the wind speeds, the return duct is the only channel which allows the air to leave the test room. Thus, the centre wind speed measurement point in the return duct was also used for the ventilation rate evaluation. The ventilation rate can be calculated by the ratio of the centre wind speed to the average wind speed in the return duct and the section area of the return duct.

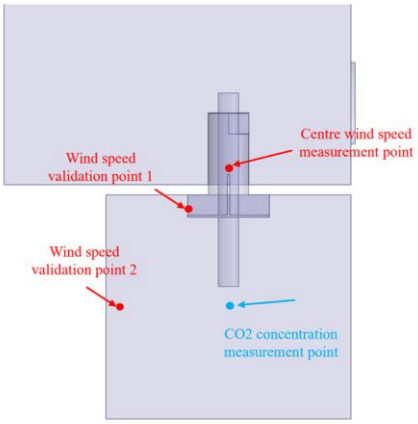


Figure 3.22 Velocity measurement points

The wind speed profiles in the return duct at different environment wind speeds, at the height of the wind speed measurement point for ventilation rate evaluation, were also measured for the simulation model validation and the calculation of the ratio of the centre wind speed to the average wind speed.

In fluid dynamics research, especially in experiments involving mechanical components like fans, measurements can be significantly influenced by transient conditions and instrumental errors. As the environmental wind speeds in the experiments were also measured rather than fixed values controlled by the fans, only one group of measurements was presented in each figure rather than combining data from different measurement groups, even though the trendlines from different measurement groups were identical. However, as the wind speed was not fixed, measuring the error range of each point by multiple tests was inaccurate. Thus, in this

study, the robust measures of scale method were employed to analyze airflow measurements obtained during experiments on fan-induced flows [125]. Given the propensity for power fluctuations in the fan and potential inaccuracies in sensor readings, the robust measures of scale method provided a more stable measure of variability.

Traditional statistical measures, such as the mean and standard deviation, often fail to provide a realistic representation of central tendency and variability under such conditions due to their susceptibility to outliers. In contrast, the robust measures of scale method offers a more resilient approach by focusing on the middle 80% of the data in this research, thereby minimizing the impact of extreme values. By focusing on the central 80% of our data—excluding the top 10% and bottom 10%—the influence of these transient deviations was minimized, which are likely not representative of the typical airflow characteristics being studied. The error bars in the presented figures were derived from the robust measures of scale method of the airflow speed measurements. As a range of 0.01 to 0.1 is a common error value in a physical measurement model, the lower boundary 10% was selected in this research for the error anlysation [126]. The error bars then extended from the first 10% and final 10% of the data for each measurement point, visually encapsulating the central 80% of the data. This method effectively illustrates the range within which the majority of our measurements fell, providing a clear visual indication of the typical variability encountered during the experiments. Utilizing the robust measures of scale method to establish error bars significantly enhanced the clarity and reliability of our findings. This approach not only highlighted the typical range of our data but also underscored the robustness of our experimental results against the backdrop of potential experimental errors. Consequently, the error bars based on the robust measures of scale method offer a transparent depiction of variability, instilling greater confidence in the repeatability and reliability of the observed phenomena.

The sensors were calibrated by Testo with certifications and the calibration results were provided in Table 3.1. As the brand new sensors were used in the measurement, the calibrations from Testo were used instead of calibrating the sensor in every measurement.

Table 3.1 Sensor calibration

| | Reference velocity $8m/s$ | References temperature 24.8℃ |
|---|---|---|

| | Permissible tolerance | Actual value | Permissible tolerance | Actual value |
|---|---|---|---|---|
| Sensor 1 | $\pm 0.7 m/s$ | 8.0m/s | $\pm 0.5$℃ | 24.7℃ |
| Sensor 2 | $\pm 0.7 m/s$ | 8.2m/s | $\pm 0.5$℃ | 24.8℃ |

## 3.7 Field test of the flap fins windcatcher

Even though the ventilation rate of the flap fins windcatcher to the environment wind speed was evaluated under different windcatcher directions, the performance of the flap fins windcatcher needs to be proved in a field test to evaluate the performance under the real conditions with varying wind directions which kept changing all the time. The wind tunnel could only generate wind speed of up to 3m/s which was not large enough to simulate the entire flow region. Thus, an experimental field test was conducted to investigate the performance of the windcatcher under real outdoor conditions.

In the field test, the flap fins louver windcatcher with the same dimension as the wind tunnel experiment was applied in a test room with similar dimensions in the experiment. Two sets of tests were conducted during a typical winter period in the UK. During the tests, the outdoor wind speeds ranged between 0 - 8m/s. The field study was carried out at the Jubilee campus at the University of Nottingham in the UK on a large open field. The outdoor temperature ranged between 16-19℃ in test 1 and 17-21℃ in test 2, and both the outdoor wind direction and speed fluctuated during the test.

The field test model (Figure 3.23), environment wind speed measurement device (Figure 3.24) and location of the model in the university (Figure 3.25) were presented. Measurements of the airflow rate were conducted using the same approach as in the wind tunnel. The measurement point of centre wind speed in the field test was about 35cm above the test room roof. The wind speed at a 1.6m height level, with the same height as the centre of the windcatcher, was measured using the same hot wire anemometer. The outdoor anemometer was about 5m away from the test room model, which could rotate according to the wind. Thus, the wind speed was measured under varying wind directions.

In the field test section, only the flap fins louver windcatcher was tested in outdoor conditions as the flap fins louver windcatcher prototype was able to operate under different wind conditions. The initial rotary scoop windcatcher used for the model validation was fully airtight without the gap for the windcatcher to rotate. The rotary scoop windcatcher model used in the rotary test was not identical to the validation model so the rotary scoop windcatcher prototype was not tested outside in the evaluation.

Figure 3.23 Field test model photo of flap fin inlet windcatcher

Figure 3.24 Environmental wind speed measurement device

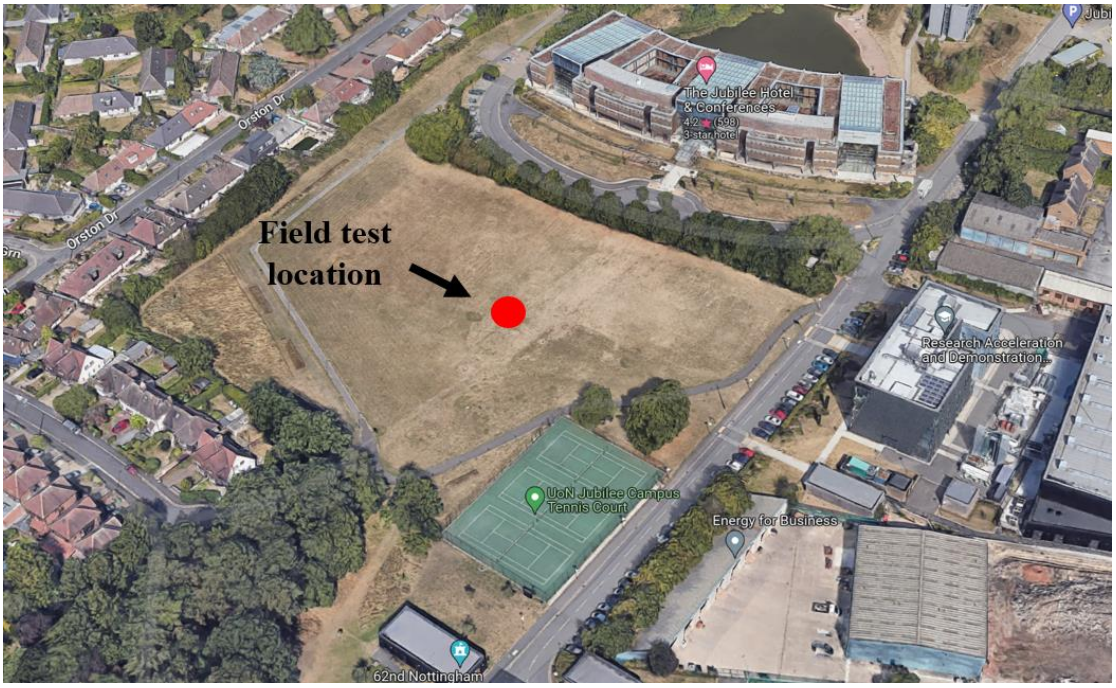


Figure 3.25 Field test location of flap fin inlet windcatcher

## 3.8 Summary

In summary, the experimental setups for the performance evaluation of two windcatcher prototypes were presented. To validate the windcatcher model, the windcatcher prototype and

test conditions were developed in this section. The manufacturing of the wind tunnel was presented in detail including the design to improve the airflow distribution and stability. A specially designed test room simulated real-world conditions, incorporating an Anti-Short-Circuit Device (ASCD) to address airflow direction. In this section, the dimensions and components of the wind tunnel and test rooms in the experiment were presented. In the section on the windcatcher prototype development, the design concept and the components of the rotary scoop windcatcher and flap fins louver windcatcher prototype were presented. The operation principle of the rotary scoop windcatcher and flap fins louver windcatchers were presented in this section and the dimensions of the rotary scoop windcatcher and different flap fins louver windcatchers were explored. The field test model of the flap fins louver windcatcher and measurement device were also explored in this section.

# Chapter 4 Numerical CFD method

## 4.1 Introduction

Computational Fluid Dynamics (CFD) is a cost-effective numerical technique and algorithm to execute and scrutinize an extensive volume of data pertinent to fluid dynamics. The precipitous advancement in CFD and computational technology has paved the way for its burgeoning application in aerodynamic design, augmenting conventional methodologies like wind tunnel experimentation. CFD furnishes a deeper comprehension of flow configurations that are challenging, costly, or implausible to investigate by employing experimental procedures. The CFD analysis has been deemed more beneficial compared to wind tunnel assessments for the exploration of specific attributes of wind tower systems, including phenomena such as flow short-circuiting and recirculation, vortex regions, as well as supply and extract segments. The parametric analysis and model optimizations in the CFD simulation are more convenient than the wind tunnel experiments as the control of model geometry and environmental variables in CFD simulation is more cost-effective and time-saving than manufacturing new experiment models.

In this section, the CFD theory including the algorithms and calculation model for the CFD simulation were presented. The modelling and meshing of each simulation model and domain with the mesh independence analysis were also presented. The simulation setups of different validation models of the rotary scoop windcatcher and flap fins louver windcatcher were also conducted, and the visualizations of simulation results were provided. The parametric analysis of the validated models for higher ventilation efficiency was also investigated in the research. The ventilation performance comparisons of the traditional conventional windcatcher to the rotary scoop windcatcher and the flap fins louver windcatcher were also discussed in this chapter.

The primary objectives of CFD modelling in this study include: (1) validating the windcatcher design through simulation against empirical data to ensure reliability, (2) conducting parametric analyses to understand the influence of design variables on system performance, and (3)

optimizing the windcatcher configurations to maximize airflow and thermal comfort while minimizing energy consumption. These objectives are systematically approached through detailed CFD simulations, providing a comprehensive understanding of the airflow patterns, pressure distributions, and thermal behaviours within the modelled windcatcher systems. By integrating CFD insights, this research contributes to the development of more effective natural ventilation solutions, aligning with sustainable building practices.

## 4.2 CFD theory

The commercial software FLUENT was used for the airflow simulation. The mass and momentum equations are solved for the airflow in this model. The Reynolds-averaged Navier-Stokes (RANS) model was employed with the k-epsilon, re-normalization group (RNG), turbulence model, which is capable of performing accurate simulations of airflow in similar natural ventilation systems, as highlighted in the literature including [127]. The SIMPLE algorithm was applied in the simulations [128]. In turbulent airflow simulations, the semi-implicit method is typically used, and a solver using pressure-linked equations segregated pressure-based algorithm is applied due to its robustness and computational efficiency. A second-order upwind scheme is employed to discretize all the transport equations. The governing equations for the mass (Equation (4.1)), momentum (Equation (4.2)), and k and epsilon (Equation (4.3) and (4.4)) [129] were detailed below:

$$\frac{\partial \rho}{\partial t} + \nabla \cdot (\rho u) = 0 \tag{4.1}$$

where u refers to the fluid velocity vector, t is time, and ρ is density.

$$\frac{\partial \rho}{\partial t} + \nabla \cdot (\rho u \nabla u) = -\nabla p + \rho g + \nabla \cdot (u \nabla u) - \nabla \cdot \tau_t \tag{4.2}$$

where g is a vector of gravitational acceleration, p is the pressure, $\tau_t$ is the stress tensor associated with the turbulence stresses, and μ is dynamic molecular viscosity.

$$\frac{\partial (\rho k)}{\partial t} + \nabla \cdot (\rho u k) = \nabla \cdot \left[ \left( \mu + \frac{\mu_t}{\sigma_k} \right) \nabla k \right] + P_k - \rho \varepsilon$$

$$\frac{\partial (\rho \varepsilon)}{\partial t} + \nabla \cdot (\rho u \varepsilon) = \nabla \cdot \left[ \left( \mu + \frac{\mu_t}{\sigma_\varepsilon} \right) \nabla \varepsilon \right] + \frac{C_{1\varepsilon} P_k}{k} \varepsilon - C_{2\varepsilon} \rho \frac{\varepsilon^2}{k} \tag{4.4}$$

where μ is molecular viscosity, $\mu_t$ is the turbulent viscosity, $\sigma_k$ and $\sigma_\varepsilon$ are turbulence model constants, $P_k$ is the turbulent production of kinetic energy, $C_{1\varepsilon}$ and $C_{2\varepsilon}$ are empirical constants.

The validation CFD model was based on the open wind tunnel experiment and the CFD settings are detailed in Table 2.2. The inlet wind speed and profile were based on the open wind tunnel experiment. The pressure outlet was set to atmospheric or 0 Pa. Default values were set for the turbulence kinetic energy. As the experiment measurement device is limited, measuring the turbulence intensity in the test was challenging and inaccurate. Thus, the default turbulence intensity, 5%, in Fluent was used in the simulation, which is a limitation of the simulaton work. . The convergence criteria were set based on the values in Table 4.1.

Table 4.1 CFD settings and boundary conditions

| **Term** | **Value and settings** |
|---|---|
| *Inlet* | |
| Velocity (m/s) | 0-3 (wind profile based on the wind tunnel) |
| | 1-7 (uniform wind condition) |
| Initial Gauge Pressure (Pa) | 0 |
| Turbulence Model | K-epsilon RNG |
| Turbulence intensities | Default value 5% |
| *Outlet* | |
| Gauge Pressure (Pa) | 0 (atmospheric) |
| *Wall (domain and windcatcher)* | |
| Shear Condition | No slip |
| Roughness Model | Standard |
| Roughness Height | 0 |
| Roughness Constant | 0.5 |
| *Converged residuals* | |
| Continuity / k / Epsilon | 0.001 |
| X/Y/Z velocity | 0.0001 |

## 4.3 CFD modelling and meshing of rotary scoop windcatcher

This section aims to develop and evaluate the rotary scoop windcatcher design in the CFD method. Several objectives of this research are achieved, including developing the CFD windcatcher model according to the prototype in the experiment validating the CFD model with the experiment results, evaluating the performance of the proposed windcatcher and comparing its performance against current commercial systems and building regulations.

### 4.3.1 CFD Modelling

The model was created by the 3D modelling software SpaceClaim in the Ansys Workbench. The solid model of the rotary scoop windcatcher and the test room for experiment model validation are presented in Figure 4.1 based on the dimension of the scaled experiment model. The volume of fluid for rotary scoop windcatcher CFD simulation was created using the solid geometry and half of the simulation zone was presented in Figure 4.2. The fluid domain of the rotary scoop windcatcher validation model was separated into the environment part and the room part so the ventilation rate could be evaluated by the amount of air passing through the interface between the environment and the room.

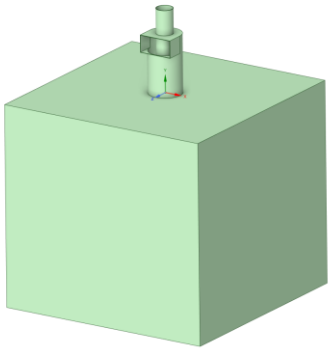

Figure 4.1 Solid SpaceClaim model of the rotary scoop windcatcher and test room

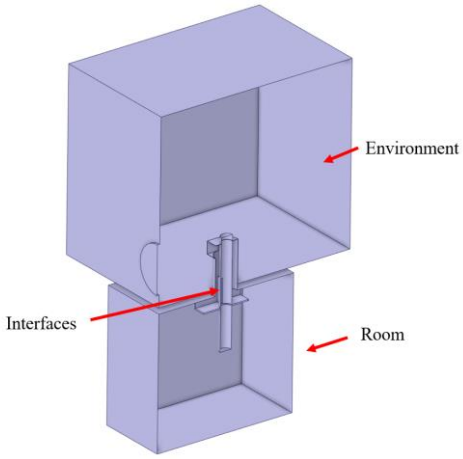


Figure 4.2 Fluid simulation domain in the Validation (half)

In the CFD validation model in Figure 4.2, the full wind tunnel geometry was not included in the simulation, and instead, a circular inlet was modelled to simulate the outlet of the open wind tunnel. Only the region around the windcatcher and inside the room was simulated in the CFD model to simplify the simulation. The inlet wind speed profile measured from the experiment was applied in the simulation first to validate the CFD simulation model. The wind speed functions at each average wind speed for rotary scoop windcatcher validation are presented in Table 4.2. After validating the simulation model, the uniform inlet wind speed was applied to the entire rectangular area in the full-scale simulation to evaluate the ventilation performance of the windcatcher. As the scaled model was designed for the experiment in a wind tunnel with limited space, the dimension of the experiment model is insufficient to provide a fresh air supply for a large room in practice. Thus, the scaled model was modified by increasing the dimensions of the validation model. The size of the full-scale model was determined by a previous windcatcher research, which was about 0.5m wide [39]. The dimensions of the scaled model and the full-scale model are presented in Figure 4.3. The extended return duct was removed in the full-scale model as it's designed for the experimental measurement but may slightly decrease the ventilation performance.

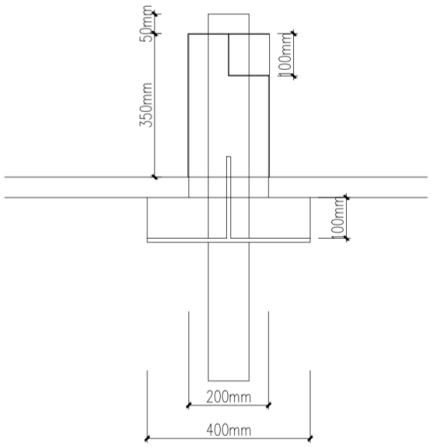


(a) Scaled model

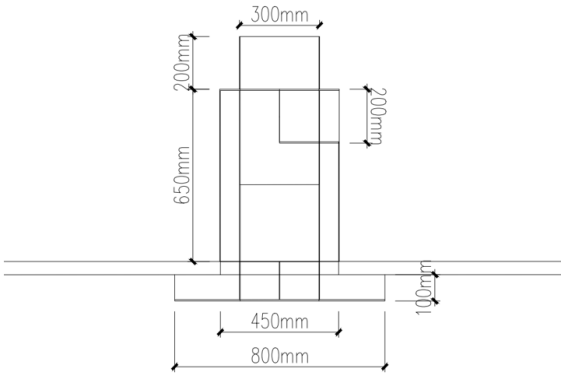


(b) Full-scale model

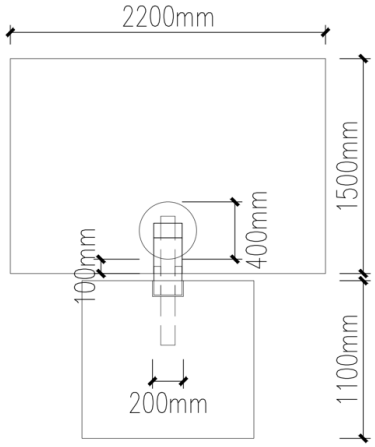


(c) Scaled model simulation domain

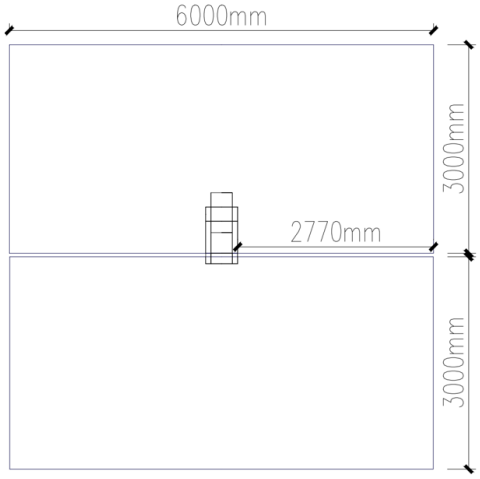


(b) Full-scale model simulation domain

Figure 4.3 Dimensions of the scaled (validation), full-scale windcatcher and simulation domain

Table 4.2 Wind speed functions for rotary scoop windcatcher validation

| Average wind speed (m/s) | Wind speed profile function (m/s) |
|---|---|
| 2.31 | $v = -48.2 \times r^2 + 7.7 \times r + 2.33$ |
| 2.10 | $v = -42.8 \times r^2 + 6.3 \times r + 2.27$ |
| 1.90 | $v = -16.4 \times r^2 + 2.2 \times r + 1.98$ |
| 1.68 | $v = -27.2 \times r^2 + 3.8 \times r + 1.79$ |
| 1.40 | $v = -17.4 \times r^2 + 1.7 \times r + 1.53$ |
| 1.03 | $v = -14.1 \times r^2 + 1.8 \times r + 1.07$ |
| 0.79 | $v = -8.2 \times r^2 + 1.2 \times r + 0.81$ |

| | |
|---|---|
| 0.48 | $v = -6.5 \times r^2 + 0.9 \times r + 0.49$ |

### 4.3.2 Meshing and mesh independence analysis

In CFD simulation, a mesh is a collection of small, non-overlapping elements that divide the geometric domain of the problem into a discrete grid. This meshing process is a critical step in the numerical approximation methods used to solve the governing equations of fluid dynamics. For the complex geometry of a windcatcher with different cylindrical tubes and rectangular components, applying the structure mesh was not effective and most of the current CFD solvers can calculate the unstructured mesh with a high accuracy and speed. The unstructured mesh was applied in the meshing stage.

The meshing element size of the flow region was 0.008m, and the face sizing on the windcatcher surface was 0.004m in the fine mesh. The final mesh node number was 4.22 million, and the elements were 2.48 million. For the mesh sensitivity analysis, three mesh sizes were generated and simulated. The ventilation rates of the windcatcher with different mesh sizes to environment wind speed were presented in Figure 4.4. The mesh node numbers of 0.22 million, 0.88 million and 4.22 million had almost no impact on the ventilation rate of the windcatcher and the relationship between the ventilation rate and the environmental wind speed. The difference between the three mesh sizes was ignorable for the ventilation efficiency evaluation, with an average difference of 2.97% to the model with 4.22 million mesh elements. The $R^2$ values of the results for all the mesh sizes were higher than 0.999 and the trendlines of all the mesh quality was almost the same. In the first data point with a low ventilation rate, a small difference would result in a large error percentage. Excluding the first data point, most of the data points achieved a low difference within 2%. Thus, in the ventilation rate evaluation, the CFD model can be treated as a mesh-independent model in this research.

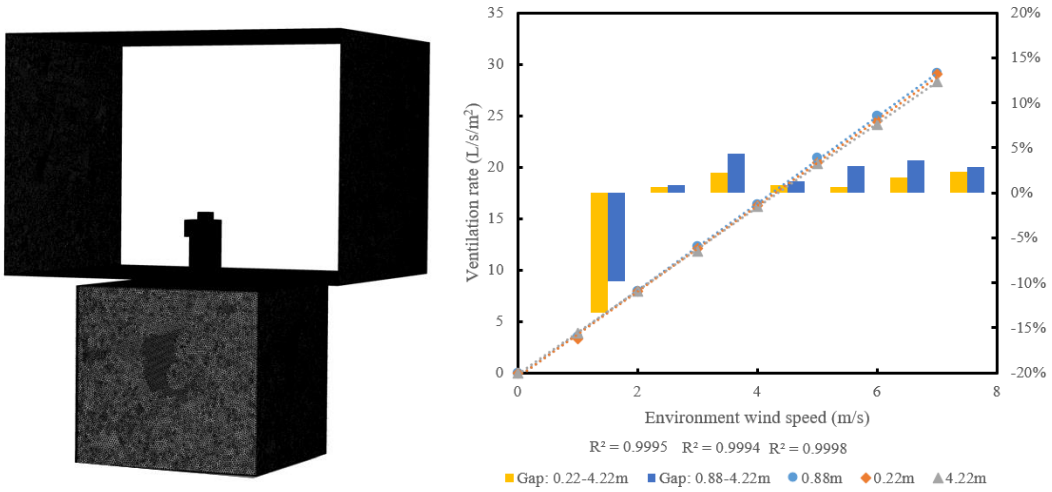


Figure 4.4 The surface mesh around the windcatcher and room model, and mesh independence analysis results

## 4.4 CFD modelling and meshing of flap fins windcatcher

### 4.4.1 CFD Modelling

The modelling process of the flap fins windcatcher is identical to the modelling process of the rotary scoop windcatcher. However, the opening angle of each flap fin in the flap fins windcatcher is not identical under different environmental wind speeds and using dynamic mesh to simulate the angle of fins was challenging for a complex model. Thus, the opening angle of the fins under different wind speeds was measured in the experiment and applied in each model with different environment wind speeds. The opening angles in the validation simulation are shown in Table 4.3 and Table 4.4.

Table 4.3 Wind speed profile of test about double height single fin model (0.1mm fins/0.91g per fin), wind from face direction (0° wind)

| Average wind speed (m/s) | Front fin open-angle (°) | Wind speed profile function (m/s) |
|---|---|---|
| 2.50 | 21 | $v = -35.79 \times r^2 + 5.41 \times r + 2.49$ |
| 2.21 | 20.6 | $v = -21.44 \times r^2 + 2.87 \times r + 2.24$ |
| 1.80 | 18.4 | $v = -18.31 \times r^2 + 2.03 \times r + 1.88$ |

| | | |
|---|---|---|
| 1.64 | 17.5 | $v = -24.99 \times r^2 + 4.1 \times r + 1.60$ |
| 1.34 | 14.5 | $v = -15.16 \times r^2 + 1.23 \times r + 1.47$ |
| 1.10 | 10.8 | $v = -10.28 \times r^2 + 0.94 \times r + 1.17$ |
| 0.81 | 8.1 | $v = -1.33 \times r^2 - 10.2 \times r + 0.96$ |
| 0.61 | 6.7 | $v = -0.14 \times r^2 - 0.97 \times r + 0.73$ |

Table 4.4 Wind speed profile of test about double height single fin model (0.1mm fins/0.91g per fin), wind from edge direction (22.5° wind)

| Average wind speed (m/s) | Fin open angle 1 (°) | Fin open angle 2 (°) | Wind speed profile function (m/s) |
|---|---|---|---|
| 2.34 | 12 | 13 | $v = -43.02 \times r^2 + 6.50 \times r + 2.40$ |
| 2.03 | 10 | 12 | $v = -38.37 \times r^2 + 6.36 \times r + 2.05$ |
| 1.81 | 9 | 11 | $v = -14.79 \times r^2 + 0.52 \times r + 2.06$ |
| 1.63 | 8 | 10 | $v = -19.25 \times r^2 + 1.55 \times r + 1.83$ |
| 1.39 | 7 | 9 | $v = -14.75 \times r^2 + 1.25 \times r + 1.56$ |
| 1.06 | 6 | 8 | $v = -9.54 \times r^2 + 0.04 \times r + 1.24$ |
| 0.80 | 5 | 7 | $v = -12.34 \times r^2 + 1.55 \times r + 0.84$ |
| 0.60 | 4. | 6 | $v = -3.85 \times r^2 + 0.07 \times r + 0.67$ |

The volume of fluid for flap fin inlet windcatcher CFD simulation was created using the solid geometry and half of the simulation zone was presented in Figure 4.5. The fluid domain was also separated into the environment part and the room part and the dimensions of the simulation domain were presented in Figure 4.6.

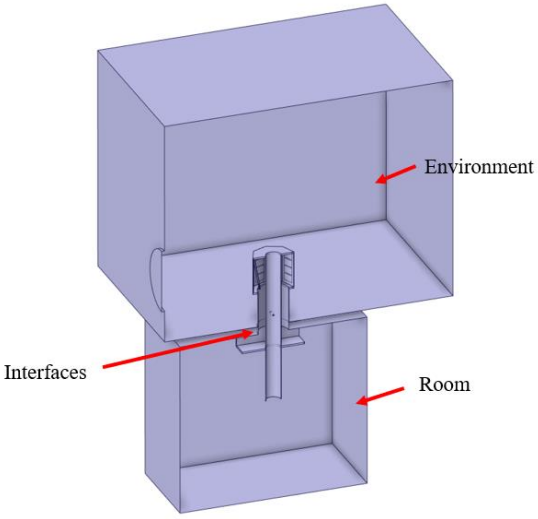


Figure 4.5 Fluid domain of the flap fin windcatcher simulation

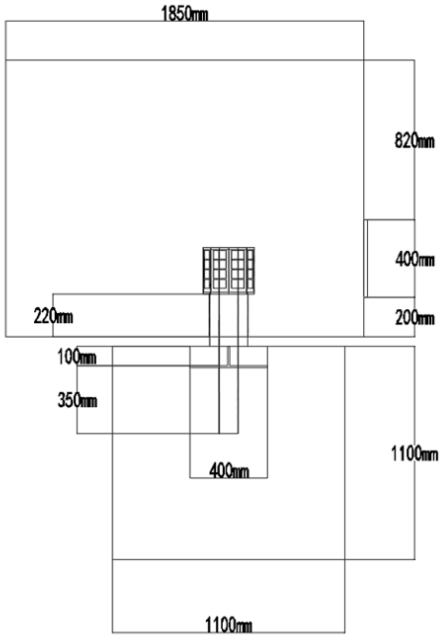


Figure 4.6 Dimensions of the fluid domain of the flap fin windcatcher simulation

### 4.4.2 Meshing and mesh independence analysis

In the CFD simulation model, the full wind tunnel geometry was not included in the simulation, and instead, a circular inlet was modelled to simulate the outlet of the open wind tunnel. Only the region around the windcatcher and inside the room was simulated in the CFD model to simplify the simulation. By using the wind speed profile at the outlet of the open wind tunnel measured from the experiment, the inlet wind speed profile was applied in the simulation first

to validate the CFD simulation model.

The mesh of the flap fin inlet windcatcher simulation is shown in Figure 4.7. The element numbers of the fine, medium and coarse mesh in the independence analysis were 3.2 million, 1.2 million and 0.3 million, respectively. The double height with single fin model was selected for the mesh independence analysis, and the results are shown in Figure 4.8. The ventilation rates predicted by the model with different mesh sizes were compared for the mesh independence analysis to support the model verification.

In the model with different mesh qualities, most of the results in the model with different mesh qualities were identical and the trend lines of the ventilation rate to the outdoor wind speed matched well. However, an error at a wind speed of about 2.2m/s occurred and the difference between the coarse and fine mesh reached 0.5L/s. After excluding this error point, the trendlines of models with three mesh qualities were identical. Although the $R^2$ values of the simulation results achieved from the three mesh qualities were not identical, all the $R^2$ values were higher than 0.98, which provided a linear relationship between wind speed and ventilation rate. Thus, for the ventilation rate evaluation in this research, the simulation model was not perfectly independent of the mesh quality but the model with fine mesh had a sufficient quality for the model validation. The fine mesh quality with about 3.2 million mesh elements, in Figure 4.7, was selected for the final simulation validation, with the highest $R^2$ value in the research and the closed result to the experiment measurements.

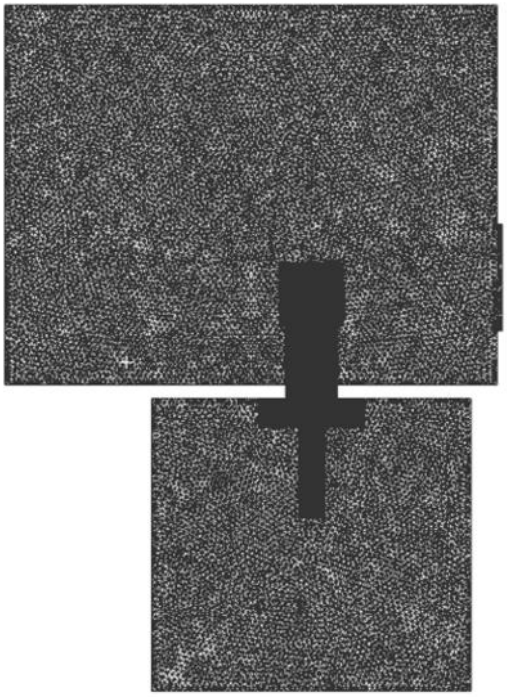

Figure 4.7 Mesh of the simulation model of the flap fins windcatcher

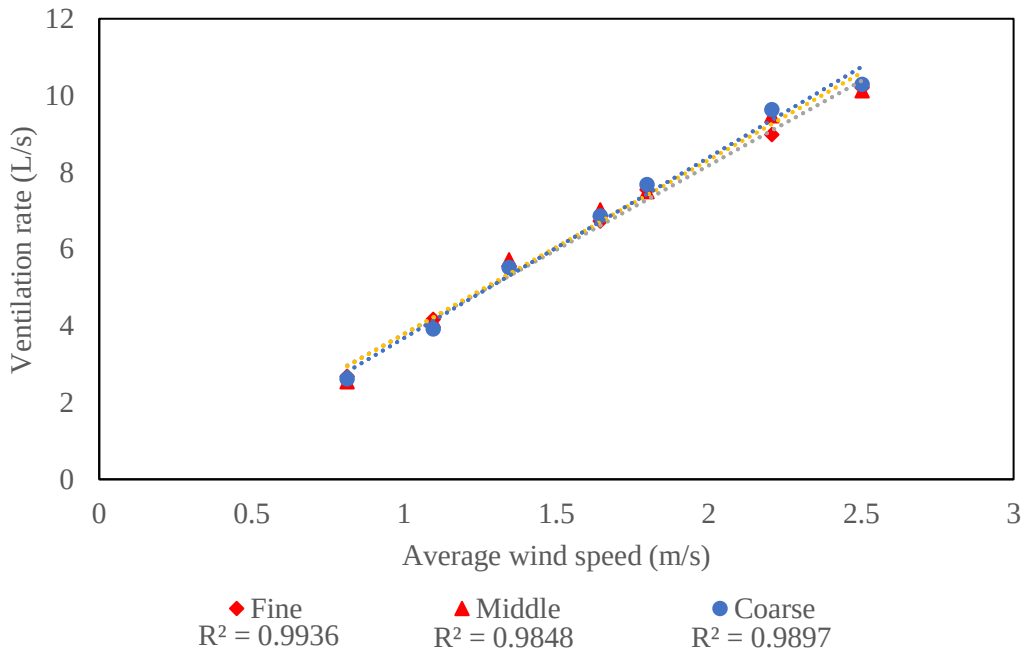


Figure 4.8 Mesh independence analysis result of the flap fins windcatcher

## 4.5 CFD parametric analysis

To address the challenges posed by unstable windcatcher performance under varying wind directions and the limitations of passive technologies in conventional windcatchers, a novel dual-channel windcatcher is proposed to provide wind-driven natural ventilation, which is independent of the wind direction and suitable for passive technology integrations [130]. As shown in Figure 4.9, the dual-channel windcatcher was developed to facilitate the intake and extraction of air within a room. It includes two concentric ducts with the outer duct incorporating a rotary wind scoop with a central aperture through which the return duct passes. A vertical tail fin positioned at the back generates torque to rotate the wind scoop, ensuring the fin aligns with the incoming wind. Consequently, the outer duct consistently serves as the supply duct, benefiting from the positive pressure generated by the wind scoop, enabling seamless integration with passive technologies. Simultaneously, the central chimney extracts stale air from the building, designating the inner duct as the constant return duct.

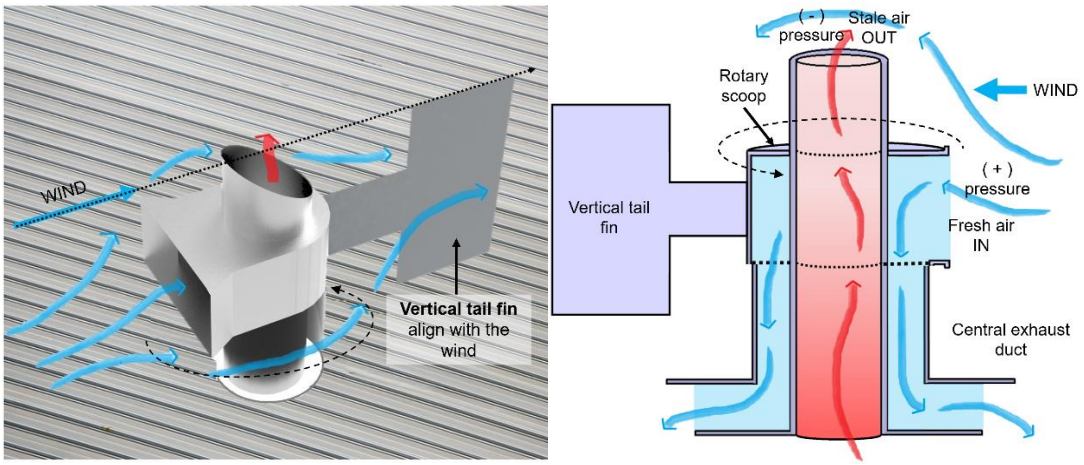


Figure 4.9 Proposed rotary scoop windcatcher with dual channels for supply and exhaust streams.

This section aims to improve the ventilation performance of the proposed system by implementing diverse strategies to optimize the pressure differential between the inlet and outlet, thereby enabling the system to operate effectively even under low wind speed conditions. Achieving a higher ventilation rate is crucial, particularly when integrating additional technologies that may introduce a pressure drop and reduce the airflow rate. The parametric

analysis will focus on attaining this objective without increasing the size of the windcatcher, while simultaneously enhancing ventilation efficiency and meeting the required ventilation demand within a smaller footprint. To accomplish this, the work will consider various design scenarios and operating conditions, employing a CFD approach validated through experimental validation. This combined approach will expedite the research process and facilitate the identification of an optimized solution.

Parametric analysis in the evaluation of a windcatcher involves systematically altering and studying the effects of various design parameters on the performance of the windcatcher. It provides a quantitative way to understand how different design choices impact the windcatcher's ability to provide natural ventilation. Conducting a parametric analysis of the proposed rotary dual-channel windcatcher is imperative to refine the design. The parametric analysis will encompass several key aspects, as presented in Figure 4.10: (1) adjusting the diameter of the internal tube to achieve varying supply-to-return channel area ratios; (2) Implementing wing walls at the wind scoop inlet to generate a higher positive pressure; (3) modifying the height of the wind scoop inlet to optimize its performance; (4) chamfering the back of the chimney to create a wind cowl that facilitates increased air extraction; (5) adjusting the height of the anti-short circuit device (ASCD) within the room to further enhance airflow patterns; (6) modifying the height of the windcatcher tube and evaluating the influence of windcatcher height through comprehensive full-scale simulations.

The optimized parameters obtained from these analyses will be integrated into an optimized windcatcher model. Subsequently, the ventilation performance of this optimized model will be compared to that of a conventional four-sided windcatcher, serving as a benchmark for evaluation.

The flow diagram of the parametric analysis section, depicted in Figure 4.10, outlines the sequential progression of our study. To ensure the accuracy and reliability of our findings, we conducted an experimental validation of the Computational Fluid Dynamics (CFD) simulation model. The full-scale model served as the foundational model for the subsequent parametric analysis and optimization within the CFD simulation framework.

The optimized parameters, comprising the wind scoop's inlet area, wing wall dimensions and

orientation, supply-to-return area ratio, and the chamfered chimney, were implemented in the final optimized model. This model was then utilized to compare the performance of the windcatcher to that of a conventional four-sided windcatcher and the initial prototype. By conducting this comprehensive evaluation, we can ascertain the improvements achieved through our optimization process and better understand the advantages of the proposed design over existing windcatcher configurations.

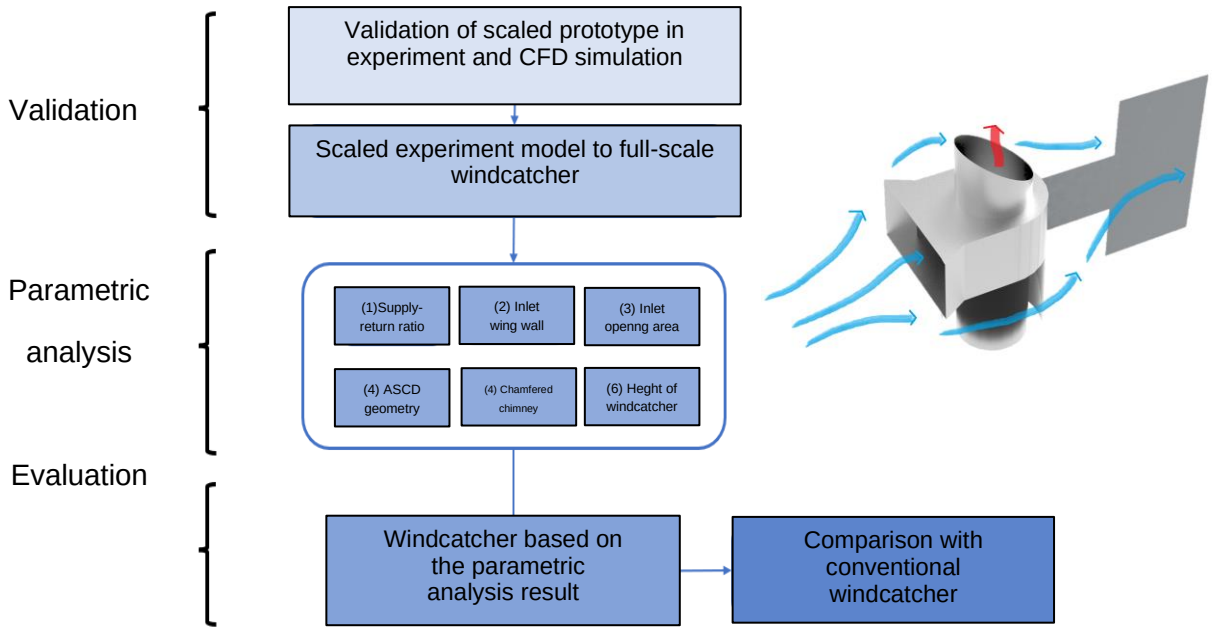


Figure 4.10 Research Process for the parametric analysis of the proposed rotary windcatcher

### 4.5.1 Dual-channel rotary scoop windcatcher for parametric analysis

The dual-channel rotary wind scoop windcatcher evaluated in this study is shown in Figure 4.11. It included the following major components: including a rotary component with a scoop inlet, a cowl outlet and a tailplane, the bearing and connection beam and the windcatcher foundation [28]. Unlike the initial design, the present windcatcher device incorporates a chamfered edge on the back side of the central chimney and wing walls at the entrance of the wind scoop to enhance the ventilation performance. The central chimney in the present design is also separated between the upper wind scoop and the lower section. This will combine the chimney outlet and wind scoop into a single component, replacing the initial prototype's ring-shaped bearing with a cost-effective bar-bearing design, reducing friction. As a result, the

torque required to rotate the wind scoop and the size of the tailplane will be minimized. However, it should be noted that this aspect is not evaluated in the numerical modelling.

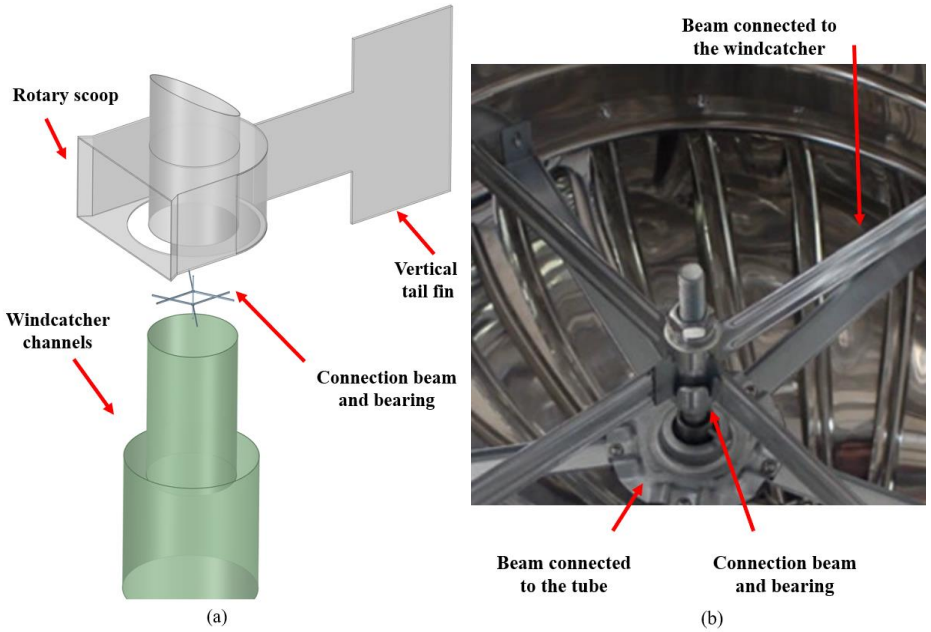


Figure 4.11 Diagram of the proposed dual-channel rotary scoop windcatcher (a) Components of the windcatcher, (b) beams and bearing connecting the windcatcher and concentric ducts.

Preventing down draught in a chimney is necessary for the ventilation system design to ensure the polluted air can be extracted from the chimney [30]. Figure 4.9 illustrates the airflow directions within the windcatcher, where two concentric circular tubes create two distinct channels. With this dual-channel ductwork configuration and the presence of the rotary scoop, the external channel consistently functions as the supply channel, while the internal channel consistently serves as the return channel, irrespective of changes in wind direction. This setup facilitates a stable airflow, essential for seamless integration with passive technologies like passive heat recovery or cooling devices. The rotary component and windcatcher foundation can be manufactured from stainless steel or transparent plastic, while the beams are typically made of stainless steel. This choice of materials ensures structural durability and efficiency within the windcatcher system.

The dimensions of the final models before and after the parametric analysis are shown in Figure 4.12.

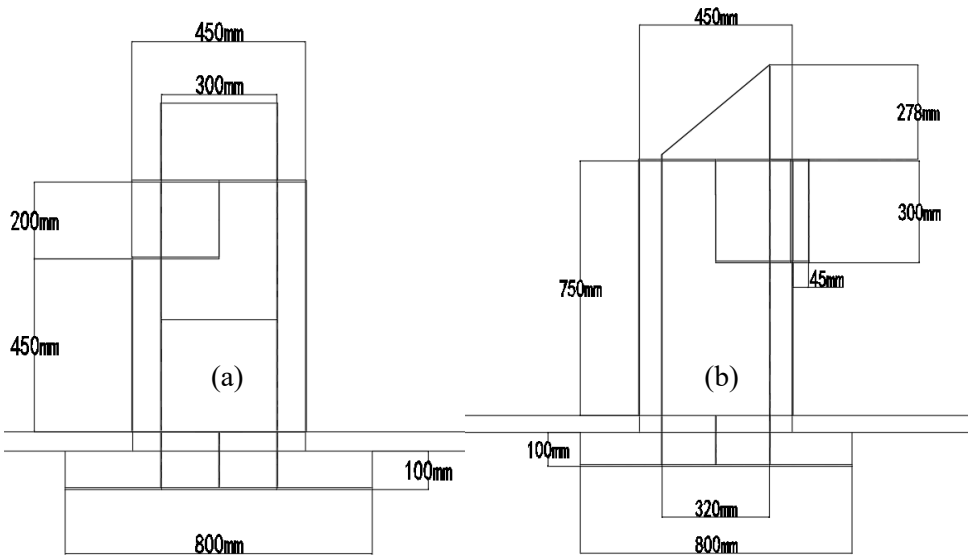


Figure 4.12 Dimension of the full-scale model of the (a) initial and (b) final rotary scoop windcatcher.

### 4.5.2 CFD modelling and grid verification

Conducting experimental tests on windcatcher designs with various parameters is impractical due to the associated costs and time constraints. As a result, employing CFD methods is more effective in parametric analysis research [131]. In this research, the commercial CFD software FLUENT was used to carry out the simulations of the windcatcher modifications.

The validation experiments were conducted under controlled conditions with a consistent environmental temperature and low wind speed. Therefore, assumptions were made that temperature variations would not occur within the CFD simulations. Our research primarily focused on airflow and ventilation performance within the windcatcher, consequently, we solely solved the mass and momentum equations to examine these aspects. The governing energy equation was excluded to simplify the process, as it did not apply to heat transfer or internal heat sources within the building.

The Reynolds-averaged Navier-Stokes, k-epsilon RNG equations and semi-implicit method for The mesh independence analysis of the optimized model is shown in Figure 4.13 with different mesh sizes including coarse (2.6 million element number), medium (6 million element number) and fine (11 million element number). As the research focuses on the ventilation performance of the windcatcher, the ventilation rate of the model with different mesh sizes was simulated

and compared. As observed, all the models achieved identical simulation results. The model with a medium mesh size was selected for the simulations.

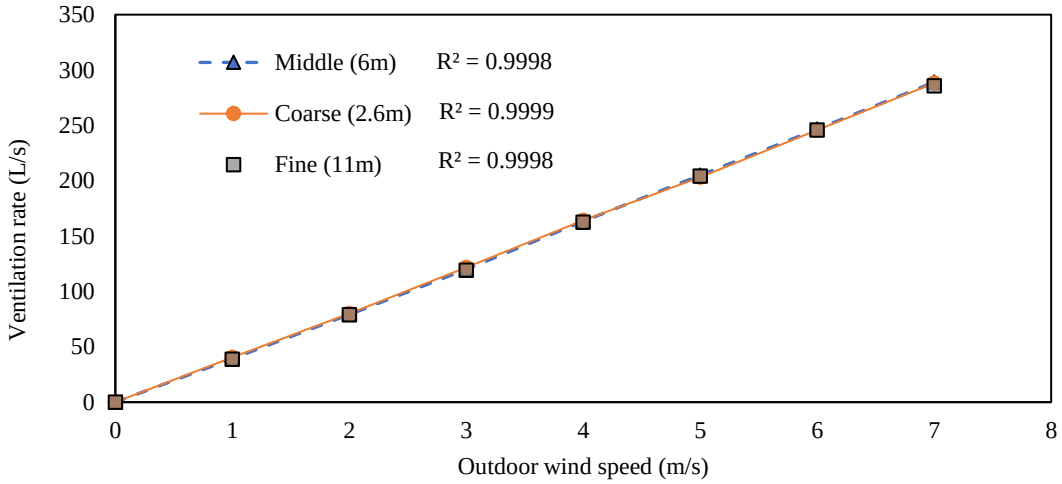


Figure 4.13 Mesh independence analysis

### 4.5.3 Proposed windcatcher parametric analysis

To enhance the ventilation rate, this research focused on parametric analysis by adjusting various factors. However, the evaluation did not involve assessing the ventilation performances of windcatchers with different cross-section areas [132]. Instead, the modifications were tested using models with identical cross-section areas. The adjustments included modifying the supply-to-return channel area ratio, incorporating wing walls with varying angles and lengths at the wind scoop inlet, adjusting the height of the wind scoop inlet, chamfering the back of the chimney at different angles, modifying the height of the ASCD within the room, and evaluating the impact of windcatcher height through ABL wind simulations. These modifications aimed to identify the most effective design parameters for enhancing the ventilation rate and improving the overall performance of the windcatcher system.

*5.5.3.1 Supply-to-return channel area ratio*

The turbulent airflow in the ventilation duct was affected by the Reynolds number in the duct and the roughness of the surface [133]. The area and shape of the channels would affect the hydraulic diameter of the system which would affect the turbulence and the Reynolds' number in the duct. The Fanning friction factor f can be used for the turbulent flow calculation [134,

135] which was increased by the increase of Reynolds' number. Thus, adjusting the shape and area of the supply and return channels to achieve a lower hydraulic diameter was necessary to decrease the Reynolds number and the system friction. In this research, the lower system friction was achieved by adjusting the diameter ratio of supply and return channels for a minimized overall system friction rather than decreasing the friction in a single channel. The diameter of the internal tube was adjusted up to 450mm to evaluate the ventilation performance with a different supply-to-return ratio.

$$\mathrm{Re} = \frac{\rho u D}{\mu} \tag{4.5}$$

where $\mathrm{Re}$ is the Reynolds' number of the system; $u$ is the velocity of airflow in the system in m/s; $D$ is the hydraulic diameter in m; $\rho$ is the density of the liquid in kg/m$^3$; $\mu$ is the viscosity of the liquid in Pa*s.

*4.5.3.2 Wing walls at the inlet*

The implementation of wing walls has been recognized as an effective natural ventilation device for enhancing the performance of single-side ventilation [136]. Adding a wing wall could provide a sharp edge at the inlet, which increases pressure, thereby improving ventilation performance [61, 137]. By adding the wing walls to the rotary wind scoop components, the inlet area can also be increased to capture more airflow to further improve the ventilation performance. Thus, wing walls with different angles, from 0° to 90°, and lengths, from 50mm to 200mm, at the wind scoop inlet were investigated as shown in Figure 4.14 (a).

*4.5.3.3 Wind Scoop Inlet Height*

Increasing the area of the windcatcher opening is a highly effective approach for enhancing airflow within a windcatcher. However, it is important to note that the benefits of increasing the opening area become limited once it reaches an excessively high level. In light of this, the present study investigated an alternative avenue for improving the ventilation rate by adjusting the height of the wind scoop inlet. This investigation sought to determine whether increasing the height of the wind scoop proved to be a cost-effective method for enhancing the ventilation rate. The range of wind scoop heights examined spanned from 0mm to 500mm, as depicted in Figure 8 (b). By analyzing the impact of varying wind scoop heights, this research aimed to identify an optimal height that would yield the desired improvements in ventilation rate while

considering practicality and cost-effectiveness.

*4.5.3.4 Chamfering the back of the chimney*

Chimneys play a crucial role in extracting polluted air from buildings, and their performance remains unaffected by the wind direction, making them suitable components for multidirectional windcatcher designs. However, the performance of a chimney in a fixed design does not fully leverage the advantages of a rotary scoop windcatcher, where the chimney component is installed within a rotating device capable of always facing the wind. As a result, the ventilation rate achievable in the current design is not maximized. To address this limitation, a novel approach involving the chamfering of the chimney was investigated, as illustrated in Figure 8(c). By incorporating a chamfered angle, a pressure cowl was created, allowing the wind to be redirected with the assistance of the tail fin. This design modification generated a larger negative pressure at the outlet, enabling the extraction of a greater volume of air. Consequently, this research focused on investigating and comparing the ventilation performance of chamfered chimneys with varying angles, ranging from 0° to 60°. Through this analysis, we aimed to identify the most effective angle for maximizing the ventilation performance of the windcatcher system.

*4.5.3.5 Impact of atmospheric boundary layer (ABL) upstream wind*

The evaluation of the windcatcher's ventilation performance in existing studies has primarily been conducted under controlled wind conditions, rather than in a real-world setting with a large-scale building and atmospheric boundary layer (ABL). It is important to note that the presence of a building's edges can significantly influence the wind speed profile above the structure, and the wind speed near the roof may be substantially lower than the ambient wind at the same height. Consequently, it becomes necessary to increase the height of the windcatcher adequately, considering the geometry of the building, to effectively capture the wind for a fresh air supply.

However, it is crucial to recognize that the total pressure loss within the windcatcher system is influenced by factors such as friction and total length. Therefore, as this research primarily focuses on the parametric analysis of windcatcher geometry, it is imperative to investigate the impact of tube length as well. This analysis aims to ensure that the windcatcher system meets

the requirements of real-world applications and effectively caters to the ventilation needs of buildings. By considering both the height and tube length, we can optimize the windcatcher design to achieve optimal performance in practical scenarios.

*4.5.3.6 Height of the ASCD*

To address potential issues related to the short-circuiting of supply air, an Anti-Short Circuit Device (ASCD) was strategically integrated within the room, directly beneath the windcatcher. This configuration aims to forestall any possible rerouting of the ventilation airflow directly from the supply to the exhaust, bypassing the intended air distribution in the room, a phenomenon known as "short-circuiting". In addition to the installation of the ASCD, a thorough examination was conducted to discern the effect of the device's height within the room on the rate of ventilation. The objective of this assessment was to find an optimal balance between the ASCD's dimensions and the ventilation rate, a crucial step towards maximizing material efficiency. This harmony ensures a sustained high-performance level of the ventilation system without unnecessary expenditure on oversized ASCDs.

The efficacy of the windcatcher was scrutinized under a variety of conditions. Initially, its performance was evaluated at both its original and modified heights, under a constant wind speed setting. This evaluation allowed for a controlled and stable understanding of the windcatcher's performance, independent of wind speed fluctuations. Further evaluation was conducted under more realistic, full-scale conditions that encompassed an atmospheric boundary layer wind speed profile.

The full-scale CFD simulation domain size and the atmospheric boundary layer were determined based on the reference [34], including 5 times the height in front (5H), 5H on the side, 5H above the building and 15H in backward.

In the full-scaled simulation with the atmospheric boundary layer, the wind speed at the windcatcher’s height level, about 4m high, was 5m/s which was identical to the constant environment wind speed simulation and the wind speed profile was 6*(height/15 m)^0.143. A pitched/curved/domed roof building can be a solution to avoid the impact of the building edge [138, 139]. Thus, a full-scale simulation of the windcatcher with a pitched roof was also applied to investigate the impact on the ventilation rate.

All the parametric analyses were conducted based on the initial windcatcher model with a 450mm external diameter with an identical environment wind speed of 5m/s, and the optimized parameters were combined for the final optimized windcatcher.

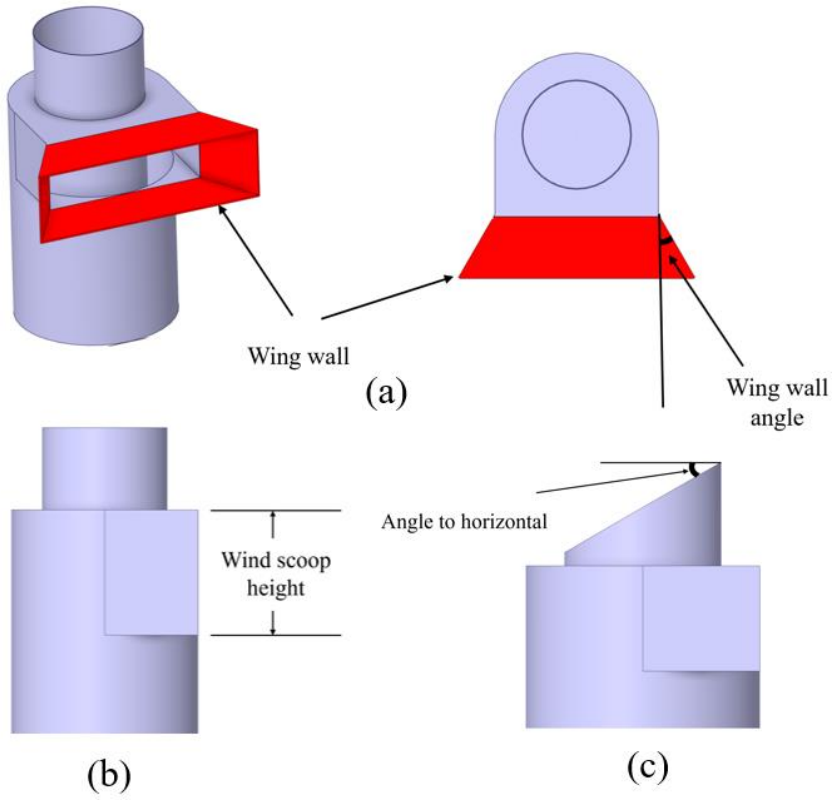


Figure 4.14 Parametric analysis of (a) wing wall at the wind scoop inlet (b) wind scoop height (c) chamfered chimney.

### 4.5.4 Comparison with the conventional 4-sided windcatcher

The primary objective of this parametric analysis is to enhance the ventilation performance of the rotary wind scoop windcatcher, with a specific focus on achieving a higher ventilation rate compared to existing models. This analysis is pivotal to advancing our understanding of how variations in design parameters can affect the windcatcher's overall performance, particularly in terms of its ability to facilitate air circulation within the enclosed space it services. Once the parametric analysis of the initial rotary wind scoop windcatcher was completed, it was crucial to gauge the effectiveness of these adjustments. This was accomplished by comparing the ventilation rate of the initial and modified versions of the rotary scoop windcatcher. To ensure a fair and balanced evaluation, the comparison was made against the conventional four-sided

windcatcher that maintained an identical diameter and opening height.

## 4.6 Summary

In summary, the CFD theory of the simulation in this research was presented in this section. The simulation models of the rotary scoop windcatcher and the flap fins windcatcher were generated based on the experiment model in this section to validate the experiment measurements. The dimensions of the simulation models and domains were presented in this section. The mesh independence analysis of two types of windcatchers was evaluated and the simulation models were independent of the mesh quality. The parametric analysis of the validated rotary scoop windcatcher was evaluated to improve the ventilation efficiency of the rotary scoop windcatcher.

# Chapter 5 Experiment results

In this section, the results of the experimental tests and field tests were presented. The ventilation rate evaluations of the rotary scoop windcatcher and wind speeds in the test room for validations were presented. The operation conditions of the flap fins louver windcatcher like opening angles and validations were also investigated in this section. The ventilation performance of different flap fins louver windcatchers with different fins and model heights were evaluated and compared to investigate the impact of each parameter in the flap fins louver windcatcher. The ventilation rates of the windcatcher under different wind directions were also evaluated and compared as the objective of this research. The field test results of the flap fins windcatcher operations were also analyzed in this section.

## 5.1 Wind tunnel results of the rotary scoop windcatcher

In Figure 5.1, the y-axis is the distance between the wind speed measure point and the centre of the wind tunnel and the x-axis is the wind speed. As shown in Figure 5.1, the wind speed profile is a quadratic function of the distance to the centre of the wind tunnel outlet. The velocity in the middle was slightly lower than the surroundings and the wind speed on the edge was lower because of the friction of the system. With the increase in average wind speed, the gap between the maximum and minimum wind speeds would also increase. The equation of the wind speed profile is detailed in the Appendix. The error range of the wind speed was determined by the percentage calculated from the hotwire anemometer sensors' accuracy based on the manufacturer's calibration.

The wind speed profiles in the outlet of the wind tunnel were presented in Figure 5.3 and the wind speed profile, at the maximum ventilation rate condition, in the return duct for the average wind speed to centre wind speed ratio calculation was presented in Figure 5.2. The wind speeds at three validation points for validation were presented in Figure 5.3 and the ventilation rate measured by the wind speed experiment and the carbon dioxide concentration change rate in Figure 5.4. In Figure 5.2, the y-axis is the distance between the wind speed measure point and the centre of the return duct and the x-axis is the wind speed. Thus, the relationship between

the centre wind velocity to the average wind velocity in the return duct was calculated, and the ventilation rate can be calculated. The correlation factor of average velocity to centre velocity was a function of the centre wind speed as the wind speed would have an impact on the Reynolds number and the development of airflow inside the tube.

The ventilation rate was calculated by Equation (5.1):

$$Q = \int V(r)\,\mathrm{d}A = 1000 * \int_0^R 2\pi r \times V(r)dr = -0.17 \times V_c^2 + 7.56 \times V_c \qquad (5.1)$$

where A is the area of the return duct of 0.00784 $m^2$ and R is the radius of the return duct of 0.05m;

Q is the ventilation rate in L/s.

As the distance from the wind speed measure point was about 0.5m which didn't reach 10 times the tube diameter, 0.1m, the airflow in the return duct was not fully developed and the speed profile was affected by the average or centre wind speed in the duct, which is still not fully developed flow. Thus, the total ventilation rate was not linear to the centre wind speed at the measure point and a decrease factor resulted in the equation.

A factor between the centre wind speed to the average wind speed in the tube was achieved in the calculation based on the experiment results of the wind speed profiles at different centre wind speed levels for a higher accuracy of ventilation rate estimation. A linear relationship between the factor and the centre wind speed was approximated to simplify the calculation and the overall ventilation rate is parabolic to the centre wind speed measured in the experiment.

The uncertainty analysis for the ventilation rate, Q, caused by the centre wind speed measurement in the return duct, needs to be calculated by Equation $= -0.017 * V_c^2 + 0.344 * V_c + 0.756$ (5.2).

$$\text{Uncertainty in } Q = \left|(\text{Uncertainty in } V_c) * \frac{dQ}{dV_c}\right| = |(0.1 + 5\% * V_c) * (7.56 - 0.34V_c)| = -0.017 * V_c^2 + 0.344 * V_c + 0.756 \qquad (5.2)$$

The uncertainty calculations were compared with the error range evaluations in the experiment and the error range was within the uncertainty range of the sensors, which proved the accuracy of the experiment measurements.

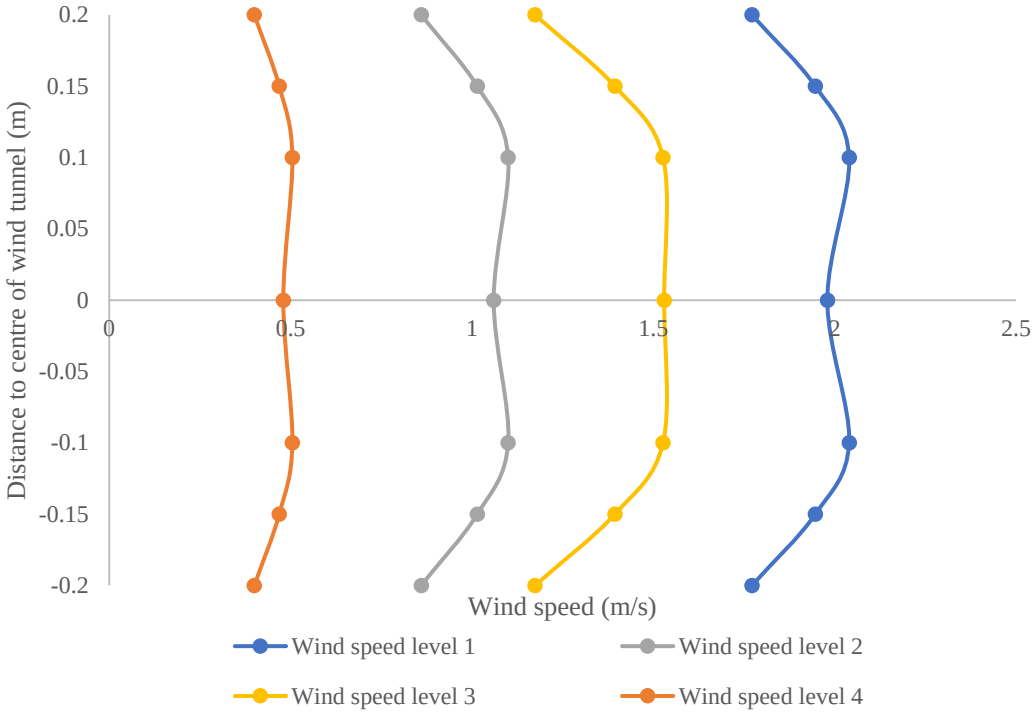


Figure 5.1 Wind speed profile in the open wind tunnel outlet

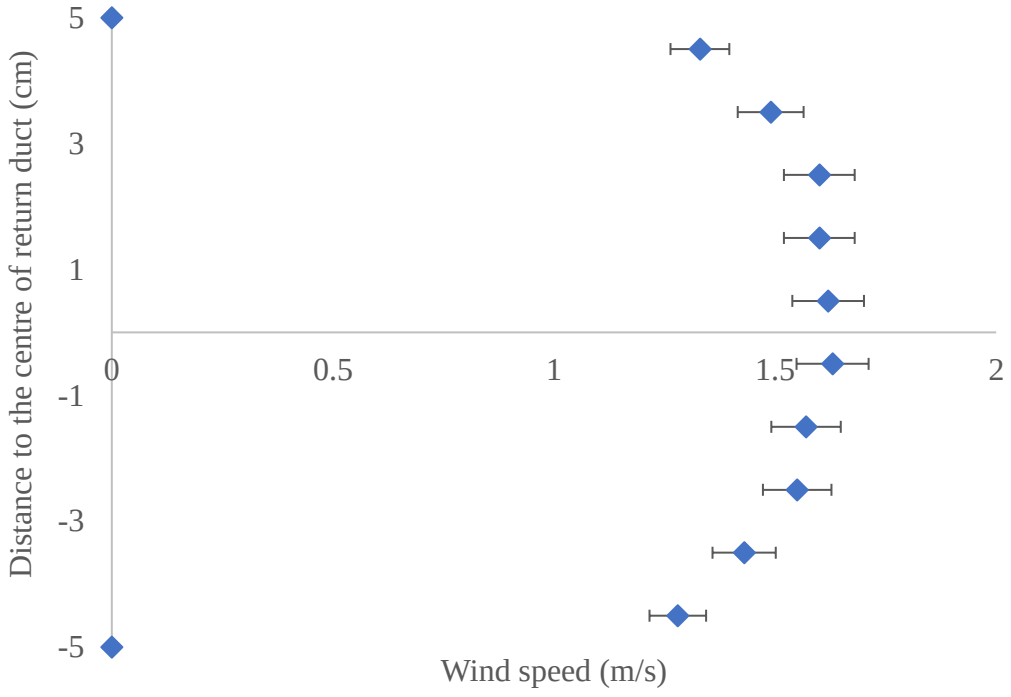


Figure 5.2 Wind speed profile in the return duct

The wind measurement points and the wind speeds measured from the experiment for CFD validation at these three different points in the test room were measured. The wind speed at

three points (Presented in Figure 3.22) fluctuated within a small range because of the accuracy of the sensor and the turbulence of the wind, but the average wind velocity in the three points was used for the model validation.

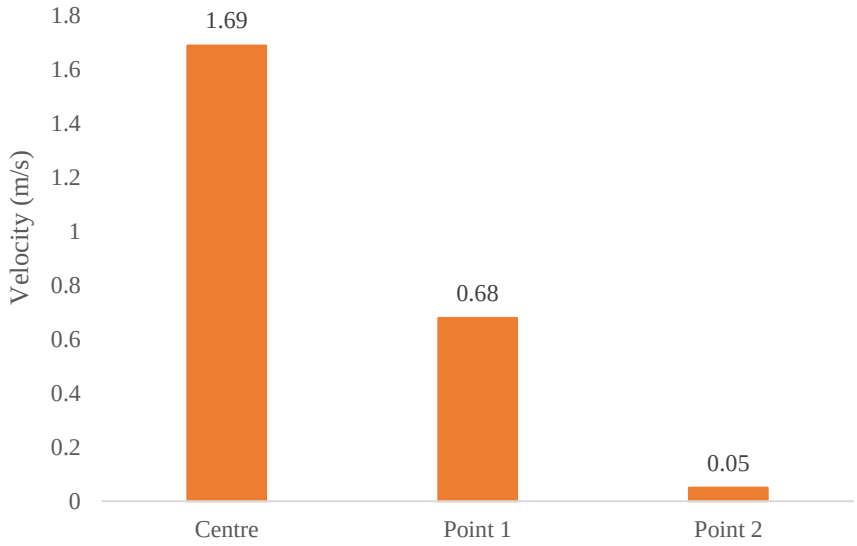


Figure 5.3 Measured velocity at different points for validation

The air change rate of the test room was also tested by the carbon dioxide concentration change rate, as shown in Figure 5.4, wind speed in the return duct and the maximum gap between the two methods was about 0.1L/s, which was ignorable for the ventilation rate evaluation of the windcatcher.

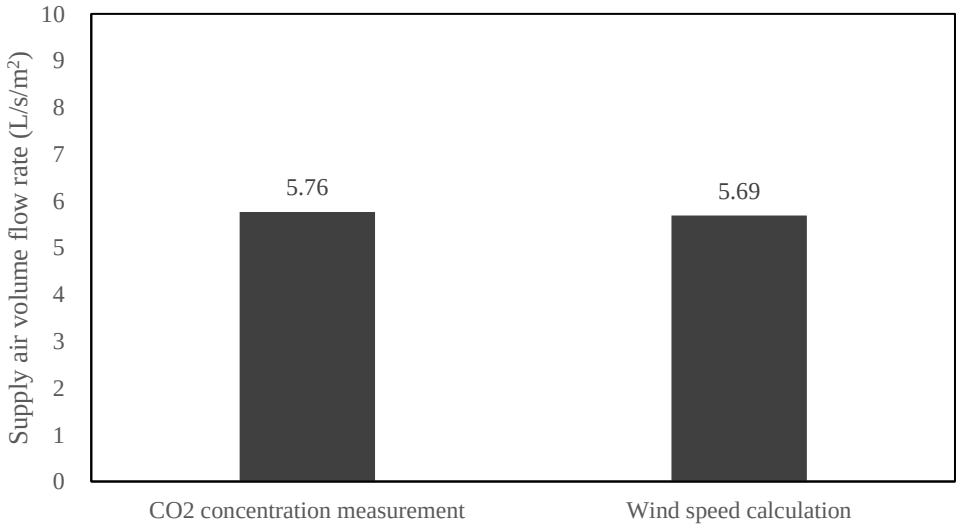


Figure 5.4 Windcatcher ventilation rate evaluation in different measurement methods

### 5.1.1 Ventilation performance of the scaled experimental model

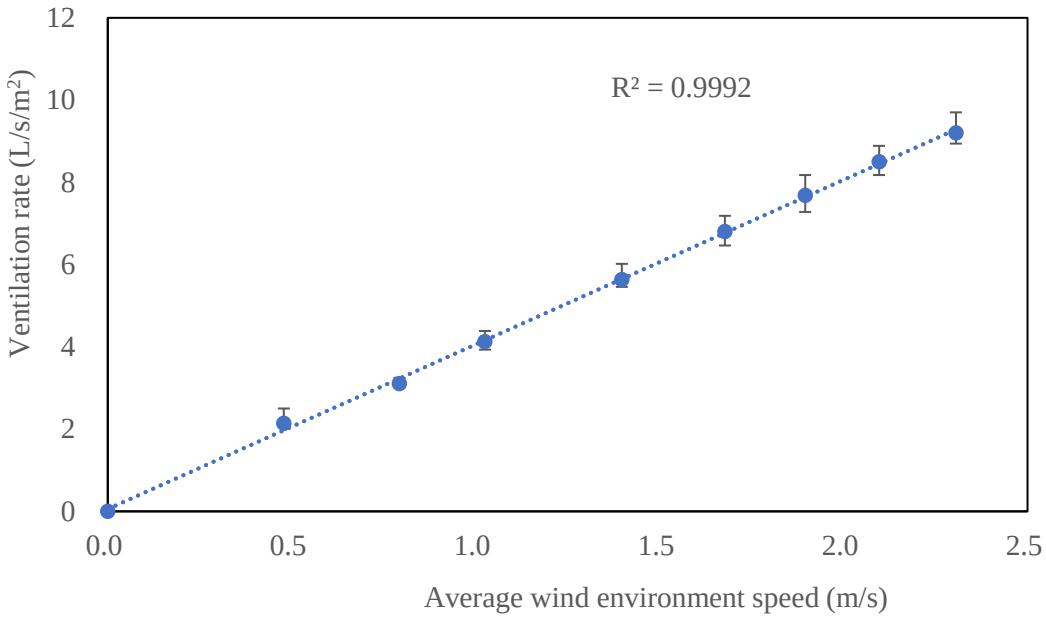


Figure 5.5 Scaled windcatcher ventilation performance

Fresh air was supplied between 1.7 L/s/m$^2$ and 9.18 L/s/m$^2$ for an outdoor wind speed of 0.5 m/s to 2.5 m/s in the scaled prototype. A linear relationship between average wind speed and ventilation rate was observed.

In the evaluation of the rotation, the wind scoop could face the wind under a wind speed of 1 m/s. The wind scoop could rotate in the correct direction fast at the beginning and stop slowly as the torque was higher when the angle of the wind to the vertical tail fin was large. The wind scoop would not fluctuate at the final place because of the friction and low torque at the final position. With the development of a commercial prototype, this necessary wind speed could be further decreased to a value lower than 0.5m/s. The position of the rotating wind scoop under 1 m/s wind is shown in Figure 5.6 and the angle change in the first three seconds was large and

stopped at the final direction that faced the wind steadily in the last 3 seconds.

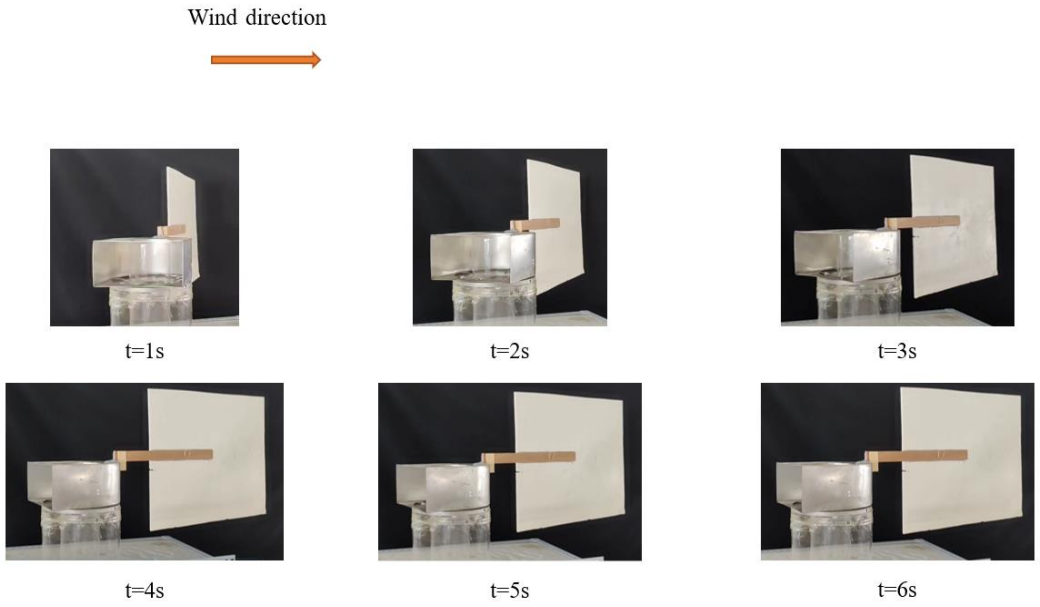


Figure 5.6 Snapshots of the rotation of the wind scoop windcatcher device

## 5.2 Wind tunnel results of the flap fin windcatcher

In this section, the experimental evaluations of different flap fins windcatcher models were presented, including the validation of the CFD model and the comparisons of the flap fins windcatcher with different parameters.

### 5.2.1 Initial single height flap fins windcatcher

The experiment test results of the initial flap fins windcatcher with a single height are presented in this section. The ventilation performance and the opening angle of the flap fins at single height single fin conditions were evaluated under two conditions including the wind blowing to the face of the windcatcher (0° wind direction) and the wind blowing to the edge of the windcatcher (22.5° wind direction).

In the 0° wind direction condition, in Figure 5.8, the ventilation rate was almost linear when the environment wind speed was higher than 0.5 m/s and the increased speed of the ventilation rate below 0.5 m/s environment wind speed was lower than the conditions with higher wind speed. The low ventilation rate at low environment wind speed conditions was caused by the

low opening angle of the flap fins at low wind speed conditions. The opening angle of the flap fins was a quadratic function to the environment wind speed in Figure 5.9. The pressure difference between the inside and outside surface of the flap fin at low wind speed conditions is insufficient to generate a torque to lift the flap fins and create a gap for air to enter the room. After the environment wind speed increased to over 0.5 m/s, the open angle of the flap fins could provide sufficient space for the air to enter the room. The opening angle of the front fin in this test is higher than the angles of the fins on two sides because of the higher pressure difference between the inside and the outside of the fins. The ventilation rate of the windcatcher at 22.5° wind direction condition is almost identical to the 0° wind direction condition. However, the opening angle of the two fins at 22.5° wind direction condition is lower than the front fin at 0° wind direction condition. Moreover, the opening angles of the two fins were not identical as the adjacent fins in this condition will block each other slightly which resulted in a higher opening angle on one side. However, as the soft fins were applied in the prototype, the block effect of the adjacent fins would not affect the ventilation rate.

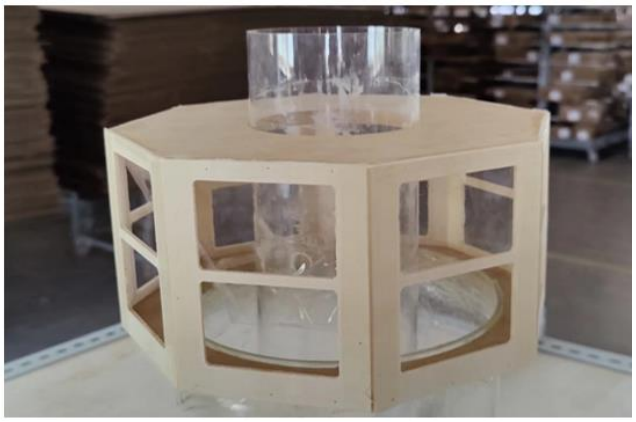

Figure 5.7 Initial experiment model with single height and single fin

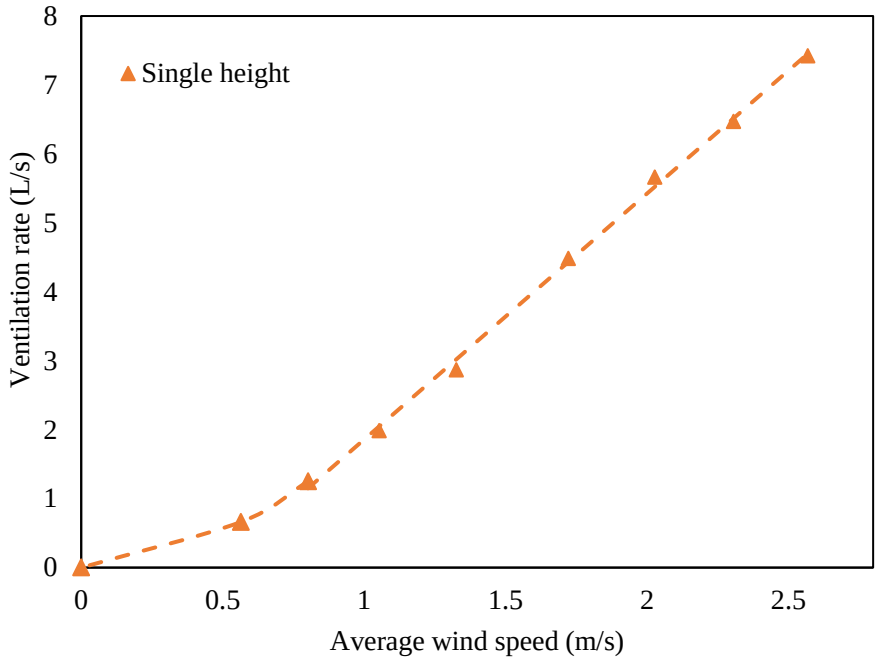


Figure 5.8 Ventilation rate of the initial single height flap fins windcatcher at 0° wind direction

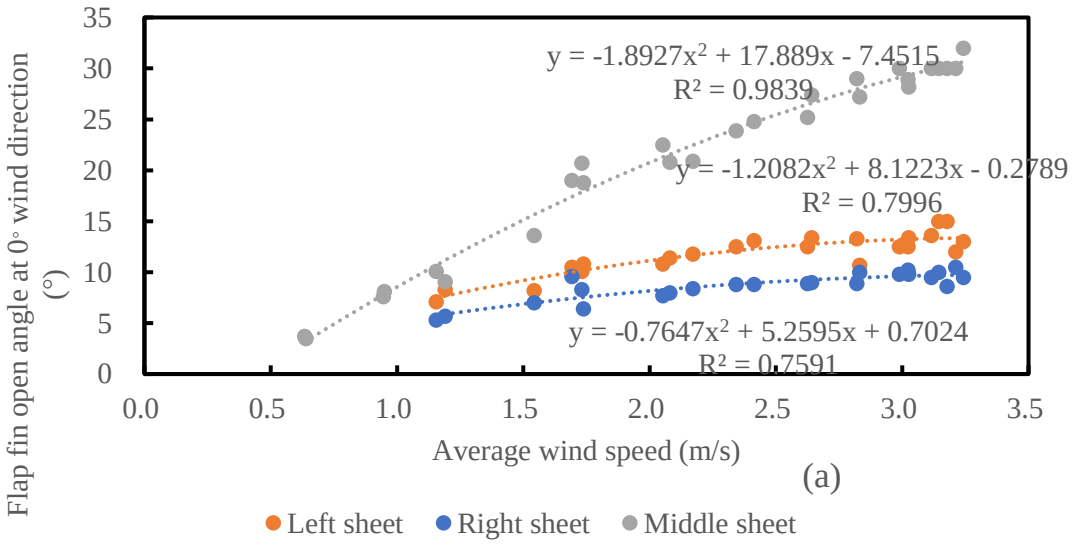

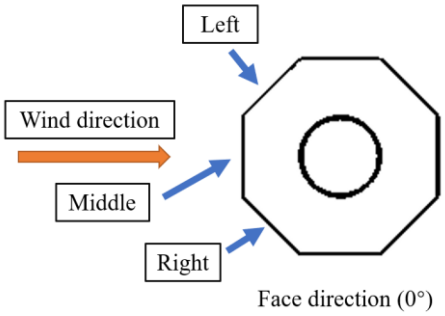


(b)

Figure 5.9 (a) Flap fins open angle and (b) locations (0° wind direction)

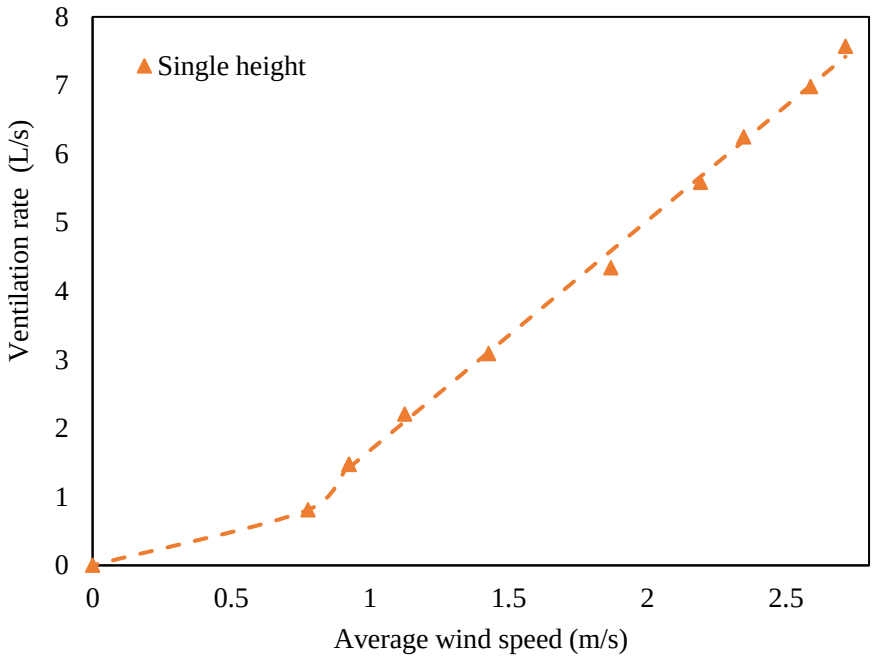


Figure 5.10 Ventilation rate of the initial single height flap fins windcatcher at 22.5° wind direction

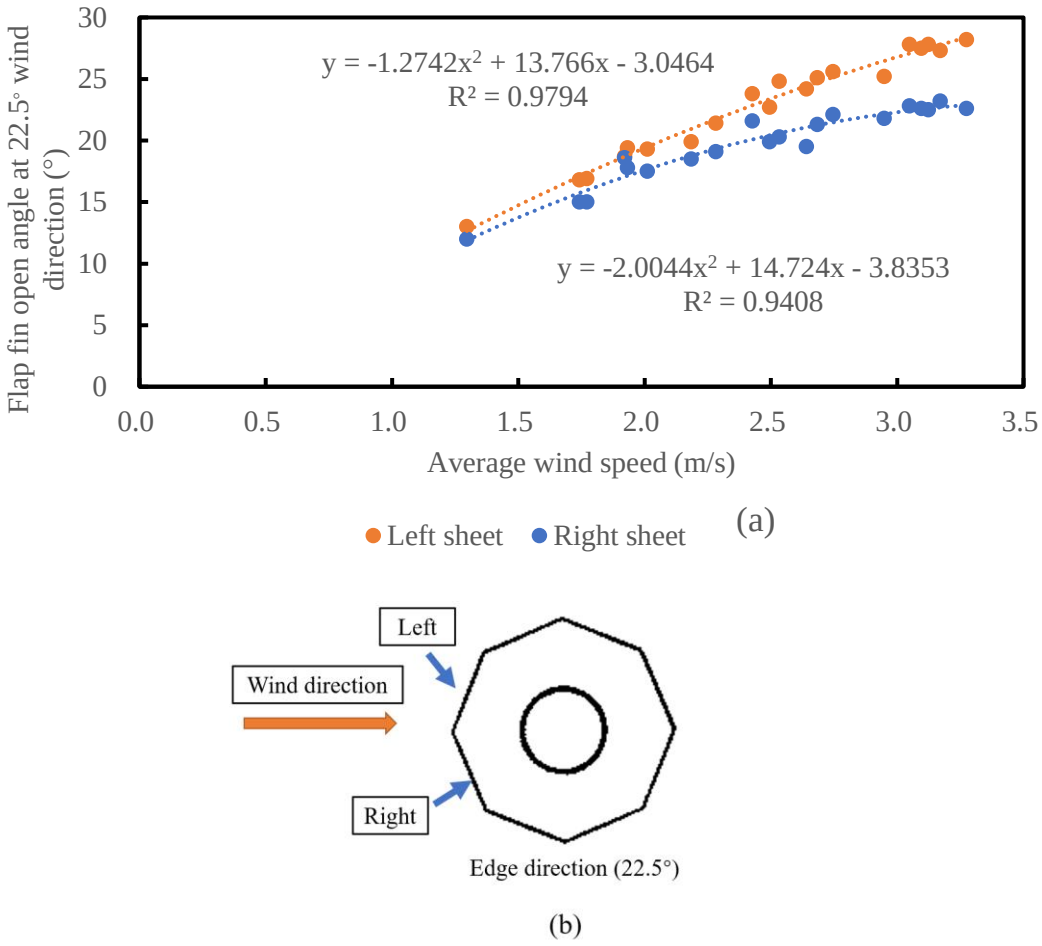


Figure 5.11 (a) Flap fins open angle and (b) locations (22.5° wind direction)

The flap fins were not stable in the operation and fluctuated within 2 degrees, which resulted in a systematic error in the measurement. When the open angle was large, the percentage of error was smaller than the small angle condition and R-value was higher than the small angle condition. The on/off performance of the plastic sheet satisfied the prediction when the average wind speed from the wind generator was higher than 2 m/s. The closed flap fins started to vibrate at wind speed lower than 2 m/s and the flap fins would leave the windcatcher wall steadily at wind speed lower than 1 m/s.

### 5.2.2 Double height flap fins windcatcher

The height of the initial flap fin windcatcher prototype was doubled to evaluate the impact of different fin lengths and areas of the inlet. The opening area and length of the flap fins were doubled in this section.

The airflow velocity at three different points (Presented in Figure 3.22) was measured in the

experiment for validation and the results were presented in Figure 5.12, which was identical to the rotary scoop windcatcher testing.

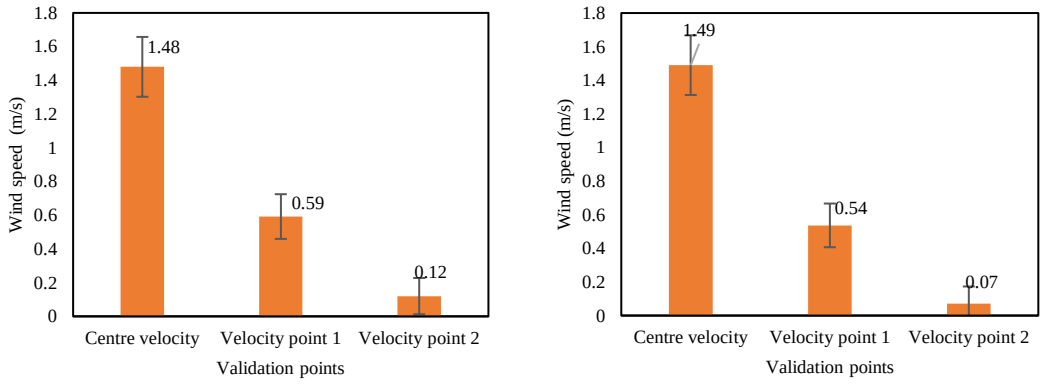


Figure 5.12 Wind speed validation results for (a) wind direction 0º and (b) wind direction 22.5º

The ventilation rate of the windcatcher model with double height and single long fins was also validated. The trendline of the ventilation rate in the model with all the fins differed from the model without the windward fins. As shown in Figure 5.13 and Figure 5.14, a linear relationship was achieved after 1 m/s wind speed in both 0° and 22.5° wind conditions. The poor ventilation rate of the flap fin louvre windcatcher was caused by the energy loss on pushing up the plastic sheet. Under the low outdoor wind speed conditions, the wind was not able to blow the fin up, and the small opening angle of the fin resulted in a block of airflow.

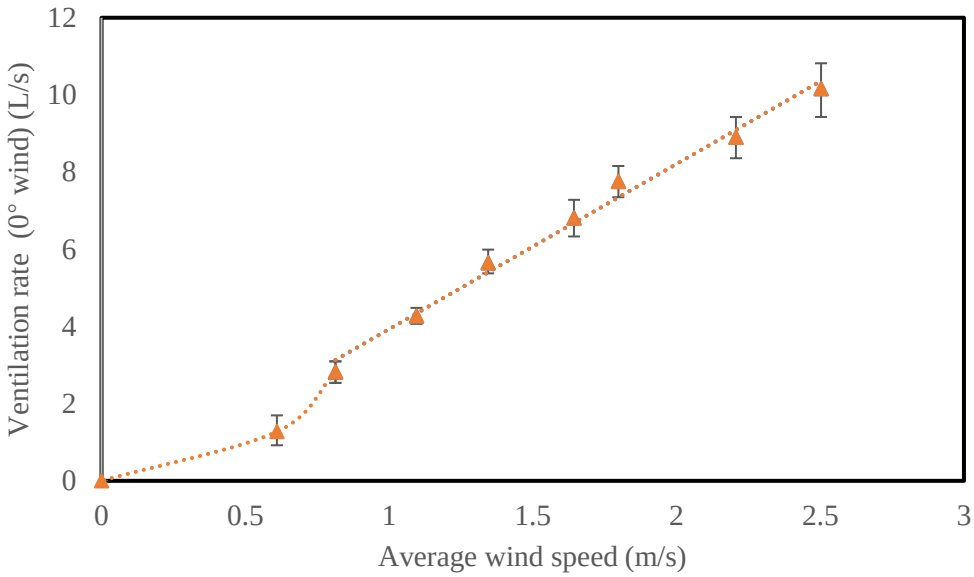


Figure 5.13 Ventilation rate validation of the windcatcher with all fins at 0° wind

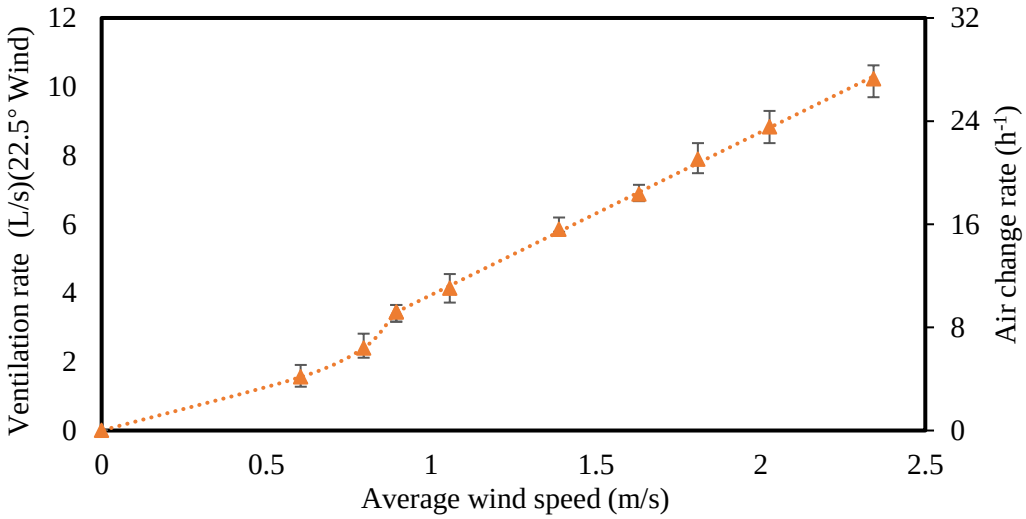


Figure 5.14 Ventilation rate validation of the windcatcher with all fins at 22.5° Wind

The average environment wind speed and ventilation rate in each measurement were measured in the experiment at the same environment wind speed. However, even though the supplied wind was already stabilized by the wind tunnel, the supplied wind was still not constant and the plastic sheet was also fluctuating around the neutral position within a small range. Overall, after comparing the wind speed profile in the return duct, wind speeds at different points, and the relationship between the ventilation rate to environment wind speed, the CFD model was

validated, and the results in the CFD simulation were qualified for this research.

By using the torque balance of the flap fins, the force and the friction can be evaluated by equation (5.3)&(5.4).

$$M = m \times g \times \frac{L}{2} \times sin\theta + M_{friction} = F_{wind} \times \frac{L}{2}$$

$$m = \rho \times T_k \times L \times W$$

$$F_{wind} = \Delta P \times L \times W$$

$$F_{wind} = \rho T_k LWgsin\theta + \frac{2M_{friction}}{L} \quad (5.3)$$

$$\Delta P = \rho T_k gsin\theta + \frac{2M_{friction}}{L^2 W} \quad (5.4)$$

where $\rho$ is the density of the flap fins in $kg/m^3$, which is about 1170 $kg/m\text{^}3$ calculated by the mass and volume of the fin,

$T_k/L/W$ is the thickness/ length/ width in $m$,

$\Delta P$ is the pressure difference between the two sides of the fins in $Pa$,

$M_{friction}$ is the torque caused by the friction at the connection of the flap fins and windcatcher wall in $Nm$,

$F_{wind}$ is the force generated by the wind pressure in $N$,

$\theta$ is the open angle of the flap fin in °.

Assuming that the friction at the connection is a fixed value and the pressure difference between the two sides of the fins is a value affected by the environmental wind speed, the decrease in the fin's thickness, $T_k$, will increase the opening angle of the flap fins. Moreover, the increase of the fin's length will decrease the impact of the friction at the connection to increase the opening angle of the flap fins to improve the ventilation efficiency of the windcatcher. As the torque generated by the friction and wind force were not measured in the experiment because of the limited prototype geometry and fin's mass, the friction torque was assumed to be a nonzero value which can not be ignored in this calculation. The relationship between the environmental wind speed and the pressure difference between the two sides of the fin can not be assumed as a function of the environmental wind speed, as the on/off status of the fin was different in the two models. For example, when the wind was facing one opening, only the front fin would be open in the double height model while three front fins in the single height model

would be open. Thus, the equation was only presented to analyze the relationship between each parameter to support the model optimizations rather than calculating the force in the experiment. The flap fins will be fully open when the flap fin is attached to the internal tube. In the single height windcatcher model with a fin length of about 10cm, the attached angle was about 45°. In the experiment, the largest opening of the short fin was about 30° when the wind speed around the windcatcher reached about 2.8m/s. Thus, the fully open angle was not evaluated in the single height windcatcher model. In the double-height windcatcher model with a fin length of about 20cm, the attached angle was about 20°. In the experiment, the attached status was achieved when the wind speed around the windcatcher reached about 2.1m/s. Thus, the fully open wind speed for the double height windcatcher with a 20cm long fin was about 2.1m/s. After reaching the internal tube, the flap fins started to bend and the inner surface of the flap fins was attached to the internal tube.

### 5.2.3 Flap fins windcatcher without the front fins

The ventilation performance of the windcatcher without the fins in the front was evaluated in this section to investigate the ventilation potential of the flap fins windcatcher and the impact of the fins.

The ventilation performance of the model without the windward side fins was also investigated and validated as a comparison to the model with the windward side fins to evaluate the impact of the mass and the geometry of the fin. As shown in Figure 5.15, linear relationships between ventilation rate and environment wind speed were achieved which is similar to a rotary scoop windcatcher. The maximum performance in the flap fins optimization is to eliminate the impact of the flap fins and the performance of the flap fins windcatcher can be identical to a rotary scoop windcatcher but the rotary components were simplified.

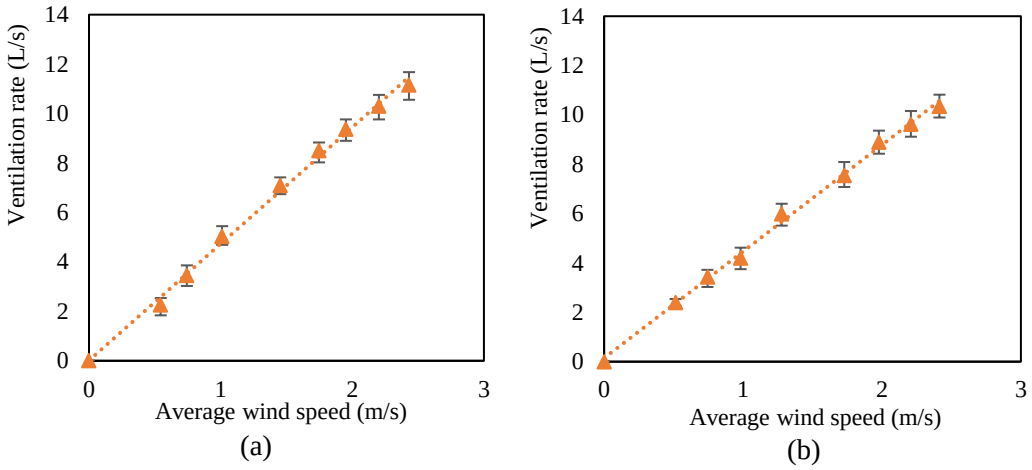


Figure 5.15 Ventilation rate of flap fins windcatcher without the windward side fins at (a) 0° wind and (b) 22.5° wind

### 5.2.4 Impact of the thickness of flap fins

In this section, the impact of the thick flap fins in the initial prototype with a single height was evaluated and presented in Figure 5.16. The length of the fin was 98mm and the width was 78mm. The mass of the 0.1mm thick fin was 0.91g per fin and the mass of the 0.25mm thick fin was 2.19g per fin.

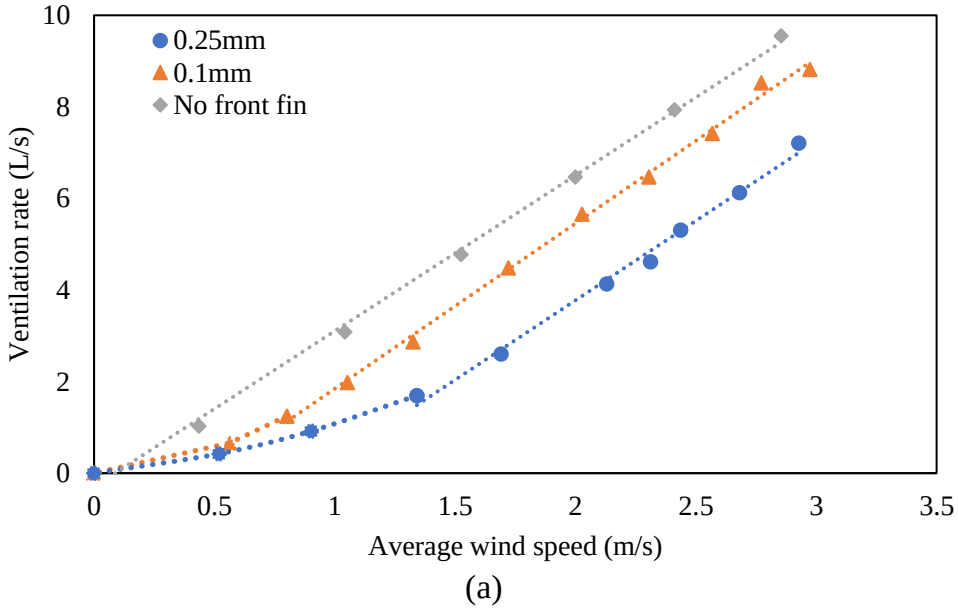

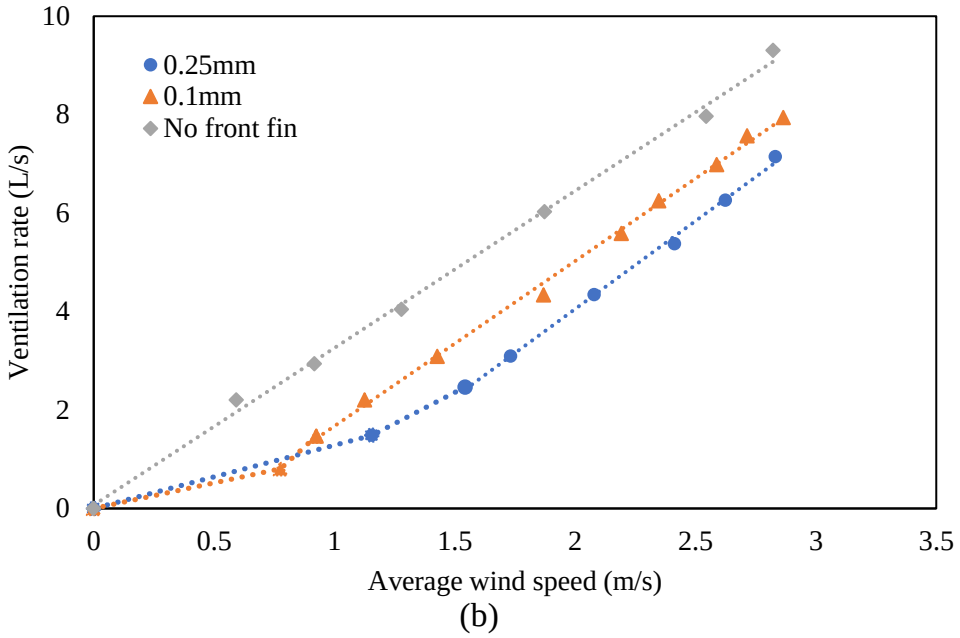


(b)

Figure 5.16 Comparison of the mass of the flap fins (a) 0° wind (b) 22.5° wind

As shown in Figure 5.16, after increasing the outdoor wind speed over 0.5m/s, the ventilation rate of the model with 0.1mm fin was linear to the outdoor wind speed and the gap between the model with and without windward fin was also decreased with the increase of environment wind speed. The same trend occurred in the model with 0.25mm fin after 1.5m/s environment wind speed. After decreasing the mass of the fin by 60%, the ventilation rate at the same wind speed was increased by 1.5L/s on average and the critical environment wind speed was also decreased from 1.5m/s to 0.5m/s. Thus, decreasing the mass of the fin was effective in improving ventilation performance.

The ventilation rate of the model without the windward fin was also compared to investigate the impact of the fins. As a fixed windcatcher without moving components, the ventilation rate was linear to the outdoor wind speed. The ventilation performance of the flap fins windcatcher increased slowly before a critical environment wind speed of around 1m/s, as the kinetic energy in the wind could not force the fin to open to a large angle and the fin was almost closed at this stage. With the increase of environment wind speed, both the gap between the model of 0.25mm and 0.1mm fin and the model of 0.1mm fin and without windward side fin were decreased. The results showed that if the outdoor wind speed was increased, the impact of the windward fin would decrease.

### 5.2.5 Impact of length of flap fins

In this section, the impact of the length of the flap fins and the opening area of the flap fins windcatcher were evaluated and presented in Figure 5.17.

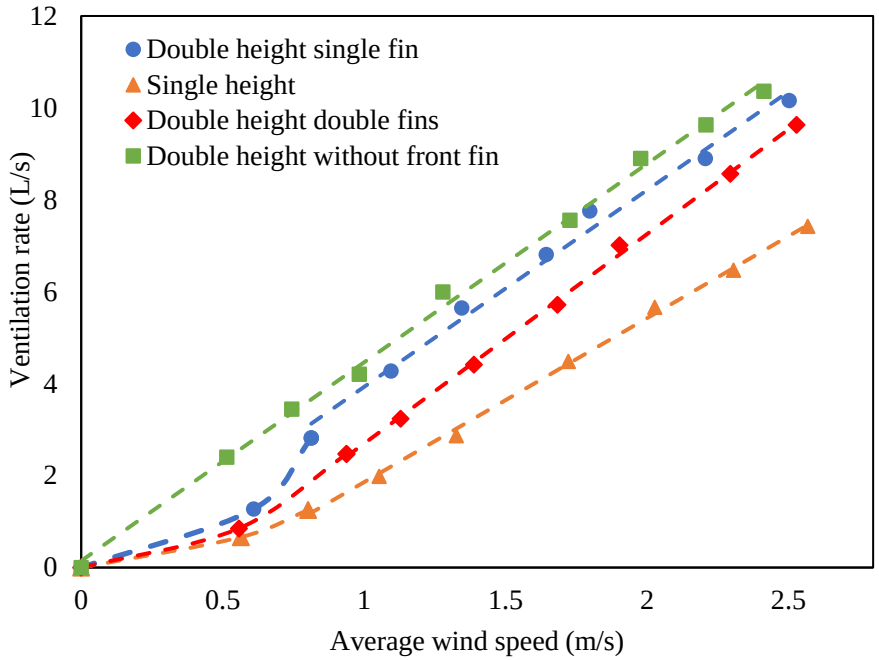


(a)

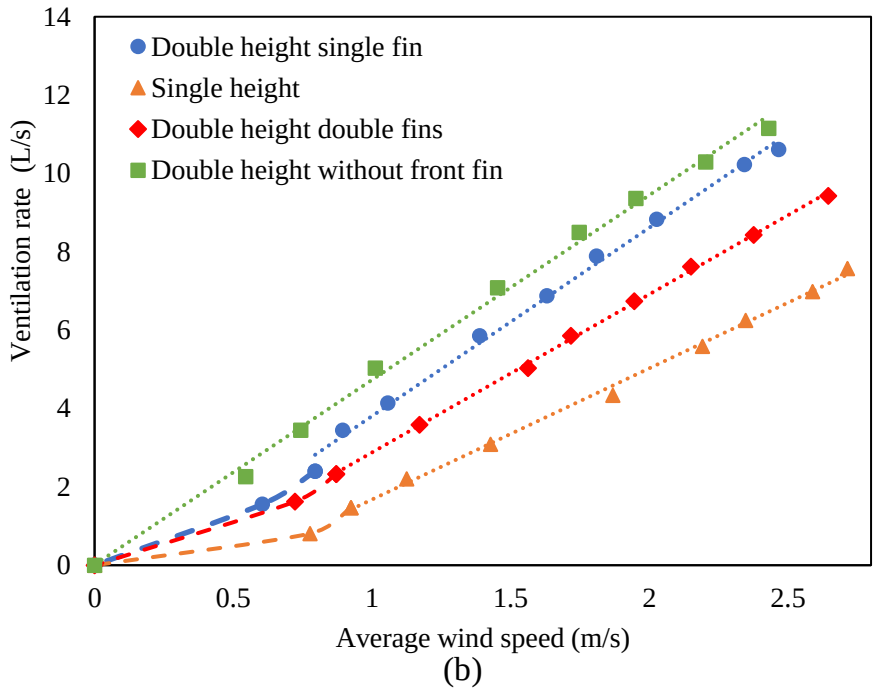


(b)

Figure 5.17 Comparison of the length of the flap fins (a) 0° wind direction (b) 22.5° wind direction

In Figure 5.17, doubling the height would not only double the length of the plastic sheet but also double the size of the opening to capture the wind. Thus, the model with a double inlet height and two plastic sheets has to be investigated to be compared with the model with a double inlet height and one plastic sheet and the model with a single inlet height. With the identical fin length, doubling the height generated a higher ventilation rate than the single-height one. Using a longer fin to replace two short fins increased the ventilation rate by over 20%.

After using a single long fin to replace two separate fins in the double-height model, the ventilation rate gap between the model with and without the front fin was decreased. Thus, increasing the length could reduce the impact of the fin on the ventilation rate of the windcatchers.

### 5.2.6 Impact of outdoor wind directions

In this section, the impact of the outdoor wind directions on the ventilation rates of flap fins windcatchers was evaluated and presented in Figure 5.18. In the single-height model, the wind from the windcatcher face direction (0° wind) could generate a slightly higher ventilation rate than the wind from the edge direction (22.5° wind), but the difference was ignorable compared to the performance of the traditional multiple-opening windcatchers. In the double-height model, the impact of wind direction was almost zero, and the ventilation rate in the two conditions was almost the same. In an eight-sided windcatcher, if the ventilation performance was stable in the range between 0° to 22.5°, the ventilation performance in the other directions would also be stable. Thus, if the fin length was long enough, which is about 20cm in this research, the windcatcher could provide a stable fresh air supply no matter how the wind

directions were changed.

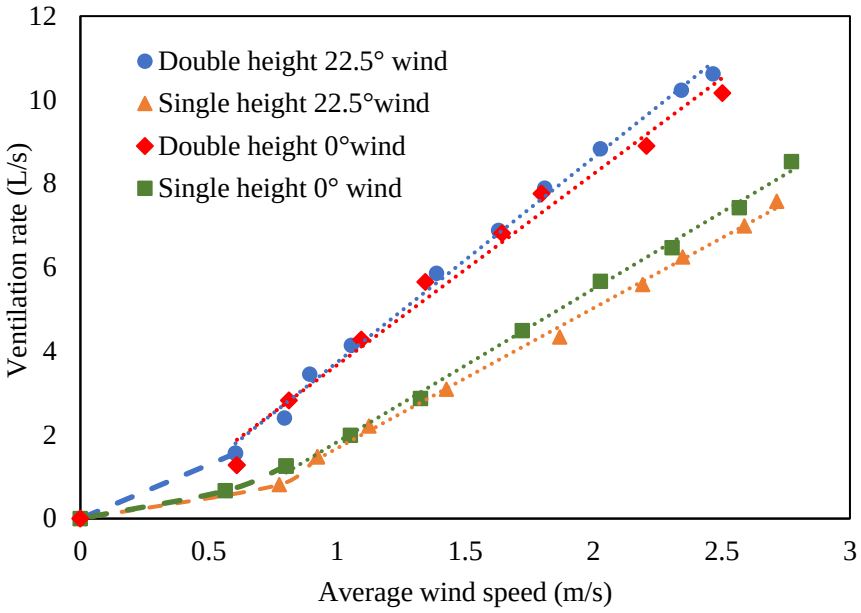


Figure 5.18 Comparison of ventilation rate under different wind directions

### 5.2.7 Impact of the layout of flap fins

In Figure 5.19, in the current research, the advantage of the horizontally hinged fin model is the impact of the mass of the fin was decreased and the impact of gravity was almost eliminated. In the vertically hinged fin model, gravity forces the plastic sheet to be closed, which limits the opening angle at low wind speed conditions. The ventilation performance of the long horizontally hinged fin model is still lower than the vertically hinged fin model. However, the result could not conclude that the vertically hinged fin had better performance than the horizontally hinged fin as the length of the vertically hinged fin was longer than the length of the horizontally hinged which generated a higher torque to open the fin. In the current prototype, the mass of the fin was minimized, and the fin was connected to the windcatcher wall by tap to minimize the impact of fin mass. The material, connection and size of the fin might be changed in further commercial products for reliable long-term operation, and the test of horizontally hinged fins was still necessary. Moreover, the adjacent fins would not block each other in the horizontally hinged fin model, so a larger opening size can be used.

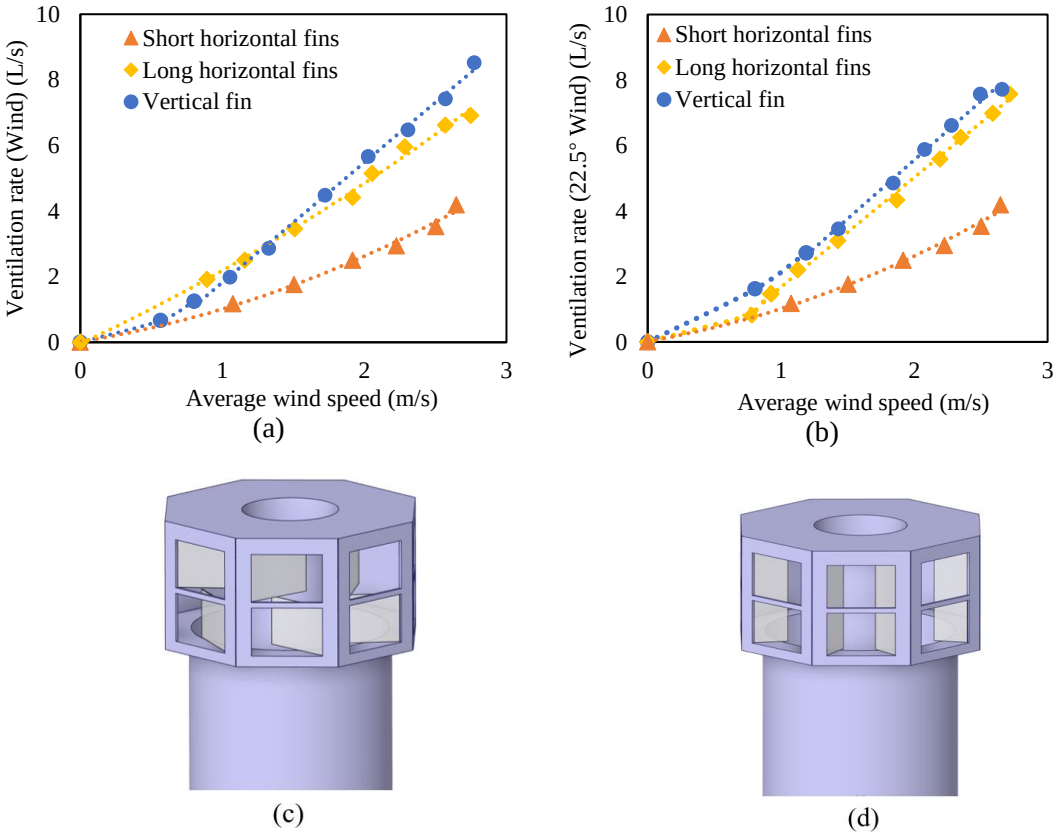


Figure 5.19 Horizontally hinged fin models and ventilation performance comparison (a) 0° wind (b) 22.5° wind (c) long horizontally hinged fins model (d) short horizontally hinged fins model

## 5.3 The field test result of the flap fins windcatcher

In this section, the results of the flap fin windcatcher's field test were presented and analysed. In the field test, when the wind direction was changed from the left-hand side to the right-hand side, the fins on the left were closed immediately, and the fins on the right opened at the same time. The could operate under varying wind directions and with a very fast response to the change in wind direction. However, the rotation of the environment wind speed measurement device had a slight delay as the rotation took time and the sensor of environment wind speed measurement was about 5m away from the windcatcher to avoid the impact of each other. Thus, in the environment with unstable wind conditions where both the wind speed and direction kept fluctuating, the ventilation rate data to environment wind speed every second was fluctuating which failed to present the relationship between the ventilation rate and to environment wind

speed. The ventilation rates every second are shown in Figure 5.20. Thus, the average ventilation rate in each minute needs to be considered in the result section.

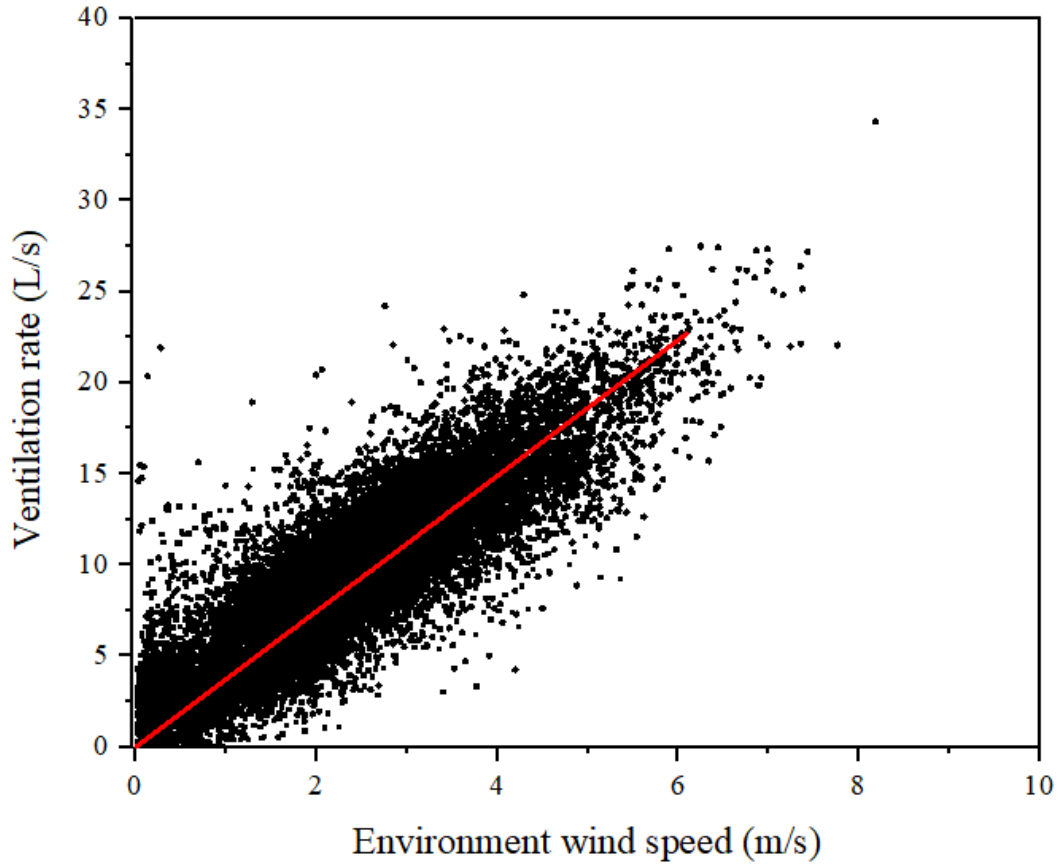


Figure 5.20 Field test ventilation rate to environment wind speed raw data in L/s

A good linear relationship between the average ventilation rate in each minute and the outdoor wind speed was achieved during the test, even though the wind conditions kept changing during the test in Figure 5.21. The results of the two field tests with high and low outdoor wind speeds were compared. The trend lines of the two tests were almost the same, with $R^2$ higher than 0.99. The stable performance of the flap fin louver windcatcher was verified by the different tests with different environment wind speeds and directions. As the wind speed generated by the wind tunnel was different to the natural wind because of the atmospheric boundary layer profile and the edge of the test room, achieving an identical performance in the field study was impossible. Thus, the average ventilation rate of the field test was slightly lower than the experiment. However, a similar ventilation performance was achieved in the field test compared to the findings of the open wind tunnel test. At low environmental wind conditions, the

ventilation rate in the experiment was slightly higher than the field study results.

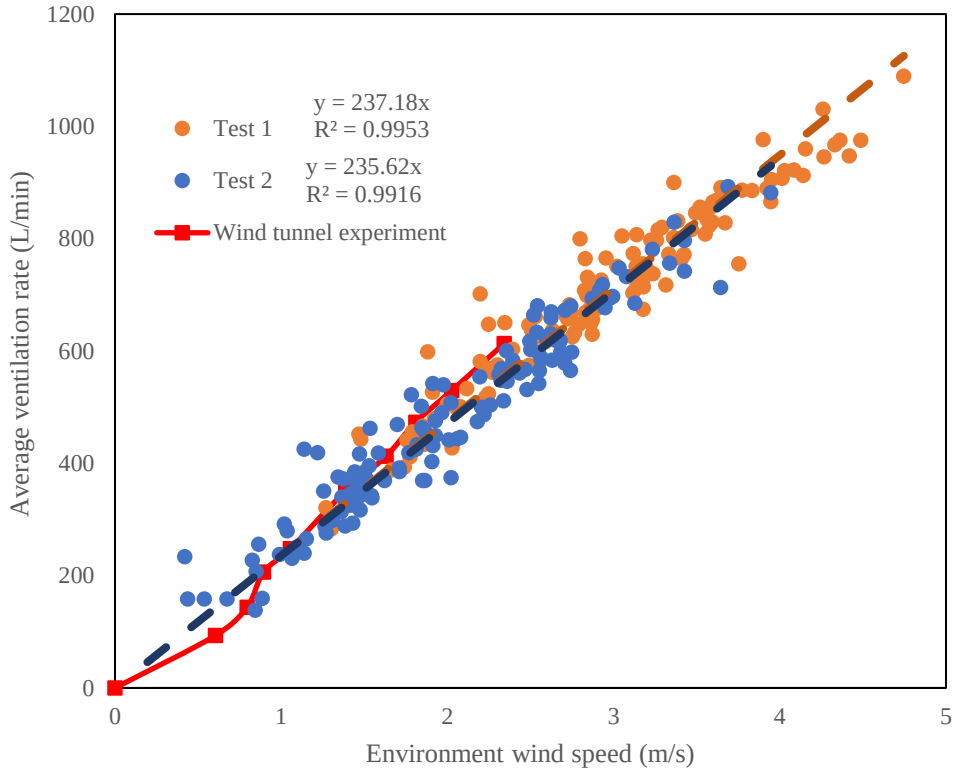


Figure 5.21 Field test results of average ventilation rate against the outdoor wind speed and the open wind tunnel experimental result

## 5.4 Summary

In summary, a linear relationship between the ventilation rate of the rotary scoop windcatcher and the environment wind speed was achieved in the experiment and the minimum environment wind speed to rotate the wind scoop was achieved. The ventilation rate and the open angle of the flap fins louver windcatcher were also presented in this section. The ventilation performance of flap fins louver windcatchers with different heights, fin lengths and fin thicknesses were compared in this section to achieve the prototype with the highest ventilation efficiency. The ventilation performance of the flap fins louver windcatcher in the field test was almost linear to the environment wind speed in minute average and the relationship between the ventilation rate to the environment wind speed was almost identical to the experiment results.

# Chapter 6 CFD results and optimizations

In this chapter, the numerical rotary scoop windcatcher model was validated by the experiment results and the details of the simulation results were presented. The ventilation performance of the full-scale rotary scoop windcatcher was also presented in this section. Different numerical flap fins louver windcatcher models were also validated by the experiment results with the details of the simulation results presented in this section. The parametric analysis result of each parameter of the rotary scoop windcatcher was presented in this section with the full-scale simulation of the rotary scoop windcatcher with the optimized value achieved from the parametric analysis. The ventilation performance comparisons of the traditional conventional windcatcher to the rotary scoop windcatcher and the flap fins louver windcatcher were also discussed in this chapter.

## 6.1 CFD model validation and simulation results of the rotary scoop windcatcher

### 6.1.1 CFD model validation of the rotary scoop windcatcher

In this section, the validation results of the rotary scoop windcatcher were presented and compared to the results measured in the experiments.

The CFD model validation was achieved by three methods, including the wind speed profile in the return duct in Figure 6.1, the wind speed in three validation points in Figure 6.2 and the ventilation rate measured by the wind speed experiment and the carbon dioxide concentration change rate in Figure 6.3 and Figure 6.4.

The wind speed profile in the return duct in the CFD simulation and experiment could match each other very well as shown in Figure 6.1. The experiment data was discussed in the previous experiment result. The y-axis is the distance between the wind speed measure point and the centre of the return duct and the x-axis is the wind speed. Thus, the relationship between the centre wind velocity to the average wind velocity in the return duct was calculated, and the ventilation rate can be calculated. The correlation factor of average velocity to centre velocity

was a function of the centre wind speed as the wind speed would have an impact on the Reynolds number and the development of airflow inside the tube.

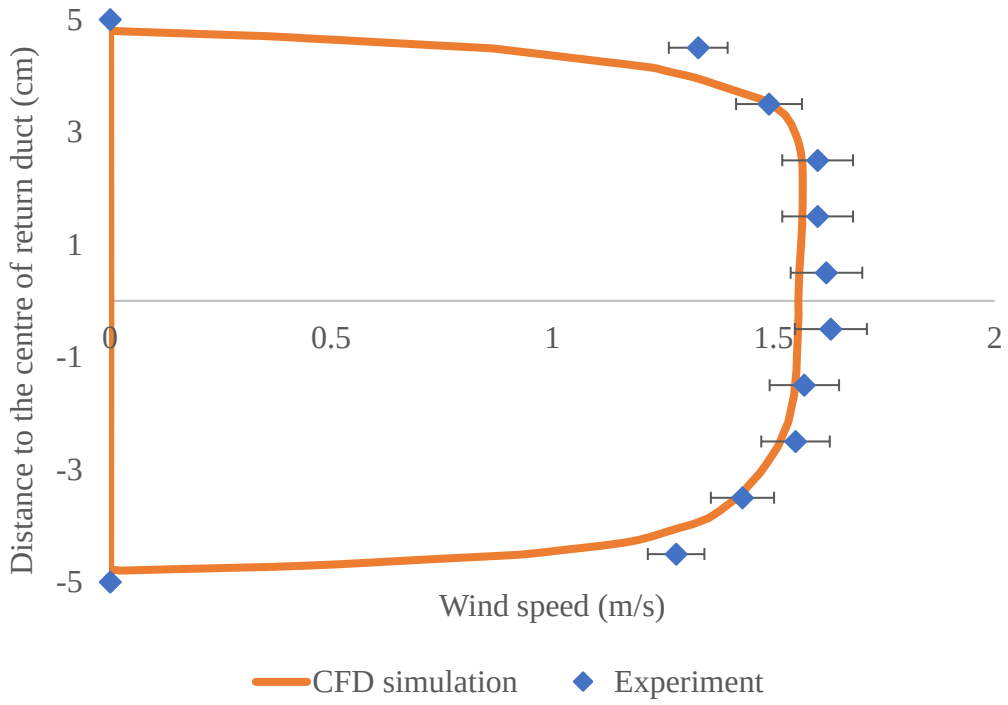


Figure 6.1 Wind speed profile in the return duct, comparing CFD results against experimental measurements

In the measurement of the wind speed profile in the return duct, two sensors were used and the volume of the sensors could not be ignored, which blocked a part of the return duct and increased the speed of airflow. The area blocked by the sensors was constant so the trend of the wind speed profile was not affected. However, in the ventilation rate measurement in the research, only one sensor was used in the experiment and modelled in the numerical model. Thus, in the numerical model, only half of the return duct was affected by the volume of the sensor which resulted in the dissymmetry of the wind speed profile. The speed of airflow in the middle was also affected by the numerical model so the numerical result was not perfectly quadratic.

The wind measurement points and the wind speeds measured from the experiment and CFD simulation at these three different points in the test room were measured for the CFD model validation, as shown in Figure 6.2. The wind speed at three points fluctuated within a small range because of the accuracy of the sensor and the turbulence of the wind, but the average

wind velocity in the three points could match the steady state condition in the CFD simulation. The relationship between validation point 1 to the centre wind speed measurement point was about 0.45 times the centre velocity.

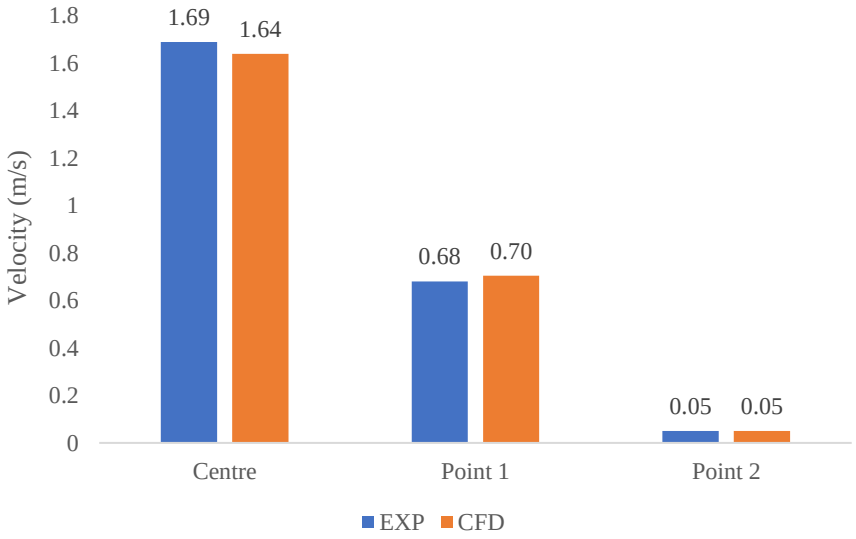


Figure 6.2 Validation of the velocity predictions using measured velocity at different points

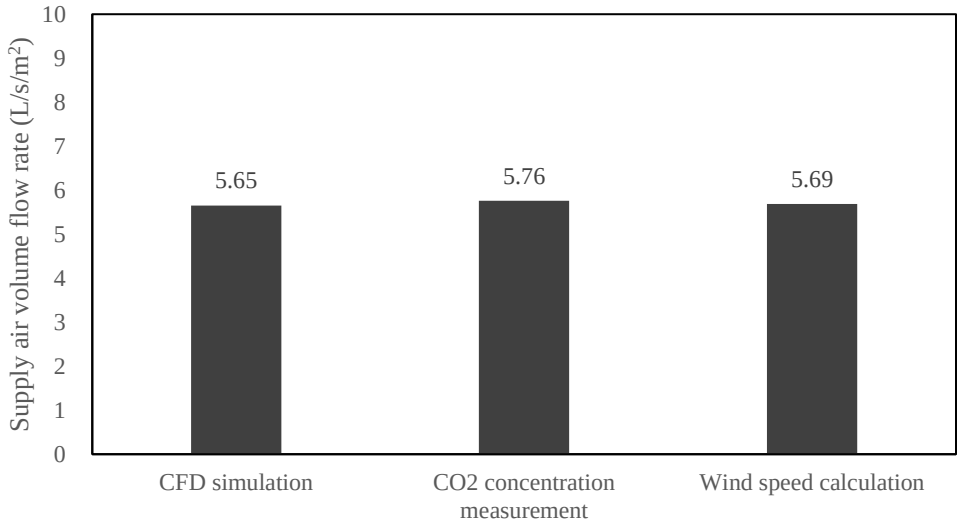


Figure 6.3 Supply air volume flow rate calculated by three evaluation methods

The ventilation rate achieved in the CFD simulation was also compared with the CO2 concentration measurement result and the wind speed calculation in Figure 6.3. The maximum gap between each method was about 0.1L/s, which was ignorable for the ventilation rate evaluation of the windcatcher.

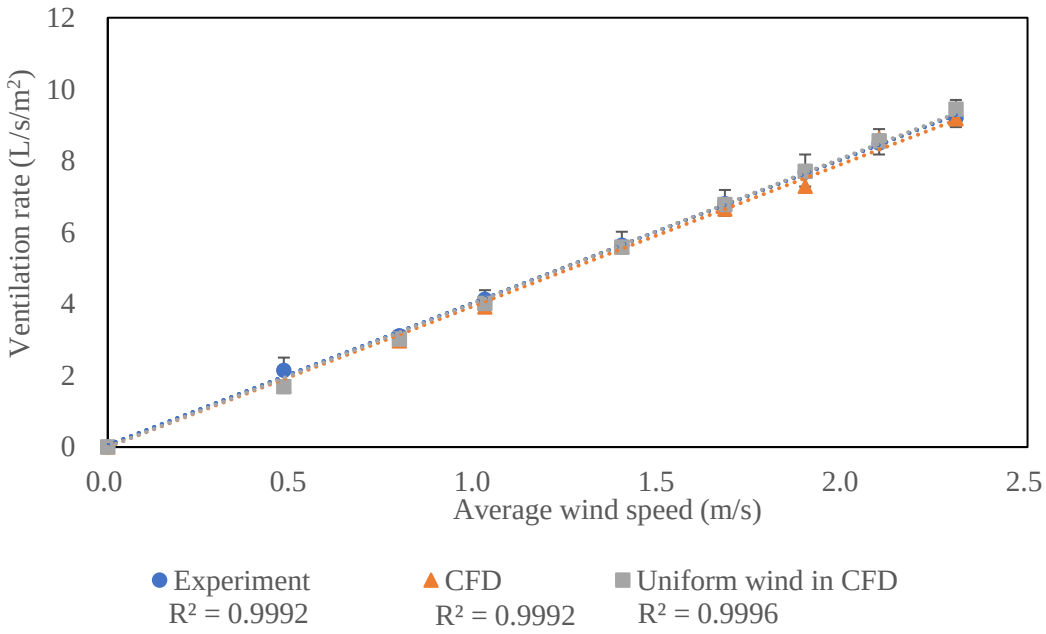


Figure 6.4 Scaled windcatcher ventilation performance: comparison between CFD and experimental results

As shown in Figure 6.4, fresh air was supplied between 1.7 L/s/m$^2$ and 9.18 L/s/m$^2$ for an outdoor wind speed of 0.5 m/s to 2.5 m/s in the scaled prototype. The average ventilation rate gap between the CFD simulation and experiment was 0.156 L/s/m$^2$ with an average difference of 4.5%. A linear relationship between average wind speed and ventilation rate was observed. As observed the difference between the ventilation rate of the CFD model with profiled wind from the open wind tunnel and uniform environment wind under identical average wind speed was minimal. Even though perfectly matched results were not achieved in the experiment and simulation, the difference in this research is much lower than other research investigating the windcatcher ventilation system, which has an average difference of 8% and highest error up to 15% [140]. Overall, the ventilation performance simulation in the CFD method was validated by three different methods, including the carbon dioxide concentration change rate, wind speed profile in the return duct and the wind speed at a different location in the test room. A good agreement was observed between different approaches.

### 6.1.2 Simulation results of the rotary scoop windcatcher

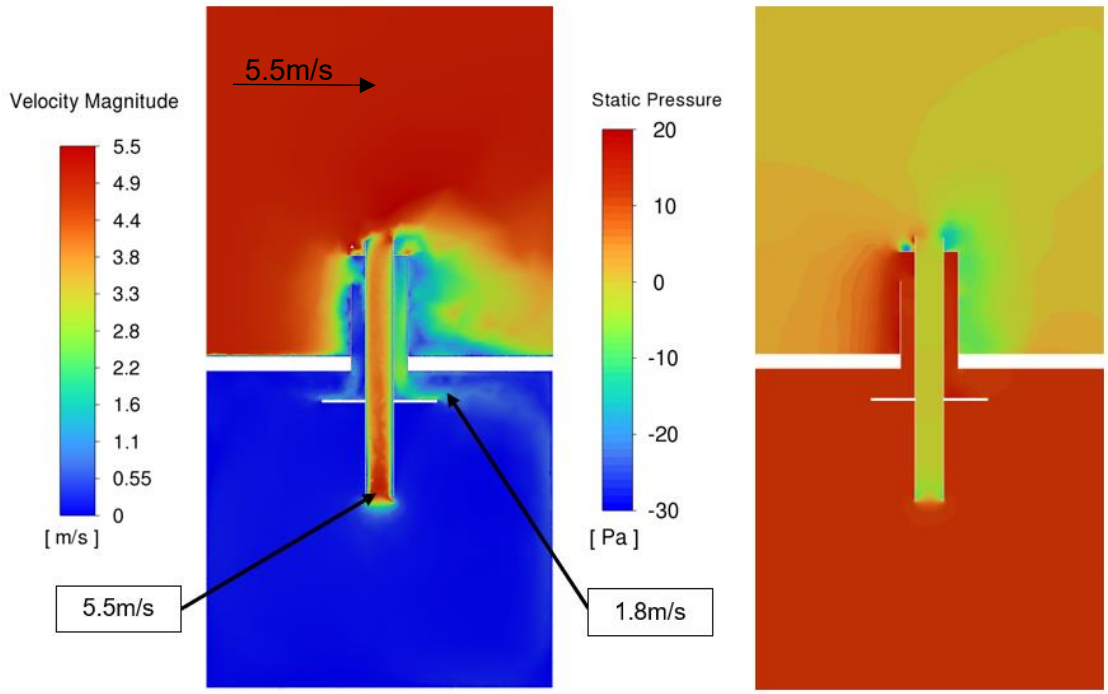


Figure 6.5 Cross-sectional contours showing the velocity and static pressure distribution in the scaled windcatcher model, outdoor wind speed at 5.5m/s

As windcatcher research investigated the ventilation performance of windcatcher system using experiment and CFD method under environmental wind speed over 5m/s, the windcatcher performance at wind speed about 5.5m/s was provided [140]. Moreover, the windcatcher was placed above the roof and a wind speed range of 4-6m/s was not uncommon in urban wind conditions. As shown in the pressure contour in Figure 6.5, the biggest pressure loss in the system came from the return duct. In the validated scaled model, the supply and return duct section areas were not perfectly balanced, because of the available products, resulting in a higher airflow velocity in the return duct and a higher pressure loss, compared to the full-scale model in Figure 6.8. As shown in Figure 6.5, the return duct was extended into the room to increase the distance between the wind speed measurement point and the inlet of the return duct which reduced the airflow velocity difference between the middle and the side. The airflow in the return duct got more uniform after entering the return duct for a longer distance which increased the ventilation rate measurement accuracy in the experiment. However, the extension of the return duct also increased the pressure loss of the system which will be modified in the

full-scale model.

The air was diffused by the anti-short circuit device and the velocity of air at the occupancy level in the room was lower than 0.5m/s at 5m/s environment wind speed which would not cause discomfort and air draught. The correct airflow direction was achieved and the indoor air was circulated well when the ASCD were added as shown in Figure 6.6. The wind speed on the two sides was not identical in the experiment model as the environment wind came from the left side but the wind speed in the highest part of the room was still lower than 1m/s at 5m/s environment wind speed. The pressure at the wind scoop was higher than the room to force the air entering the environment into the room. The pressure at the outlet was lower than the room to extract the air leaving the room from the chimney. The overall replacement ventilation was achieved by the appropriate airflow direction created by the pressure differences between the inlet, room and outlet.

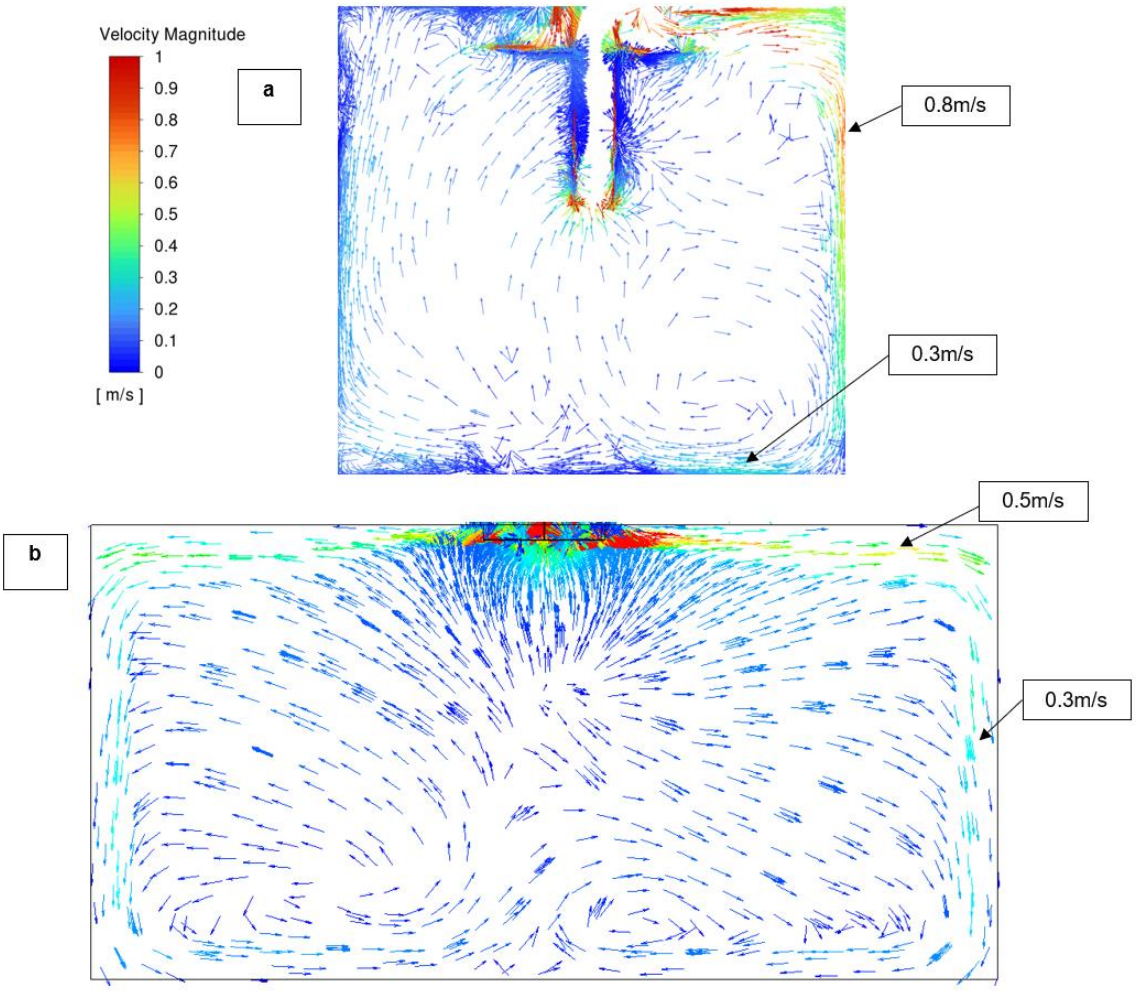


Figure 6.6 Air circulation inside the room at 5m/s environment wind speed (a) experiment model (b) full-scale model

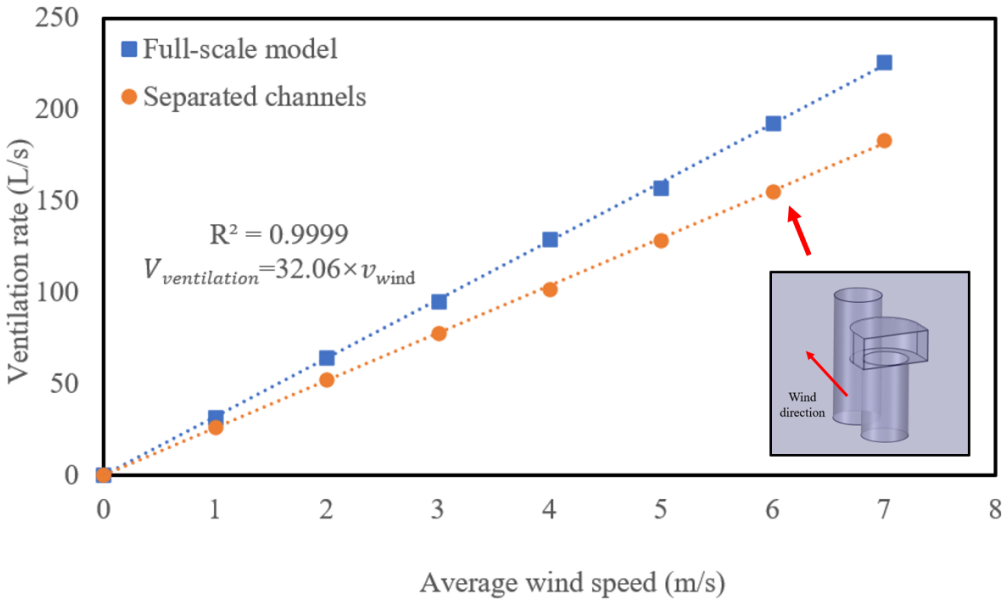


Figure 6.7 Impact of outdoor wind speed on the ventilation rate of the full-scale windcatcher model

For the full-scale model, the overall diameter of the windcatcher was increased from 200 mm to 450mm, and the size of the test room was increased to 6 m × 6 m × 3m. The increase of the windcatcher scale effectively increased the ventilation rate in the same wind conditions. However, it should be noted that the room volume also increased to 108 $m^3$, and hence a larger volume is ventilated. As observed, a linear relationship between the ventilation rate and outdoor wind speed was achieved. The full-scale rotary scoop windcatcher could provide a ventilation rate from 32 L/s to 226 L/s at 1-7 m/s environment wind speed as presented in Figure 6.7, while the fresh air supply at low outdoor wind speed conditions over 30 L/s was sufficient for three occupants, with 10 L/s/person in CIBSE Guide A for occupants working in an office [141].

The ventilation performance of the windcatcher system with separated inlet and outlet channels was also evaluated and compared to the full-scaled rotary scoop windcatcher system. The ventilation rate of the full-scaled rotary scoop windcatcher system was 26% higher than the separated system with an identical opening area and duct section area at the same location. Because the adjacent windcatcher channels would block each other when the environment wind direction was fluctuating, the ventilation efficiency would also decrease to a lower level so the performance of the separated system was always lower than the combined system proposed in

this research. Considering the windcatcher was normally placed on the top of a building with a higher environment wind speed, the windcatcher with 450mm diameter could provide sufficient fresh air supply for commercial use and a damper is necessary to avoid over-ventilation.

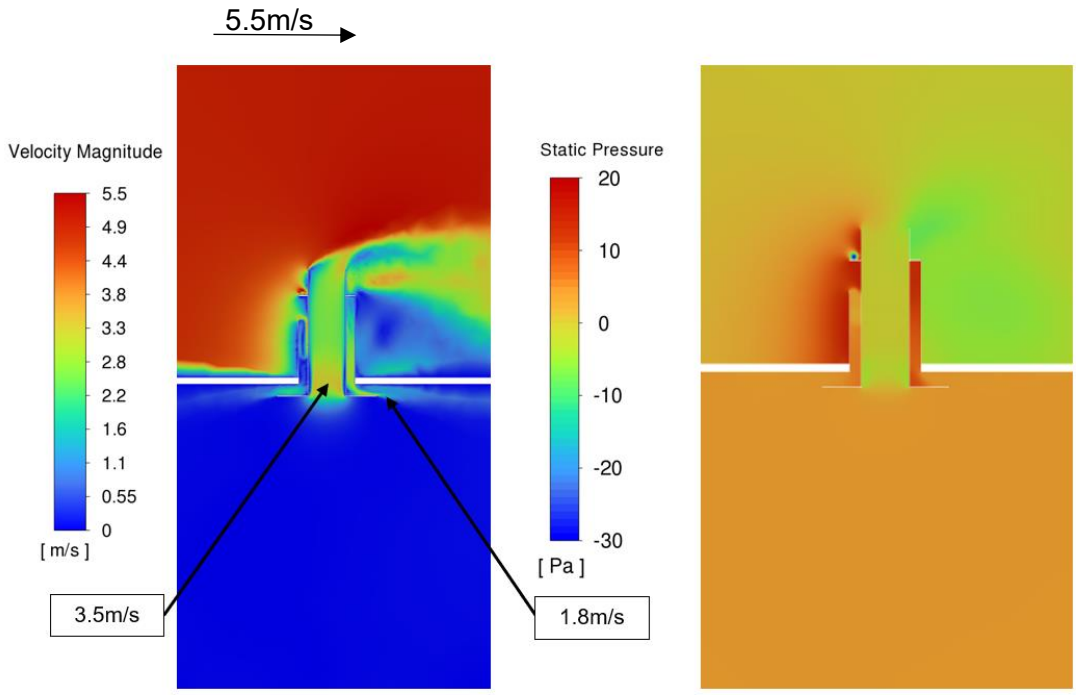


(a) Velocity (b) Static pressure

Figure 6.8 Cross-sectional contours showing the velocity and static pressure distribution in the full-scale wind catcher model, outdoor wind speed at 5.5m/s

As shown in Figure 6.8, the wind speed in the return duct in the full-scale model was lower than the initial scaled model at the same outdoor wind speed, which decreased the system friction and pressure loss and increased the total ventilation rate. Although the airflow velocity was decreased from 5.5m/s to 3.5m/s in the return duct under the same environment wind speed, the section area was increased, and the overall ventilation rate was increased. The size of the full-scale windcatcher was about three times larger than the scaled model but the ventilation rate in the full-scale model was over five times of the scaled model. The airflow on two sides of the ASCD was also more balanced than in the initial model. After reaching the side wall of the room, the airflow was diffused in different directions and the airflow velocity was decreased from 1.8 m/s to about 0.3 m/s close to the wall and the occupancy level.

In the pressure contour, the static pressure in the outside environment was identical to the initial

condition but the internal pressure in the full-scale model was lower than the initial scale model, which was caused by the lower pressure loss in the return duct that the full-scale building was not as pressurized as the scaled building. As the pressure at the inlet and opening was identical at the same wind speed, the pressure gradient was fixed, and the ventilation efficiency was increased by lower system friction.

### 6.1.3 Comparison to the conventional windcatcher

To achieve a windcatcher for practical application, the ventilation performance of the novel design had to be compared to the traditional products. The current single windcatcher product for natural ventilation under changing wind directions was normally a multi-opening windcatcher with four or more opening numbers to different sides. In the traditional three-sided or four-sided windcatcher, the ventilation rate was sensitive to the wind direction, but increasing the opening number could decrease the effect of changing wind directions [56]. Thus, an eight-sided windcatcher was selected to compare with the rotary windcatcher in this research. The ventilation performance of the scaled rotary scoop windcatcher was compared with a conventional eight-side windcatcher in Figure 6.9 which also had the function of providing fresh air under changing wind directions.

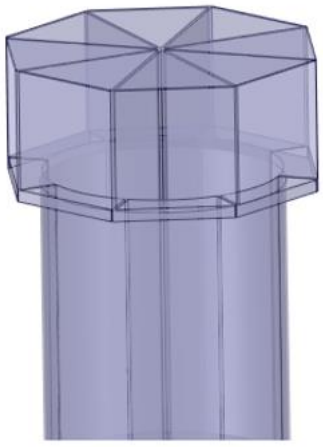

Figure 6.9 Geometry of the 8-sided windcatcher for ventilation rate comparison [142]

As observed in Figure 6.10, the ventilation performance of the rotary wind scoop windcatcher is slightly higher, about 10%, than the conventional eight-side windcatcher as the inlet area facing the wind with high positive pressure, and the outlet was on the top with a high negative

pressure which resulted in a higher pressure difference between inlet and outlet to force the airflow. The balanced supply and return duct area can decrease the system pressure loss to increase the ventilation performance as the supply duct number in the conventional eight-side windcatcher was always less than the return duct.

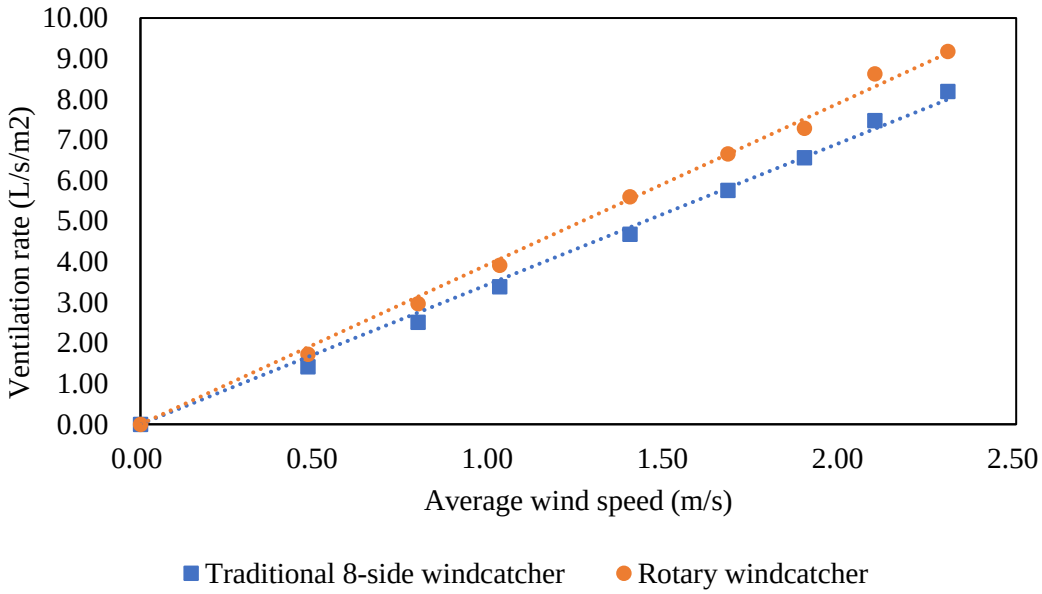


Figure 6.10 Comparison of conventional windcatcher and full-scale rotary scoop windcatcher

## 6.2 CFD model validation and simulation results of the flap fins windcatcher

### 6.2.1 CFD model validation of the flap fins windcatcher

In this section, the validation results of the flap fins windcatcher were presented and compared to the results measured in the experiments.

The wind speeds at different locations in the flap fins windcatcher test were measured in the experiment for the CFD model validation and the results were compared in Figure 6.11. The wind speeds under different wind directions are presented in Figure 6.11 (a) and (b). The difference between the wind speed measurement and the CFD model result was negligible compared to the accuracy range of the anemometer.

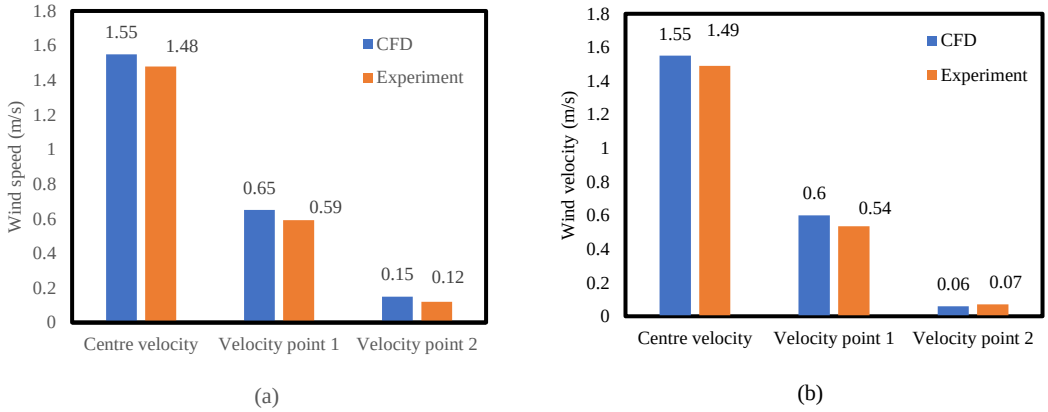


Figure 6.11 Wind speed validation results for (a) wind direction 0º and (b) wind direction 22.5º

The ventilation performance of the model without the windward side fins was also investigated and validated as a comparison to the model with the windward side fins to evaluate the impact of the mass and the geometry of the fin. As shown in Figure 6.12, a linear relationship between ventilation rate and environment wind speed was achieved. The average difference between the ventilation rate in the experiment and simulation was 0.25L/s with an average error of 4.1% in the condition with wind from the edge direction (22.5° wind). The average gap between the ventilation rate in the experiment and simulation was 0.23L/s with an average error of 5.6% in the condition with wind from the face direction (0° wind). The trendlines of the simulation and experiment results were almost overlapped, and the error was within the accuracy range of the anemometer.

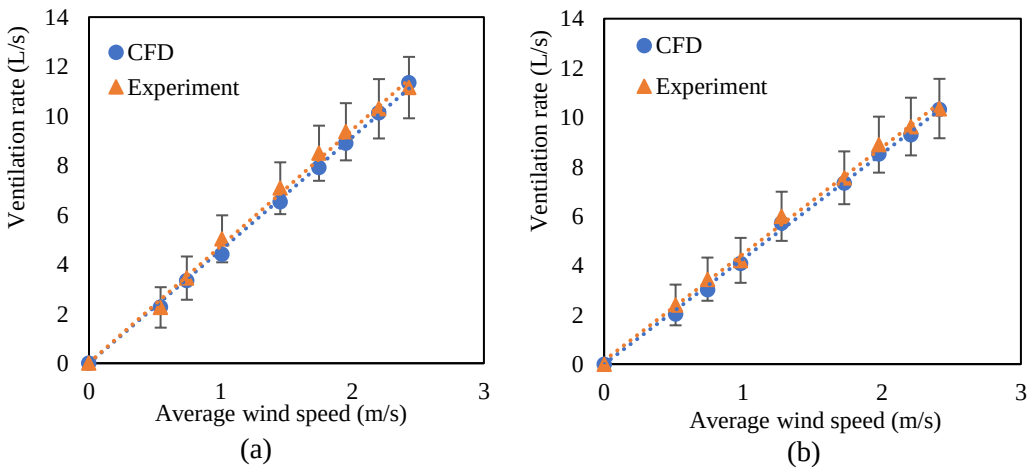


Figure 6.12 Validation of the ventilation rate for the windcatcher without the windward side

fins at (a) 0° wind and (b) 22.5° wind

The ventilation rate of the windcatcher model with double height and single long fins was also validated. The trendline of the ventilation rate in the model with all the fins differed from the model without the windward fins. As shown in Figure 6.13, a linear relationship was achieved after 1 m/s wind speed. The poor ventilation rate of the flap fin louver windcatcher was caused by the energy loss on pushing up the plastic sheet. Under the low outdoor wind speed conditions, the wind was not able to blow the fin up, and the small opening angle of the fin resulted in a block of airflow. The average gap between the ventilation rate in the experiment and simulation was 0.16L/s with an average error of 4.5% in the condition with wind from the edge direction (22.5° wind). The average difference between the ventilation rate in the experiment and simulation was 0.09L/s with an average error of 2.3% in the condition with wind from the face direction (0° wind). The trendlines of the simulation and experiment results almost overlapped, and the error was within the accuracy range of the anemometer.

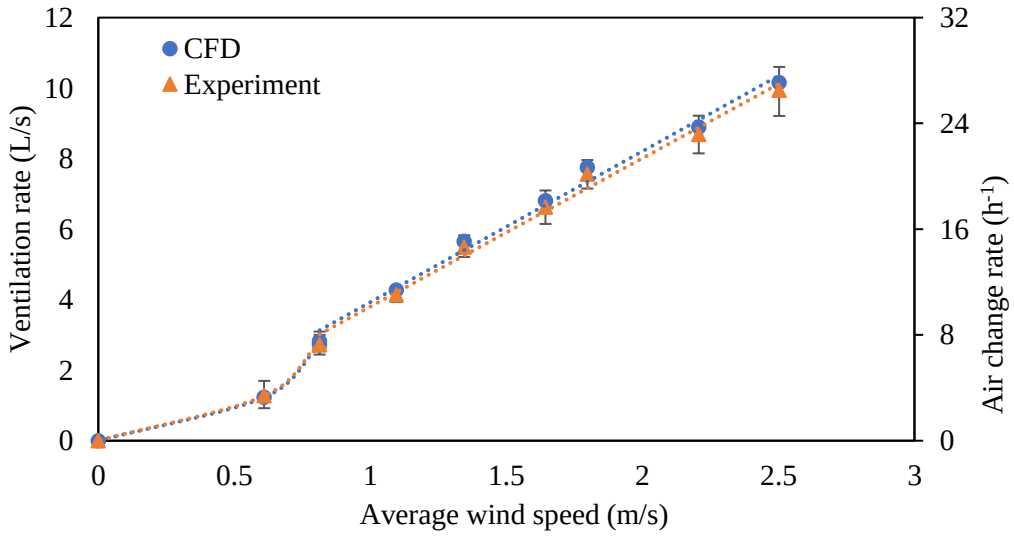


(a)

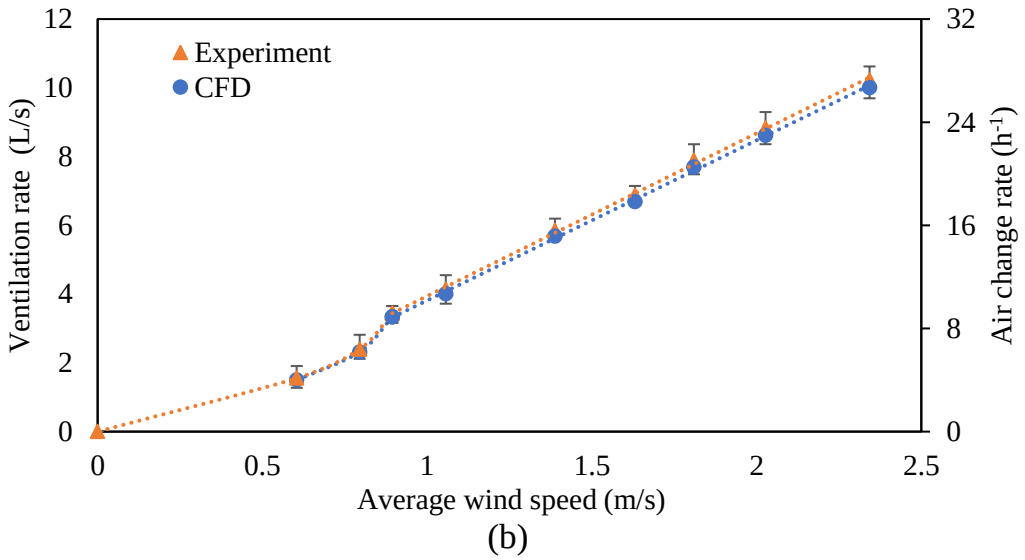

(b)

Figure 6.13 Ventilation rate validation of the windcatcher with all fins (a) 0° wind (b) 22.5° Wind

The average environment wind speed and ventilation rate in each measurement were measured in the experiment at the same environment wind speed. However, even though the supplied wind was already stabilized by the wind tunnel, the supplied wind was still not constant and the plastic sheet was also fluctuating around the neutral position within a small range. Overall, after comparing the wind speeds at different points and the relationship between the ventilation rate to environment wind speed in different models, the CFD model was validated, and the results in the CFD simulation were qualified for this research.

### 6.2.2 Simulation results of the flap fins windcatcher

The airflow velocity contour is shown in Figure 6.14. The wind speed started decreasing before arriving at the windcatcher because of the size of the wind tunnel. The air was diffused by the anti-short circuit device and the velocity of air at the occupancy level in the room was lower than 0.2m/s at 2.5m/s environment wind speed which would not cause discomfort and air draught. Even though the velocity of air inside the room was low, the air was well circulated and the fresh air from the windcatcher can be supplied to the level of occupants. The average wind speed at the plane with a height of 0.5m was 0.03m/s and the circulation of air would not cause discomfort. In the current test room, a slow but well-circulated airflow was achieved in

the experiment. However, to circulate the air in a large room, the size of the supply opening inside the room can be decreased and the supply air velocity could be increased to circulate in a large region. The ventilation rate would be slightly decreased by the higher system friction but better air circulation is more beneficial for the application.

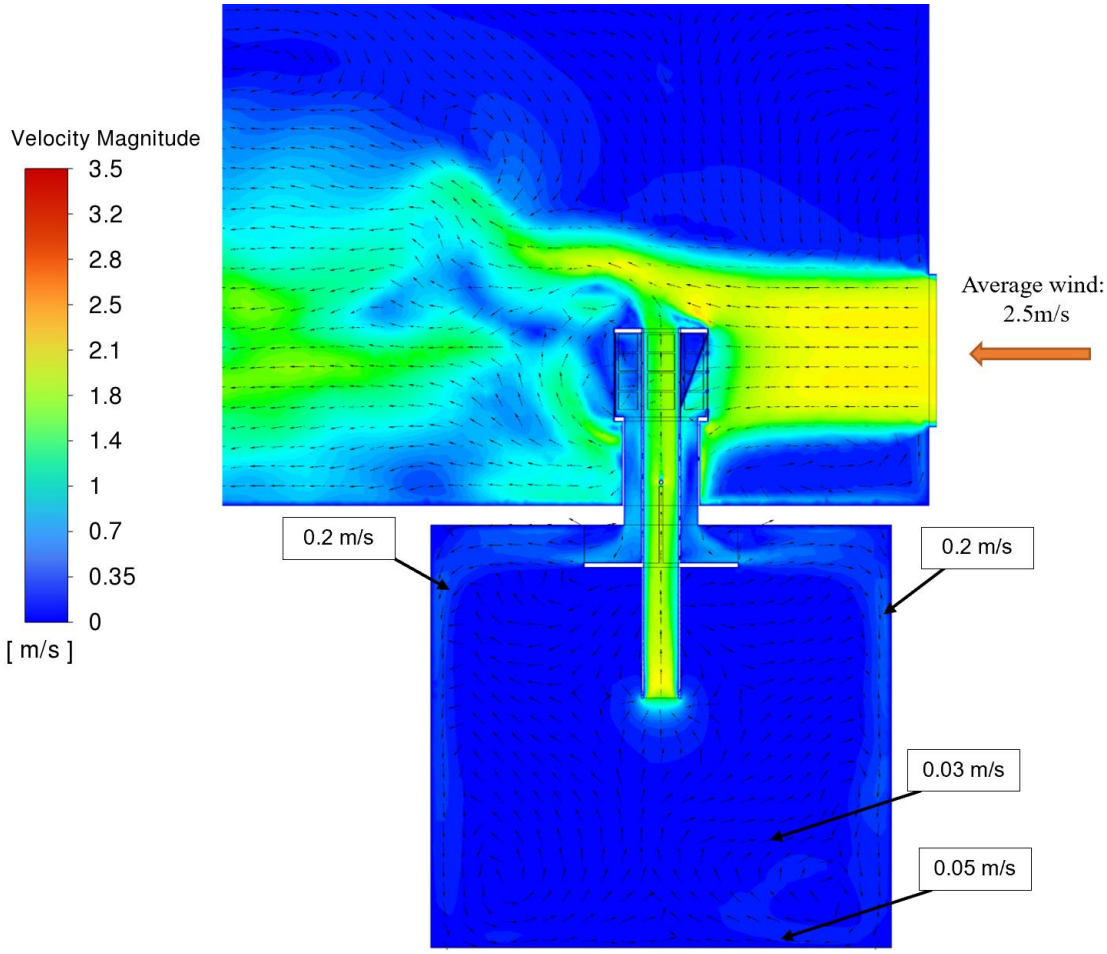


Figure 6.14 Wind speed contour and vector (in-plane) in the model

The pressure distribution (at 2m/s wind speed) and the open/off condition around the flap fin louver windcatcher at 0º and 22.5º wind direction are presented in Figure 6.15(a). A high-pressure region occurred in the front of the windward side that opened the fin in the front. The high-pressure region inside the windcatcher was caused by the lower wind speed inside than the outside. The outside pressure around the leeward side fins was all negative, and the pressure difference between the inside and outside of the fin would force the fin to attach to the windcatcher wall and close the opening.

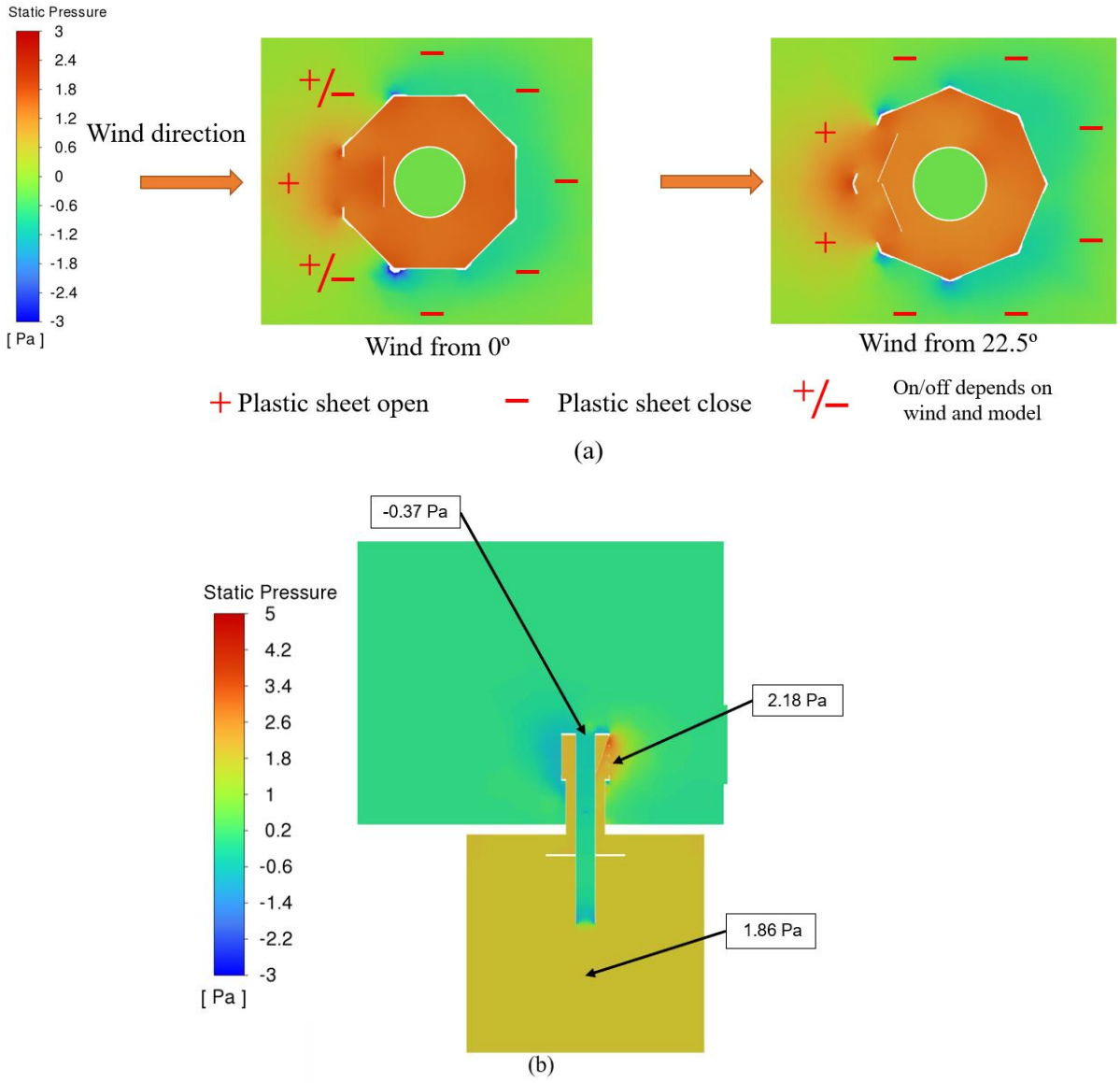


Figure 6.15 Pressure contour of the flap fins inlet windcatcher (a) Open and close status of flap fins at each opening (Top view) and (b) Static pressure around the windcatcher and the whole model (Side view)

In Figure 6.15, the pressure at the inlet was higher than the room to force the air entering the environment into the room. The pressure at the outlet was lower than the room to extract the air leaving the room from the chimney. A low-pressure zone was created above the windcatcher around the outlet opening because of the sharp edge in the front. Thus, placing the opening on the top of the windcatcher could increase the ventilation rate with a larger negative pressure around the outlet. The overall replacement ventilation was achieved by the appropriate airflow direction created by the pressure differences between the inlet, room and outlet.

### 6.2.3 Comparison to the conventional windcatcher

A conventional 8-sided windcatcher with similar geometry to this research was selected for ventilation performance comparison. After increasing the opening number to over 6 openings the ventilation rate of the 8-sided windcatcher was almost independent of the wind direction [39]. A fixed 8-sided windcatcher model with the same opening size as the flap fin louver windcatcher in this research was made. The simulation settings and outdoor wind speeds in the 8-sided windcatcher simulation were identical to the previous validation model.

The traditional 8-sided windcatcher used for comparison is shown in Figure 6.16(a), and the comparison result is shown in Figure 6.16 (b). At wind speed higher than 1m/s, the ventilation performance of the flap fin louver windcatcher was higher than the 8-sided windcatcher. In the 8-sided windcatcher, most of the air would enter the room through the two or three openings in the front, which resulted in a higher wind speed at the supply channels and a higher total pressure loss than the windcatcher with balanced supply and return channels area. Moreover, the low-pressure zone at the top of the flap fin louver windcatcher had a larger negative pressure than the back and the side of the 8-sided windcatcher and extracted more air from the outlet openings. Even though the ventilation performance of the flap fin louver windcatcher was affected by the flap fin, the ventilation performance of the flap fin louver windcatcher was still higher than the 8-sided windcatcher. As shown in Figure 6.15, the region above the windcatcher had a relatively lower pressure caused by the sharp edge in the front of the windcatcher. Thus, a larger negative pressure was created at the outlet of the flap fin louver windcatcher to extract more air from the room, which made the ventilation more effective than a traditional 8-sided windcatcher.

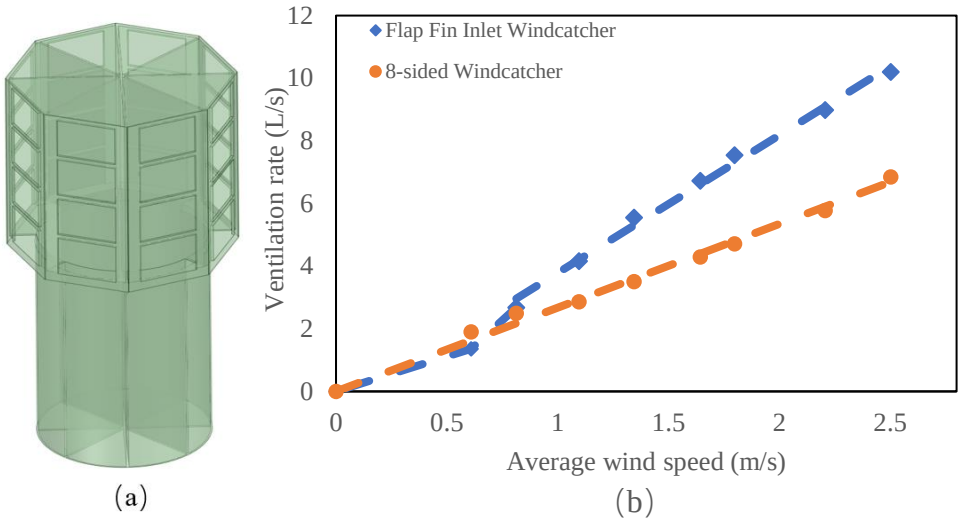


Figure 6.16 Comparison of the ventilation rate between the (a) traditional 8-sided windcatcher and (b) flap fin louver windcatcher at 0° wind

## 6.3 CFD parametric analysis of the rotary scoop windcatcher

In this section, only the parametric analysis of the rotary scoop windcatcher was conducted. As the geometry change of the flap fins louver windcatcher would have impacts on the open angle of the fins which resulted in the inaccuracy of the flap fins louver windcatcher simulation in the CFD simulation, the geometry optimization of the flap fins louver windcatcher was conducted in the experiment.

### 6.3.1 Supply-to-return channel area ratio

The impact of the supply-to-return channel area ratio on the ventilation rate was assessed and shown in Figure 6.17. It was observed that achieving an optimal ventilation rate required equivalent areas for both the supply and return channels. Deviations from this balanced ratio resulted in significant alterations in the wind speed within the channels, subsequently leading to varying levels of pressure loss. For instance, when the supply channel area was considerably smaller than that of the return channel, a substantial increase in wind speed was observed within the supply channel. This, in turn, escalated the pressure loss within the system. Similar consequences were noted when the area of the return channel was reduced.

As the shapes of the supply, circular tube, and return channel, ring-shape tube, were not

identical, the balanced velocity in different channels could not guarantee the minimization of the system friction and the parametric analysis of the supply-to-return area was necessary for the geometry optimization. By ensuring that the areas of the supply and return channels were identical, a balanced ventilation configuration was achieved in the parametric. In such cases, the wind speeds designed for both channels were equal, thus minimizing pressure loss within the system while maintaining a constant ventilation rate. Consequently, it became evident that an unbalanced supply-to-return channel ratio could significantly impact the overall ventilation rate within the room.

Furthermore, the diameter of the ducts played a crucial role in determining the ventilation rate. The final optimized model demonstrated that a balanced duct diameter of 320mm yielded the highest ventilation rate when considering a constant diameter. However, it is important to consider the manufacturing costs associated with producing a windcatcher with a specific diameter. Opting for a ready-made product available in the market, such as 300mm or 400mm, may prove to be a more cost-effective solution, despite potential slight deviations from the ideal diameter.

To minimize any discrepancies in the area difference between the supply and return channels, it is recommended to maintain a ratio of approximately 0.707 between the internal and external diameters. This approach helps to achieve a more balanced airflow distribution and enhances the overall efficiency of the windcatcher system.

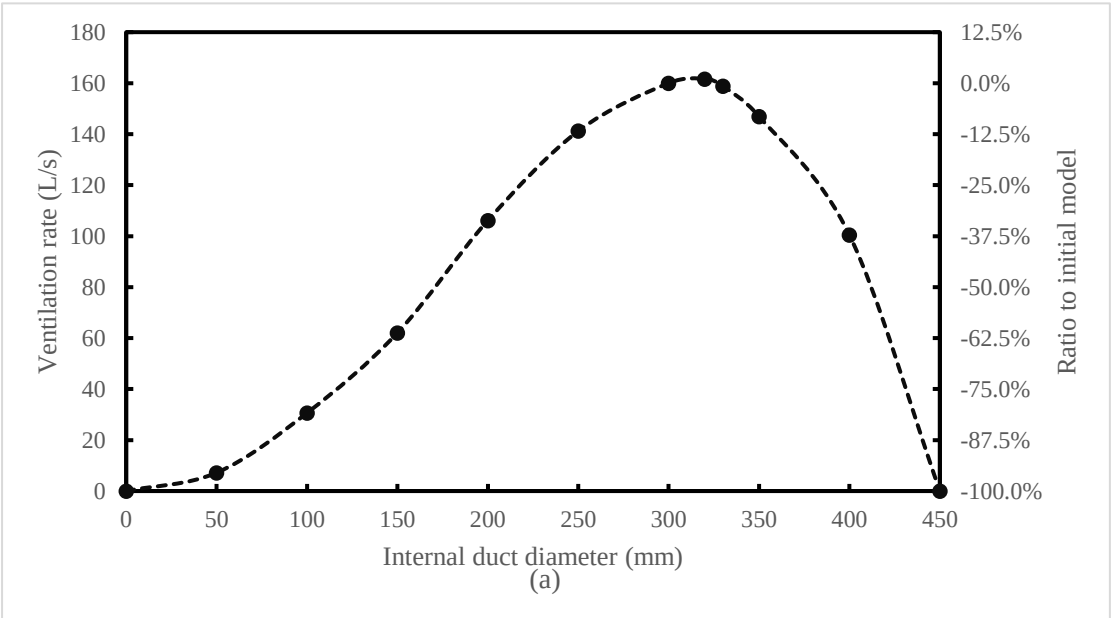

(a)

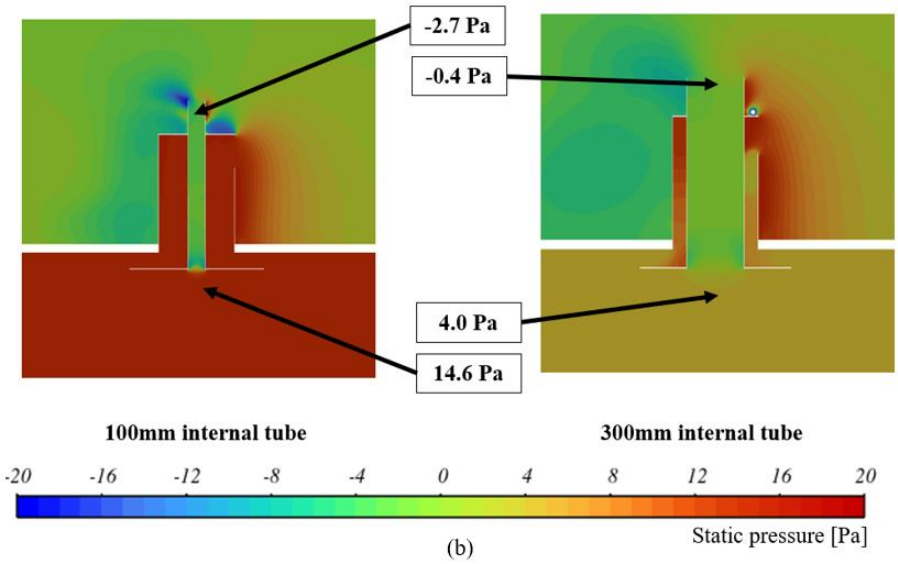


Figure 6.17 Impact of the internal duct diameter on the ventilation rate at 5m/s environment wind speed (a) Ventilation performance and (b) cross-section pressure contour comparing 2 designs.

### 6.3.2 Wing wall angle and length

The impact of both the angle and length of the wing wall on the ventilation rate has been meticulously examined and is graphically depicted in Figure 6.18. It was observed that all the windcatchers equipped with wing walls outperformed the original model in terms of ventilation performance.

In scenarios where the angle of the wing wall was less than 50 degrees, it was found that shorter wing walls led to an enhanced ventilation rate. This can be attributed to the fact that introducing a lengthy wing wall under low-angle conditions essentially extended the supply channel's length without increasing the wind scoop's area. This caused an upsurge in pressure loss without a corresponding increase in air capture, an unfavourable outcome for ventilation efficiency.

Low-angle wing walls at the wind scoop inlet could generate an extended sharp edge outside the windcatcher foundation, thus amplifying the pressure coefficient at the front. However, a longer wing wall did not contribute to a more significant increase in the pressure coefficient when compared to a shorter one. As a result, models fitted with shorter wing walls achieved a higher ventilation rate relative to those with longer wing walls.

In contrast, for larger angles exceeding 50 degrees, increasing the length of the wing wall

essentially expanded the inlet area. Consequently, windcatchers with longer wing walls demonstrated superior ventilation performance in comparison to their counterparts with shorter wing walls.

However, it is essential to consider the practical implications of extending the wing wall, as it inherently increases the size of the wind scoop. A wind scoop that is substantially larger than the windcatcher channel may not present a cost-efficient solution compared to simply opting for a larger-diameter windcatcher. As such, while a 200mm wing wall with an 80-degree angle could potentially reach the maximum ventilation rate, a more pragmatic and efficient design, considering material usage and spatial constraints, was found to be a 50mm wing wall with a 20-degree angle. This design managed to strike a balance between achieving an optimal ventilation rate and maintaining cost and space efficiency.

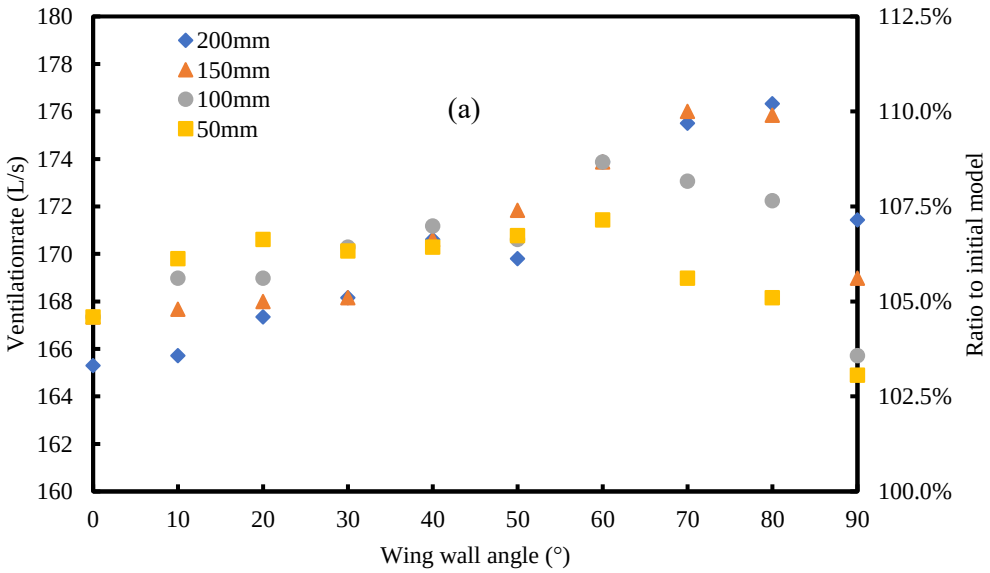

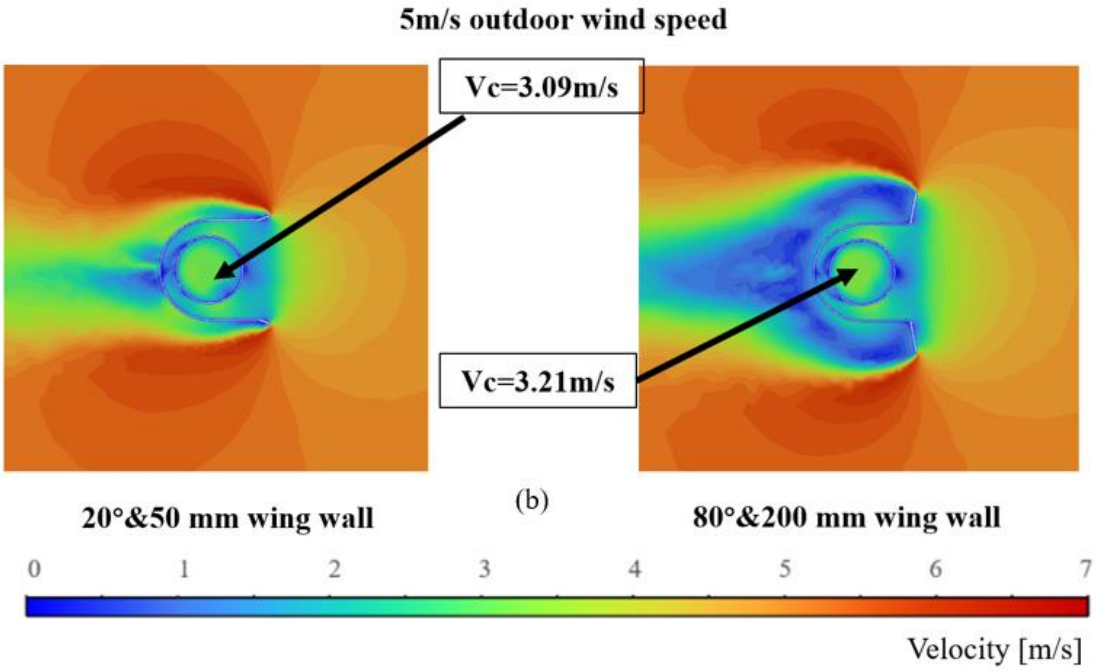


Figure 6.18Impact of the wing wall angle on the ventilation rate at 5m/s environment wind speed (a) Ventilation performance and (b) velocity contour comparisons.

### 6.3.3 Height of wind scoop and Anti-Short Circuit Device (ASCD)

The area of wind capture in a windcatcher constitutes a crucial determinant of its ventilation efficiency. The effect of modifying the height of the wind scoop on the ventilation rate was examined, with the results shown in Figure 6.19. An increase in the ventilation rate was noted when the height was increased to 200mm. This boost is largely attributable to the considerable system friction and a diminished frontal area for wind capture associated with a small inlet opening. Nonetheless, once the area of the wind scoop was expanded to approximately twice that of the supply channel area, the subsequent improvement in the ventilation rate was negligible. This observation indicates that despite further enlargements of the wind scoop area beyond 300mm, the pressure differential created by the wind was inadequate to propel additional airflow through the system. When analysing improvements in the ventilation rate, a height increment from 200mm to 300mm led to an estimated uplift of approximately 12%. Conversely, doubling the height of the wind scoop from 200mm to 400mm only resulted in a relatively modest 15% increase under identical environmental wind conditions. Hence, a height increase of the wind scoop to 300mm was determined to be the ideal strategy for ventilation

enhancement. This adjustment not only ensured a high ventilation rate but also promoted more efficient material usage, which is crucial in striking a balance between enhancing performance and reducing resource consumption.

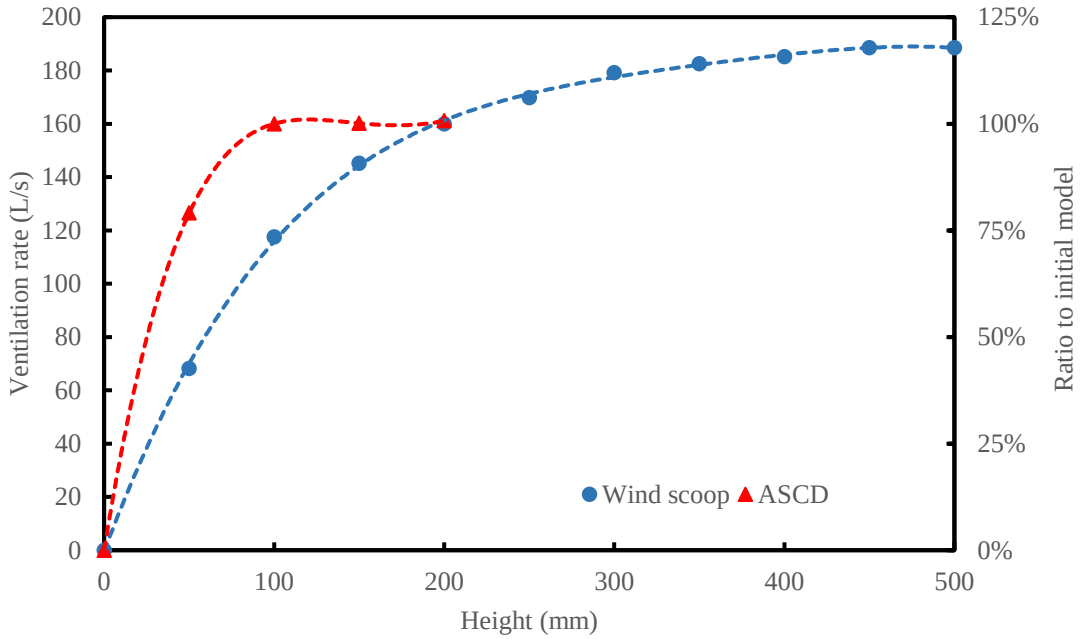


Figure 6.19 Ventilation rate to the wind scoop height at 5m/s environment wind speed.

As shown in Figure 6.19, the results showed that after reaching a height of 100mm, the ventilation rate demonstrated a near-constant trend. This plateau effect in the ventilation rate, beyond the 100mm mark, underscores the importance of this particular ASCD height in the ventilation performance of the model. Based on these findings, the initial ASCD height of 100mm was retained for further investigation. This was rooted in the understanding that any increase in height beyond this threshold would not significantly enhance the ventilation rate. Thus, maintaining the ASCD at this height aligns with the principle of optimization – achieving the highest possible ventilation performance while minimizing unnecessary material consumption and spatial requirements. This investigation into the influence of ASCD height exemplifies the holistic approach taken in this study, where every variable, no matter how ostensibly minor, is examined for its potential impact on the overall performance of the windcatcher system.

### 6.3.4 Chamfered chimney angle

Incorporating a chamfered chimney outlet can facilitate an increase in the outlet area at the region of negative pressure, whilst concurrently generating a larger zone of negative pressure behind the outlet to promote increased extraction of air from the room. Within a model featuring a rotary wind scoop, the outlet chimney could be affixed to the wind scoop, enabling simultaneous rotation. This ensures that the wind scoop constantly faces the wind, and the chamfered chimney maintains its optimal orientation without the need for electrical power.

As presented in Figure 6.20, the introduction of a chamfered chimney enhanced the ventilation performance of the initial windcatcher, with the ventilation rate continuing to rise in line with the angle of the chamfer. However, the ventilation rate tended to stabilize once the chamfered angle reached approximately 45°, peaking around a 50° chamfered angle, which resulted in a ventilation rate improvement of about 14%. The requirement for a high chimney becomes significant for a large chamfer angle exceeding 45 degrees, leading to a considerable rise in material needs, yet the ventilation rate ceases to increase with further chamfered angle increments past 45°. Consequently, a chimney cut angle of 40 degrees was selected for the final model.

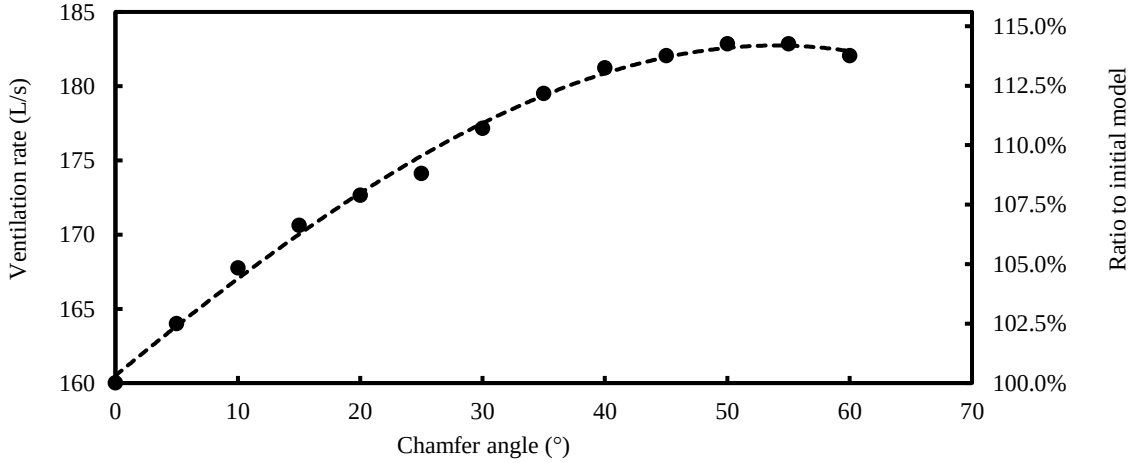


Figure 6.20 Impact of the chimney on the duct diameter at ventilation rate at 5m/s environment wind speed.

### 6.3.5 Windcatcher height and full-scale simulations

The unique sharp edge of a flat roof building, when oriented perpendicularly to the wind direction, engenders turbulent airflow above the roof surface. This turbulence, in turn, causes the wind speed profile near the building's edge in actual operational conditions to deviate substantially from those observed under controlled experimental settings. Consequently, the windcatcher's performance, when subjected to a constant environmental wind speed while simultaneously influenced by an atmospheric boundary layer shaped by the building's architecture, may differ considerably from its performance in comprehensive, full-scale simulations that also incorporate the atmospheric boundary layer. To better understand these performance variations, comparisons were drawn between full-scale simulations and those under a constant environmental wind speed.

As depicted in Figure 6.21 and Figure 6.22, the windcatcher of initial height was strategically situated at the centre of the roof, near the roof's surface. In the full-scale simulation, the wind speed near the windcatcher was nearly reduced to zero, leading to a near-zero ventilation rate. However, the ventilation rate in the full-scale simulation witnessed a significant surge when the height of the windcatcher was increased from 0.5m to 1m and thereafter, it maintained a state of equilibrium.

In contrast, under unvarying wind speed conditions in the absence of a building, the performance of the windcatcher was unaffected by the turbulence at the building edge. As a result, it demonstrated a gradual decline in response to increases in windcatcher height, mainly due to the escalating system friction. Nevertheless, the sharp edge of the building amplified the wind speed above the initial windcatcher, thereby enabling a taller windcatcher to harness the wind with a significantly greater velocity. Therefore, despite a reduction in ventilation rate due to the expanded tube length in a taller windcatcher system, the overall ventilation rate of this system still exceeded that of the initial model under constant environmental wind speed conditions.

Moreover, extending the tube length by 3m resulted in a 10% decrease in the total ventilation rate. The increase in tube length can expand the area available for sunlight capture, potentially proving beneficial for solar chimneys or other passive technologies such as heat recovery. This

finding suggests a multi-faceted approach to building design that considers the interplay between wind and solar energy, offering insights for the enhancement of both ventilation and energy efficiency.

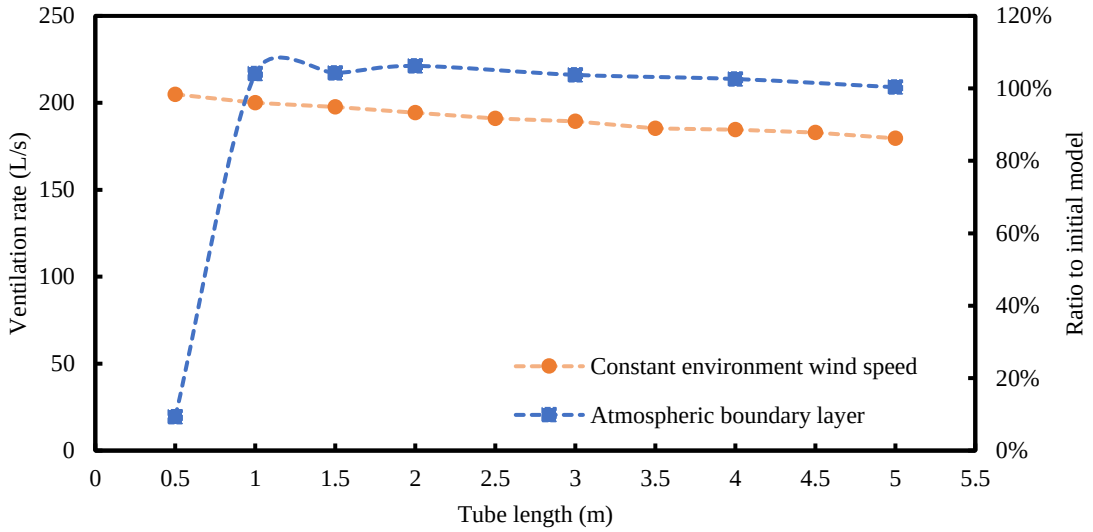


Figure 6.21 Impact of the windcatcher length at ventilation rate at 5m/s environment wind speed and full-scale simulation with atmospheric boundary layers

In the full-scale simulation, the windcatcher of initial height, when incorporated into a pitched-roof building, exhibited ventilation rates that were essentially on par with those observed under a constant environmental wind speed profile. This can be primarily attributed to the fact that the horizontal wind speed profile near the windcatcher remained remarkably stable, largely impervious to the influence exerted by the building's roof geometry. This unimpeded wind profile allows for more consistent wind-driven ventilation, closely mimicking conditions of a constant environmental wind speed.

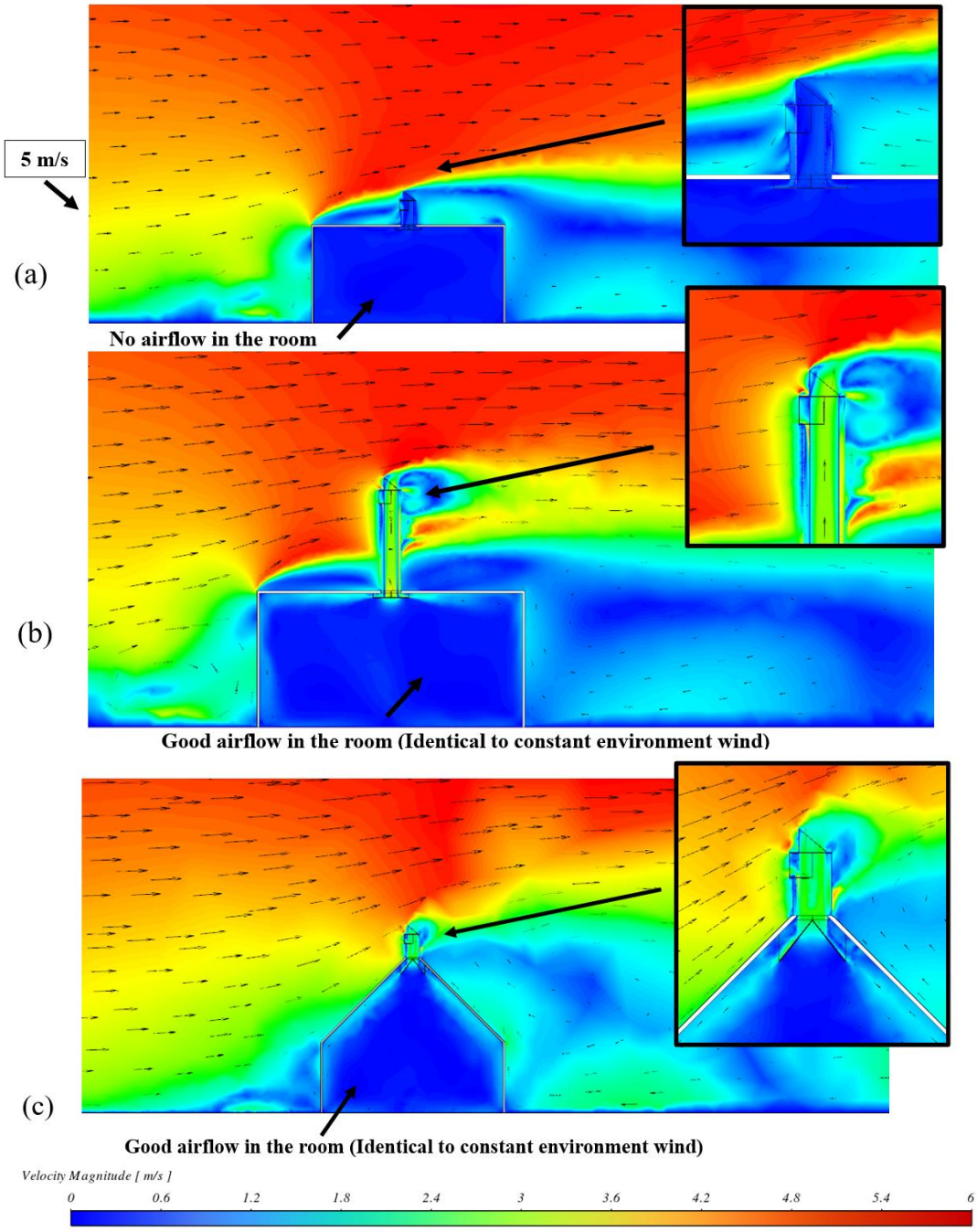


Figure 6.22 Contour of the velocity for the full-scale simulation of windcatcher with (a) initial height, (b) adjusted height (2m) and (c) initial height with pitched roof building.

In the context of the windcatcher geometry, the design process did not specifically optimize for tube length. Instead, it was recognized that the tube length would play a critical role in the windcatcher's performance, impacting factors such as wind capture, pressure differentials, and system friction. However, considering the intricate balance between these variables and the potential material and cost implications of an elongated tube, a decision was made to retain the

initial tube length for the final geometry optimization phase. Maintaining the initial tube length allowed for a focus on optimizing other elements of the windcatcher's design in the current stage of research. Meanwhile, the implications of varying tube lengths, such as changes in system friction and wind capture, can be considered in future investigations. This approach affords a more nuanced and measured design process that can better adapt to diverse architectural contexts and environmental conditions.

### 6.3.6 Combined modifications evaluation

The final iteration of the optimized model presented a combination of modifications, incorporating a chamfered angle of 40 degrees, a wind scoop height of 300mm, an internal-to-external diameter ratio of 320mm to 450mm, and a 50mm wing wall set at a 20-degree installation angle.

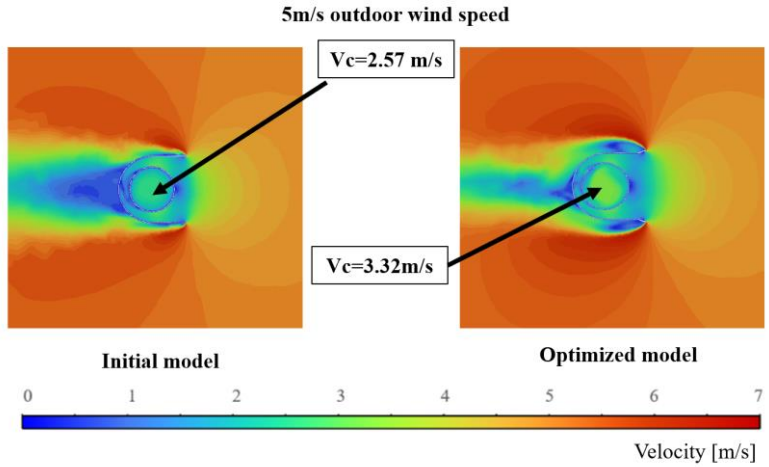

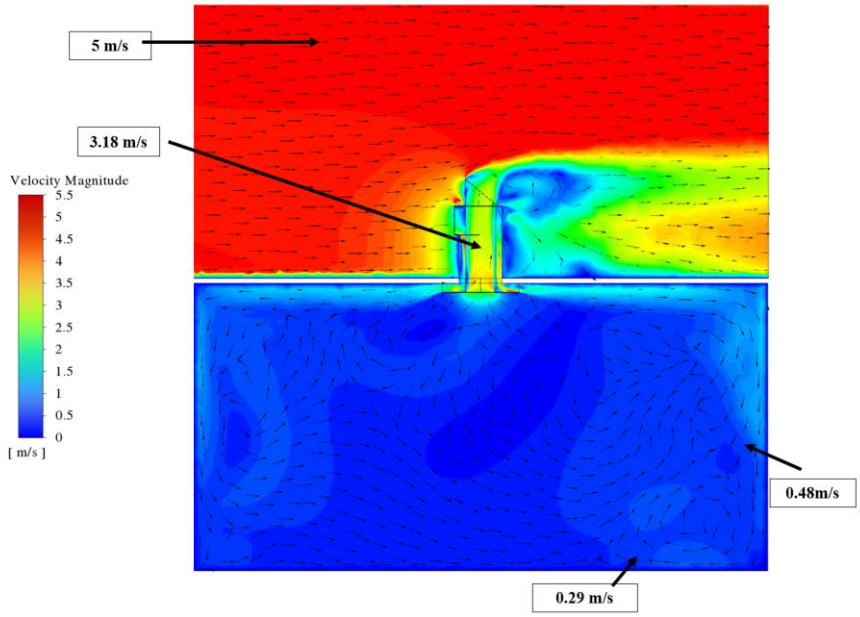


Figure 6.23 Velocity contour of the modified rotary scoop windcatcher at 5m/s environment wind speed (Top and side view)

To evaluate the performance of the optimized windcatcher, simulations were conducted under constant environmental wind speed conditions of 5m/s. The velocity distribution within the windcatcher system was analyzed and visualized through velocity contours, as shown in Figure 6.23. It was observed that the airflow within the room maintained effective circulation, ensuring the supply of fresh air to the lower levels at a comfortable velocity while facilitating efficient extraction after circulation.

Moreover, the pressure distribution within the windcatcher system was analyzed and presented through pressure contours, as depicted in Figure 6.24. Comparing the optimized windcatcher to its initial design, noticeable changes in the pressure differentials were observed. The positive pressure at the inlet experienced a slight increase from 11.4 Pa to 12.6 Pa, while the negative pressure at the outlet exhibited a significant increase from -0.7 Pa to -5.2 Pa. This substantial increase in negative pressure resulted in a rise in the pressure differential between the inlet and outlet, escalating by 47% from 12.1 Pa to 17.8 Pa. These findings demonstrate the improved performance of the windcatcher system in generating a stronger pressure differential, which facilitates enhanced airflow and ventilation efficiency under 5m/s environmental wind speed conditions.

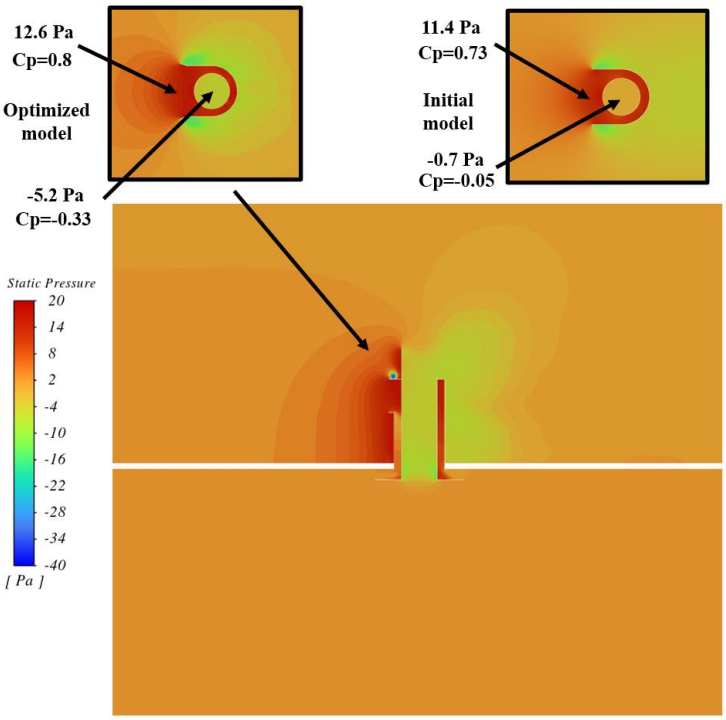


Figure 6.24 Pressure contour of the optimized rotary scoop windcatcher at 5m/s environment wind speed and the comparison of the initial and optimized model at the wind scoop region

### 6.3.7 Comparison with a conventional four-sided windcatcher

To provide a comprehensive comparative analysis, the conventional four-sided windcatcher was included alongside the optimized and initial rotary scoop windcatchers. Figure 19 presents the ventilation performance of these windcatcher designs, revealing notable differences in their capabilities. The optimized windcatcher exhibited an enhancement in overall ventilation rate, surpassing the initial model by 28% as presented in Figure 6.25. Furthermore, when compared to the four-sided windcatcher of the same dimensions and under identical environmental wind speed conditions, the modified windcatcher demonstrated an improvement in ventilation performance. Specifically, the ventilation rates achieved by the optimized windcatcher ranged from 14% to 58% higher than those of the four-sided windcatcher. The modified windcatcher not only delivered enhanced ventilation rates given the same area but also ensured a stable supply of fresh air, which remained unaffected by fluctuating wind directions in the surrounding

environment.

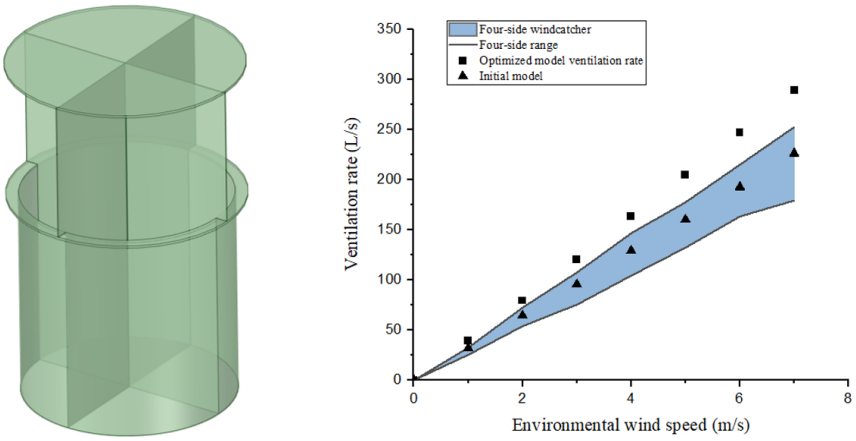


(a) (b)

Figure 6.25 Comparison to the traditional four-sided windcatcher (a) Comparison model and (b) the ventilation rates of the modified, initial rotary scoop windcatcher and the four-sided windcatcher

### 6.3.8 Discussion of study limitations and practical considerations

In the present design of the windcatcher under consideration, an open chimney structure has been employed. The primary rationale behind adopting such a straightforward construction was to simplify this investigation, with the core objective being the examination of multi-directional natural ventilation facilitated through the innovative rotary scoop design. The focus, therefore, was on exploring and optimizing the effects of the geometric parameters of the windcatcher on ventilation performance. However, it is crucial to scrutinize the practical implications of employing an open chimney in real-world applications. The feasibility of such a configuration, devoid of any protective measures, may raise concerns, given the array of potential environmental elements it could be exposed to. Key elements of potential threat include weather-based factors like rainfall, along with small animals and insects, all of which could interfere with the operation of the windcatcher and even lead to detrimental effects on indoor air quality. Given these potential vulnerabilities, it becomes clear that the incorporation of protective measures such as a chimney cap or cowl is a practical necessity. Such additions can effectively shield the outlet from various environmental elements, thereby maintaining the

functional integrity of the windcatcher. Future design iterations should thus focus not only on optimization for ventilation performance but also on ensuring robustness against external environmental factors. This will help to ensure that the windcatcher can operate effectively and consistently in a broad range of real-world conditions.

Furthermore, the current design of the windcatcher involves a bearing system that connects the rotary wind scoop to the tubes. It is observed that this bearing configuration does not provide a perfect seal between the rotating wind scoop and the static tubes, allowing for a potential gap. While this may seem like a minor oversight in design, it is of paramount importance to strive to minimize this gap, as it can provide a pathway for a possible short circuit from the inlet to the outlet. Such a short circuit would essentially bypass the intended airflow path, thereby undermining the windcatcher's ventilation performance. One potential solution to address this issue might involve the use of a ring-shaped bearing. This configuration could potentially seal off the identified gap. However, the implications of adopting such a solution must be carefully examined. The introduction of a ring-shaped bearing would likely result in increased friction, necessitating the inclusion of a larger tailplane. This, in turn, could significantly elevate both the initial capital investment and the ongoing maintenance costs relative to the current bearing system. Moreover, it would inherently increase the frictional forces, thus raising the torque requirements for rotating the wind scoop. This could introduce further complexities to the design and operational aspects of the windcatcher.

Considering these factors, for the device which will be located above the roof to enable fresh air supply, the current bearing design appears to be more advantageous. Its low maintenance demand and overall reliability appear to outweigh the potential benefits of the previously considered ring-shaped bearing. In this context, it is essential to prioritize system stability and reliability, even at the expense of some potential efficiency in ventilation performance. As such, while it remains important to strive for optimal ventilation efficiency, these other factors must also be considered in the design and implementation of the windcatcher system.

The proposed windcatcher and tube system can be manufactured from a selection of diverse materials to serve varying purposes. Transparent acrylic materials, for example, are an enticing choice for daylight to filter through, providing a natural lighting solution for the interior space.

On the other hand, the choice of metal materials could serve to enhance the system's structural strength, durability, and cost-effectiveness. A particularly intriguing application could be to construct the external duct from transparent material while coating the internal duct in black. This combination creates a fascinating interplay of solar radiation absorption and heat emission. The internal duct, being black, would efficiently absorb solar radiation, converting it into heat. The heat, in turn, is emitted to both the supply and return air. This process can serve to preheat the supply air in the outside channel and create a solar chimney in the inside channel. The system can be further refined to incorporate evaporative cooling into the supply channel. Such a mechanism can effectively precool the supply of air, particularly under suitable weather conditions. This feature can significantly enhance thermal comfort within the indoor environment, and also curtail the consumption of cooling energy, thus contributing to the overall energy efficiency of the system.

Passive heat recovery techniques such as the use of heat pipes or fins can also be integrated into the windcatcher channels. Given that the supply and return channels are in constant proximity and their airflow directions remain fixed regardless of wind direction, these heat recovery techniques could significantly enhance system efficiency.

It should be noted that in this study, the process of determining the dimensions of the windcatcher for experimental validation had to take into account several key factors. This included the dimensions of the open wind tunnel available for the experimental process, and the constraints imposed by the available spatial limits. Additional constraints, such as the need to achieve uniform wind conditions and the necessity to reach specific wind velocities, further necessitated a limit on the size of the windcatcher under examination. The overarching goal of this investigation was to validate the computational model through the use of experimental measurements. To achieve this, it was of paramount importance that the geometric properties of the windcatcher be identically replicated in the numerical modelling efforts. Moreover, any subsequent optimization processes needed to be performed based on this validated geometry. This methodological approach provided the foundation for a fair and objective comparison between the experimental and CFD investigations. In real-world applications, the determination of the windcatcher's dimensions would be governed by different factors. This might include

considering the area or volume of the building in which the windcatcher will be installed and the specific ventilation requirements associated with the building. Future research should consider investigating the ventilation performance of a full-scale windcatcher. This would entail conducting field tests or utilizing larger wind tunnels to assess the windcatcher's functionality. Additionally, comparative studies examining windcatchers of various sizes and their ventilation rates, when installed in different buildings, would further contribute to the body of knowledge surrounding this innovative ventilation technology.

In this research, the analysis of cooling effects was intentionally omitted. The decision was driven by the complexity and variability of factors influencing indoor temperatures, such as room size, the number and types of occupants and devices, and the placement and quantity of windcatchers. These variables introduce significant challenges in standardizing models to predict precise temperature reductions reliably. Consequently, this thesis focused solely on optimizing ventilation efficiency, a fundamental performance metric critical to the design and functionality of windcatchers. It is recognized that airflow distribution plays a crucial role in practical applications, significantly influenced by the strategic positioning of inlets and outlets within a space. However, these factors also depend heavily on specific requirements for passive cooling and fresh air supply, which vary widely across different building contexts. Future research will aim to incorporate these diverse parameters, potentially exploring their impact on thermal comfort and cooling load to provide a more comprehensive understanding of windcatcher performance under realistic, varied use conditions.

## 6.4 Summary

In this chapter, the numerical model of the rotary scoop windcatcher was validated by different experiment results including the ventilation rate to the environmental wind speed, wind speeds at different locations in the test room and the carbon dioxide concentration change rate measurement. The validated scaled rotary scoop windcatcher model was modified to the full-scale model and the ventilation performance was presented in this section. The parametric analysis of the full-scale rotary scoop windcatcher model was delivered and the impact of each parameter was presented in this chapter. The full-scale rotary scoop windcatcher model after

parametric analysis was investigated with uniform wind speed profiles and the ABL wind speed profiles. Different numerical flap fins louver windcatcher models were also validated by the experiment results with the details of the simulation results presented in this section.

# Chapter 7 Conclusions

## 7.1 Conclusions of the research

This research introduced two passive ventilation devices, the rotary scoop windcatcher and the flap fins louver windcatcher, designed to operate independently of environmental wind directions. A thorough review of existing literature on windcatcher technologies, including solar walls, evaporative cooling, and passive heat recovery, was performed to identify research gaps and evaluate existing solutions. These novel windcatcher systems were developed and tested using a simplified wind tunnel and test room, with various models undergoing experimentation to assess their performance in different conditions. Further, Computational Fluid Dynamics (CFD) simulations validated these experimental models and provided detailed insights into the systems' effectiveness. Moreover, the performance of the flap fin louver windcatcher was also validated in the field study with varying directions of the environment wind. Lastly, a parametric analysis of the rotary scoop windcatcher aimed to optimize ventilation efficiency by modifying design parameters like scoop size, wing walls, air channel ratios, and chimney design. In this research, the novel natural ventilation systems using multidirectional windcatchers, including a rotary scoop windcatcher design and flap fin louver windcatcher design were proposed with the function of; (1) the airflow direction and ventilation rate inside the system are fixed regardless of wind direction, (2) the supply and return airflow channels are adjacent to allow heat transfer between them for example, for heat recovery, (3) the polluted air from the outlet would not contaminate the supply air, and (4) there will be no air-short circuiting. This windcatcher addresses the issue of the incorporation of passive/low-energy heating and cooling technologies in conventional windcatchers. The multidirectional function achieved by the windcatcher system allows the windcatcher to provide a stable fresh air supply under complex environmental conditions, such as in cities with many buildings surrounding the windcatcher location. Moreover, with the fixed and adjacent supply and return channels not affected by the changing wind direction, passive/low-energy technologies can be applied in this windcatcher, such as solar heating, evaporative cooling, Phase Change Materials and heat transfer devices.

By ensuring that the passive heating and cooling can be applied to the supply air directly, the efficiency of passive heating and cooling in the ventilation system is guaranteed to reduce the building energy consumption for the low-carbon industry and indoor thermal comfort.

### 7.1.1 Conclusions of rotary wind windcatcher research

A novel dual-channel rotary scoop windcatcher was developed and tested using a prototype in a specially constructed wind tunnel and test room, demonstrating efficient ventilation unaffected by wind direction changes. The test room's airtightness was rigorously measured, and ventilation rates were evaluated under various wind speeds using both direct airspeed measurements and the tracer-gas decay method with carbon dioxide.

The wind speed at different points in the test room and the ventilation rate in the CFD model were validated by the experiment results. The average difference between the ventilation rate in the CFD model and the experiment results was 2.97%, and most of the differences were lower than 2%.

The validated experiment prototype was modified into a full-scale model in CFD to further evaluate the fresh air rates, airflow velocity and pressure distribution. The application of the anti-short circuit device (ASCD) also improved the air circulation in the ventilated space. Fresh air was supplied by the windcatcher device between 1.7 L/s/$m^2$ and 9.18 L/s/$m^2$ for an outdoor wind speed of 0.5 m/s to 2.5 m/s in the scaled experiment prototype. The full-scale rotary scoop windcatcher could provide a ventilation rate of the windcatcher from 32 L/s to 226 L/s at 1-7 m/s environment wind speed.

A parametric analysis refined the windcatcher's design, significantly enhancing airflow efficiency, including various parameters in the previously validated computational fluid dynamics (CFD) model were scrutinized to optimize the rotary scoop windcatcher. These included: (1) the ratio of supply-to-return channel area; (2) the angle and length of wing walls; (3) the height of the wind scoop; (4) chamfered chimney angles; (5) the height of the Anti-Short Circuit Device (ASCD); (6) the height of the windcatcher tube. The optimized model boasted a 28% increase in ventilation rates compared to earlier designs and performed 14% to 58% better than similar-sized conventional models under equivalent conditions. Future research

should explore passive climate control techniques and assess the performance of various windcatcher sizes in more extensive field tests.

### 7.1.2 Conclusions of the flap fin windcatcher research

A flap fin louvre windcatcher design was proposed with the same function as the rotary scoop windcatcher in the research. The windcatcher was tested in a constructed open wind tunnel and airtight test room, with the tunnel providing a stable wind speed of 0-3m/s. The ventilation performance of the flap fin louver windcatcher under different environments wind speed and directions was measured in this research, and the impact of each component was also compared, including the length, weight and open direction of the fins. Increasing the length of the fin and decreasing the mass of the fin could improve the ventilation rate effectively. With the increase of the environmental wind speeds, the ventilation rate of the flap fins windcatcher was close to the fixed windcatcher with the same opening area.

The Computational Fluid Dynamics (CFD) model was validated against experimental data, showing minimal variation in ventilation rates and an average error percentage between 2.3% and 5.6%. Field tests confirmed that the windcatcher's performance was consistent across different wind speeds and directions, and it outperformed traditional 8-sided windcatchers in terms of ventilation rate and system efficiency at wind speeds above 1m/s.

The current scaled experiment model with a diameter of 20cm could provide about 10L/s fresh air supply at 2m/s environment wind speed with an air change rate over 27 $h^{-1}$. The full-scale model investigation and ventilation rate optimization need to be tested in further research.

## 7.2 Limitations of the current research

### 7.2.1 Limitations of rotary wind windcatcher research

For a wind-induced device, the experiment and CFD simulation only consider the operations under horizontal wind directions without any internal heat gains. The buoyancy effect at low wind speed conditions and the impact of vertical wind needs to be considered in further research. The rotation part in the prototype needs to be further optimized to reduce the minimum wind

speed for rotation and improve air tightness. In future research, the geometry of the windcatcher can be further optimized, and the passive heating, cooling, dehumidification, and energy recovery technologies can be applied in the fixed supply duct. Passive heating using solar thermal and passive cooling using evaporative or absorption cooling should be investigated by experiment and field study, and the possible passive dehumidification method should be evaluated. The ventilation performance of the full-scale windcatcher should be evaluated in a larger wind tunnel and field test in further research. The optimization of the rotary wind scoop in the windcatcher also needs to be investigated to decrease the capital and maintenance cost of the windcatcher.

In the current research, the ventilation performance of the windcatcher was investigated in the experiment condition and only the horizontal wind was considered in the experiment and CFD simulation to simplify the research. However, the application of windcatchers in cities is much more complex, especially in large cities with high-rise buildings in China, where vertical wind needs to be considered in the research [143]. The solar radiation on the wall surface would also increase the vertical flow and the buoyancy effect which has to be taken into account in the actual application of the windcatcher [144]. Thus, the vertical flow and the temperature conditions need to be considered in further research including both CFD simulation and field study of the windcatcher.

The rotary wind scoop windcatcher was designed for different types of passive technology integrations. However, we only presented the initial concept and focused on the ventilation performance in the present work. The performance of the different passive cooling and heating integrations with the proposed windcatcher will be investigated in future research. Limitations of flap fins windcatcher research

Like the prototype, the windcatcher device surfaces could be constructed using transparent or glass material which could also provide some daylighting to the room and save energy from the artificial lighting system. The rotary wind scoop and tail fin could also be made of transparent materials to allow the light to pass through. The impact of this on daylighting performance should be investigated. A damper will be necessary for commercial applications to control the ventilation rate at high outdoor wind conditions to avoid discomfort and overventilation.

In the present research, the fixed supply and return channels were achieved. The airflow inside the ventilation system was similar to that of a mechanical ventilation system but the fans were replaced by natural wind power to save energy. Thus, some devices could be applied in this ventilation system with a windcatcher. Cooling devices could be added to the supply channel to reduce the temperature of the supply air or moisture in the supply air. Heat recovery devices such as heat pipes could be applied, and the heat could be transferred from the return air to the supply air continuously without the impact of changing wind directions. The moisture could be absorbed from the supply air and emitted to the return air with appropriate design in further research. So the dehumidification could also be achieved by the desiccant wheels or other passive dehumidification applications such as the silica gel [145]. Passive heating using solar energy could also be applied in the supply duct such as a solar wall. And the evaporative cooling device could be installed in the supply channel effectively reducing water wastage.

### 7.2.2 Limitations of flap fins windcatcher research

In this study, the dimensions of the windcatcher for the experiment and simulations were decided based on the size of the experimental room, the size of the experimental open wind tunnel and the available experimental space. The size of the wind tunnel was limited by the space of the experiment, uniform wind requirement and the wind speed demand which further limited the size of the windcatcher. Since we aimed to validate the numerical model with the experiment, we ensured that we replicated the same geometry in the numerical modelling work. This will ensure that a fair comparison can be made between the two approaches. In practice, the dimensions of the windcatcher can be determined based on the area/volume and ventilation demand of the building, similar to our earlier works [65, 146]. The current system is not sized based on an actual building or installation, as the current research is still in the initial stages of development. Future works can focus on evaluating how the flow rate scales on the dimensions of the windcatcher.

Regarding the materials of the windcatcher employed in the experiment, the frame in the prototype was the wood panel and the flap fin was made of 0.1mm-0.25mm polyvinyl chloride. This prototype was not designed for actual or real building installations and more work is

required to develop a close-to-market prototype, which can withstand various weather conditions. The selected materials in the experiment were due to various factors including the prototyping capabilities and cost restrictions.

The ventilation performance of the windcatcher was strongly affected by the opening angle of the fins, especially at low wind speed conditions. The connection at the joint and the mass of the fin had a large impact on the fin's open angle. In the current prototype, the fin mass was minimized by using a light and thin PVC material, but other materials like metal foil/film could be considered. Balancing the mass of the fin to reduce the impact of fin mass and decrease the friction at the hinge joint is necessary for optimizing performance.

The initial results showed that the adjacent fins would be in contact with each other, limiting the open angle of fins in specific wind directions, and this issue resulted in the different fin open angles at the wind from edge condition (22.5° wind). The blocking effect limited the performance of the flap fin louver windcatcher when the flap fin design was applied in the traditional four-side windcatcher. Thus, the final windcatcher in this research had an eight-sided design. In future research, the face number of the flap fin louver windcatcher can be further increased, and the issue can be avoided by a larger angle between the adjacent windcatcher face. The opening size could also be smaller than the face of the windcatcher to avoid the adjacent fins blocking each other.

Furthermore, to increase the opening angle of the flap fin, a necessary gap between the external to internal duct has to be provided in the prototype. With the limitation of the total windcatcher area and the gap, the current section area of the supply duct and return duct was not balanced and the ventilation rate was not maximized. Further optimization of the supply-to-return area ratio needs to be applied in the later application to improve ventilation performance.

An open exhaust or chimney was used in this windcatcher design. However, an open chimney without any protection was not practical for real applications because of the entry of rain, snow and insects. The exhaust outlet needs to be integrated with a chimney cap or cowl to protect the outlet from the rain or be combined with a rotary turbine ventilator or a flap fin outlet design.

Finally, the current research tests the ventilation performance of the flap windcatcher and the windcatcher integrated with the passive technologies needs to be investigated further, including

solar heating using the windcatcher tube or roof, evaporative cooling, heat pipe heat recovery, earth-air heat exchanger or phase change materials. The internal duct could be further extended above the top of the windcatcher and painted black to generate a solar chimney effect and increase the ventilation rate. The water spray system could also be placed in the supply channel to cool the supply air. The heat recovery can be achieved with metal fins, tubes or heat pipes between the supply and return channels as the channels were adjacent and the airflow direction would not be changed during the operation.

## 7.3 Future works

In future research, the geometry of the flap fins windcatcher needs to be further optimized, such as adjusting the surface of the windcatcher faces and using deformable fins. The ventilation performance of a larger windcatcher with an appropriate flap fin design should be evaluated in a larger wind tunnel in further research. The flap fin design was applied in this research to create a controlled inlet, and a similar flap fin design could also be used in an extract chimney as an outlet with a reversed fin direction, which can avoid the reverse flow of pollutants. The prototype of the rotary scoop windcatcher needs to be further developed based on the results of the parametric analysis for field tests and commercial use.

Passive heating, cooling, and energy recovery technologies need to be applied in the rotary scoop windcatcher and flap fins windcatcher. Passive heating using solar thermal and passive cooling using evaporative or absorption cooling should be investigated by experiment and field study, and the possible passive dehumidification method should be evaluated. The passive heat recovery using metal fins or heat pipes needs to be applied in the windcatchers and investigated in the field test and experiment results.

The passive cooling achieved by the windcatcher systems should also be applied to the industry beyond residential buildings, such as the passive cooling of the workstation and battery in the room.

## 7.4 Contributions to knowledge

In this research, the research gap of multidirectional natural ventilation devices for passive technologies integration is filled with experimental and numerical methods. The achievements of this research are summarised in the following points:

1. Two passive ventilation devices were proposed which had a ventilation performance independent of the environmental wind directions.
2. A rotary scoop windcatcher was developed from the current ventilation device, wind scoop and chimney, and the rotary scoop windcatcher had a higher ventilation performance than the current four-side conventional windcatcher after the parametric analysis.
3. A flap fins windcatcher provided the same function as the rotary scoop windcatcher without the rotating components using a new flap fin mechanism which was never applied in the natural ventilation device.
4. The prototypes of the rotary scoop windcatcher and the flap fins windcatcher were manufactured and tested in the wind tunnel experiments.
5. The numerical models of the rotary scoop windcatcher and the flap fins windcatcher were generated based on the experiment prototypes and validated by the experiment results.
6. The parametric analysis of the rotary scoop windcatcher and the flap fins windcatcher was investigated to improve the ventilation performance of the windcatchers.
7. A heat recovery design with a high heat recovery efficiency for the dual-channel windcatcher was proposed which can be applied in the rotary scoop windcatcher and the flap fins windcatcher.

# References


1. Saadatian, O., L.C. Haw, K. Sopian, and M.Y. Sulaiman, *Review of windcatcher technologies.* Renewable and Sustainable Energy Reviews, 2012. **16**(3): p. 1477-1495.
2. He, B.-j., L. Yang, M. Ye, B. Mou, and Y. Zhou, *Overview of rural building energy efficiency in China.* Energy Policy, 2014. **69**: p. 385-396.
3. Pérez-Lombard, L., J. Ortiz, and C. Pout, *A review on buildings energy consumption information.* Energy and Buildings, 2008. **40**(3): p. 394-398.
4. Liu, P., M. Justo Alonso, and H.M. Mathisen, *Heat recovery ventilation design limitations due to LHC for different ventilation strategies in ZEB.* Building and Environment, 2022. **224**: p. 109542.
5. IEA, *The Future of Cooling-Opportunities for energy-efficient air conditioning*. 2018.
6. Chan, H.-Y., S.B. Riffat, and J. Zhu, *Review of passive solar heating and cooling technologies.* Renewable and Sustainable Energy Reviews, 2010. **14**(2): p. 781-789.
7. Zomorodian, Z.S., M. Tahsildoost, and M. Hafezi, *Thermal comfort in educational buildings: A review article.* Renewable and Sustainable Energy Reviews, 2016. **59**: p. 895-906.
8. Li, J., C. Jimenez-Bescos, J.K. Calautit, and J. Yao, *Evaluating the energy-saving potential of earth-air heat exchanger (EAHX) for Passivhaus standard buildings in different climates in China.* Energy and Buildings, 2023: p. 113005.
9. Jomehzadeh, F., H.M. Hussen, J.K. Calautit, P. Nejat, and M.S. Ferwati, *Natural ventilation by windcatcher (Badgir): A review on the impacts of geometry, microclimate and macroclimate.* Energy and Buildings, 2020. **226**: p. 110396.
10. Ghalam, N.Z., M. Farrokhzad, and H. Nazif, *Investigation of optimal natural ventilation in residential complexes design for temperate and humid climates.* Sustainable Energy, Grids and Networks, 2021. **27**: p. 100500.
11. Nasrollahi, N. and P. Ghobadi, *Field measurement and numerical investigation of natural cross-ventilation in high-rise buildings; Thermal comfort analysis.* Applied Thermal Engineering, 2022. **211**: p. 118500.
12. Bay, E., A. Martinez-Molina, and W.A. Dupont, *Assessment of natural ventilation strategies in historical buildings in a hot and humid climate using energy and CFD simulations.* Journal of Building Engineering, 2022. **51**: p. 104287.
13. Zhang, H., D. Yang, V.W.Y. Tam, Y. Tao, G. Zhang, S. Setunge, and L. Shi, *A critical review of combined natural ventilation techniques in sustainable buildings.* Renewable and Sustainable Energy Reviews, 2021. **141**: p. 110795.
14. Bamdad, K., S. Matour, N. Izadyar, and T. Law, *SIntroducing extended natural ventilation index for buildings under the present and future changing climates.* Building and Environment, 2022: p. 109688.
15. Pelletier, K. and J. Calautit, *Analysis of the performance of an integrated multistage helical coil heat transfer device and passive cooling windcatcher for buildings in hot climates.* Journal of Building Engineering, 2022. **48**: p. 103899.
16. Sangdeh, P.K. and N. Nasrollahi, *Windcatchers and their applications in contemporary architecture.* Energy and Built Environment, 2022. **3**(1): p. 56-72.

17. He, Y., Y. Chu, H. Zang, J. Zhao, and Y. Song, *Experimental and CFD study of ventilation performance enhanced by roof window and mechanical ventilation system with different design strategies.* Building and Environment, 2022. **224**: p. 109566.
18. Jafari, S. and V. Kalantar, *Numerical simulation of natural ventilation with passive cooling by diagonal solar chimneys and windcatcher and water spray system in a hot and dry climate.* Energy and Buildings, 2022. **256**: p. 111714.
19. Ghoulem, M., K. El Moueddeb, E. Nehdi, F. Zhong, and J. Calautit, *Analysis of passive downdraught evaporative cooling windcatcher for greenhouses in hot climatic conditions: Parametric study and impact of neighbouring structures.* Biosystems Engineering, 2020. **197**: p. 105-121.
20. Noroozi, A. and Y. Veneris, *Thermal Assessment of a Novel Combine Evaporative Cooling Wind Catcher.* Energies, 2018. **11**: p. 442.
21. Calautit, J.K., B.R. Hughes, and S.S. Shahzad, *CFD and wind tunnel study of the performance of a uni-directional wind catcher with heat transfer devices.* Renewable Energy, 2015. **83**: p. 85-99.
22. Gilvaei, Z.M., A.H. Poshtiri, and A.M. Akbarpoor, *A novel passive system for providing natural ventilation and passive cooling: Evaluating thermal comfort and building energy.* Renewable Energy, 2022.
23. Varela-Boydo, C.A., S.L. Moya, and R. Watkins, *Analysis of traditional windcatchers and the effects produced by changing the size, shape, and position of the outlet opening.* Journal of Building Engineering, 2021. **33**: p. 101828.
24. Afshin, M., A. Sohankar, M.D. Manshadi, and M.K. Esfeh, *An experimental study on the evaluation of natural ventilation performance of a two-sided wind-catcher for various wind angles.* Renewable Energy, 2016. **85**: p. 1068-1078.
25. Montazeri, H., F. Montazeri, R. Azizian, and S. Mostafavi, *Two-sided wind catcher performance evaluation using experimental, numerical and analytical modeling.* Renewable Energy, 2010. **35**(7): p. 1424-1435.
26. Dorizas, P.V., S. Samuel, M. Dejan, Y. Keqin, M.-M. Dimitris, and L. Tom, *Performance of a natural ventilation system with heat recovery in UK classrooms: An experimental study.* Energy and Buildings, 2018. **179**: p. 278-291.
27. Jiang, Y. and Q. Chen, *Effect of fluctuating wind direction on cross natural ventilation in buildings from large eddy simulation.* Building and Environment, 2002. **37**(4): p. 379-386.
28. Li, J., J. Calautit, C. Jimenez-Bescos, and S. Riffat, *Experimental and numerical evaluation of a novel dual-channel windcatcher with a rotary scoop for energy-saving technology integration.* Building and Environment, 2023: p. 110018.
29. Mahon, H., D. Friedrich, and B. Hughes, *Wind tunnel test and numerical study of a multi-sided wind tower with horizontal heat pipes.* Energy, 2022. **260**: p. 125118.
30. Khan, N., Y. Su, and S.B. Riffat, *A review on wind driven ventilation techniques.* Energy and Buildings, 2008. **40**(8): p. 1586-1604.
31. Li, J., J.K. Calautit, and C. Jimenez-Bescos, *Experiment and numerical investigation of a novel flap fin louver windcatcher for multi-directional natural ventilation and passive technology integration.* Building and Environment, 2023. **242**: p. 110429.
32. Kumar, N., R. Bardhan, T. Kubota, Y. Tominaga, and M. Shirzadi, *Parametric study on*

*vertical void configurations for improving ventilation performance in the mid-rise apartment building.* Building and Environment, 2022. **215**: p. 108969.
33. Liu, M., C. Jimenez-Bescos, and J. Calautit, *CFD investigation of a natural ventilation wind tower system with solid tube banks heat recovery for mild-cold climate.* Journal of Building Engineering, 2022. **45**: p. 103570.
34. Nejat, P., M. Salim Ferwati, J. Calautit, A. Ghahramani, and M. Sheikhshahrokhdehkordi, *Passive cooling and natural ventilation by the windcatcher (Badgir): An experimental and simulation study of indoor air quality, thermal comfort and passive cooling power.* Journal of Building Engineering, 2021. **41**: p. 102436.
35. Moghtader Gilvaei, Z., A. Haghighi Poshtiri, and A. Mirzazade Akbarpoor, *A novel passive system for providing natural ventilation and passive cooling: Evaluating thermal comfort and building energy.* Renewable Energy, 2022. **198**: p. 463-483.
36. Foroozesh, J., S.H. Hosseini, A.J. Ahmadian Hosseini, F. Parvaz, K. Elsayed, N. Uygur Babaoğlu, K. Hooman, and G. Ahmadi, *CFD modeling of the building integrated with a novel design of a one-sided wind-catcher with water spray: Focus on thermal comfort.* Sustainable Energy Technologies and Assessments, 2022. **53**: p. 102736.
37. Moosavi, L., M. Zandi, M. Bidi, E. Behroozizade, and I. Kazemi, *New design for solar chimney with integrated windcatcher for space cooling and ventilation.* Building and Environment, 2020. **181**: p. 106785.
38. Ghoulem, M., K. El Moueddeb, E. Nehdi, F. Zhong, and J.K. Calautit, *Design of a Passive Downdraught Evaporative Cooling Windcatcher (PDEC-WC) System for Greenhouses in Hot Climates.* Energies, 2020. **13**: p. 2934.
39. Farouk, M., *Comparative study of hexagon & square windcatchers using CFD simulations.* Journal of Building Engineering, 2020. **31**: p. 101366.
40. Harrouz, J.P., K. Ghali, and N. Ghaddar, *Integrated solar – Windcatcher with dew-point indirect evaporative cooler for classrooms.* Applied Thermal Engineering, 2021. **188**: p. 116654.
41. Jones, B.M. and R. Kirby, *Quantifying the performance of a top–down natural ventilation Windcatcher™.* Building and Environment, 2009. **44**(9): p. 1925-1934.
42. Chohan, A.H. and J. Awad, *Wind Catchers: An Element of Passive Ventilation in Hot, Arid and Humid Regions, a Comparative Analysis of Their Design and Function.* Sustainability (Switzerland), 2022. **14**(17).
43. Elmualim, A.A., *Evaluating the performance of windcatchers for natural ventilation*. 2003, University of Reading.
44. Ionescu, C., T. Baracu, G.-E. Vlad, H. Necula, and A. Badea, *The historical evolution of the energy efficient buildings.* Renewable and Sustainable Energy Reviews, 2015. **49**: p. 243-253.
45. Calautit, J.K., B.R. Hughes, and D.S.N.M. Nasir, *Climatic analysis of a passive cooling technology for the built environment in hot countries.* Applied Energy, 2017. **186**: p. 321-335.
46. Aydin, Y.C. and P.A. Mirzaei, *Wind-driven ventilation improvement with plan typology alteration: A CFD case study of traditional Turkish architecture.* Building Simulation, 2017. **10**(2): p. 239-254.
47. Jomehzadeh, F., H.M. Hussen, J.K. Calautit, P. Nejat, and M.S. Ferwati, *Natural*

*ventilation by windcatcher (Badgir): A review on the impacts of geometry, microclimate and macroclimate.* Energy and Buildings, 2020. **226**.
48. Bahadori, M.N., A. Dehghani-Sanij, and A. Sayigh, *Wind Towers*. 2016: Springer.
49. Morales, X., F.Z. Sierra-Espinosa, S.L. Moya, and F. Carrillo, *Thermal effectiveness of wind-tower with heated exit-wall and inlet-air humidification: Effects of winter and summertime.* Building and Environment, 2021. **204**: p. 108110.
50. Reyes, V.A., F.Z. Sierra-Espinosa, S.L. Moya, and F. Carrillo, *Flow field obtained by PIV technique for a scaled building-wind tower model in a wind tunnel.* Energy and Buildings, 2015. **107**: p. 424-433.
51. Haghighi, A.P., S.H. Pakdel, and A. Jafari, *A study of a wind catcher assisted adsorption cooling channel for natural cooling of a 2-storey building.* Energy, 2016. **102**: p. 118-138.
52. O'Connor, D., J.K. Calautit, and B.R. Hughes, *A novel design of a desiccant rotary wheel for passive ventilation applications.* Applied Energy, 2016. **179**: p. 99-109.
53. Montazeri, H. and R. Azizian, *Experimental study on natural ventilation performance of one-sided wind catcher.* Building and Environment, 2008. **43**(12): p. 2193-2202.
54. Pan, W., S. Liu, S. Li, X. Cheng, H. Zhang, Z. Long, T. Zhang, and Q. Chen, *A model for calculating single-sided natural ventilation rate in an urban residential apartment.* Building and Environment, 2019. **147**: p. 372-381.
55. Zhang, B., H. Hu, H. Kikumoto, and R. Ooka, *Turbulence-induced ventilation of an isolated building: Ventilation route identification using spectral proper orthogonal decomposition.* Building and Environment, 2022. **223**: p. 109471.
56. Farouk, M., *Comparative study of hexagon & square windcatchers using CFD simulations.* Journal of Building Engineering, 2020. **31**.
57. Saif, J., A. Wright, S. Khattak, and K. Elfadli, *Keeping cool in the desert: Using wind catchers for improved thermal comfort and indoor air quality at half the energy.* Buildings, 2021. **11**(3).
58. Poshtiri, A.H. and S.M. Mohabbati, *Performance analysis of wind catcher integrated with shower cooling system to meet thermal comfort conditions in buildings.* Journal of Cleaner Production, 2017. **148**: p. 452-466.
59. Ghoulem, M., K. El Moueddeb, E. Nehdi, F. Zhong, and J. Calautit, *Design of a Passive Downdraught Evaporative Cooling Windcatcher (PDEC-WC) System for Greenhouses in Hot Climates.* Energies, 2020. **13**(11): p. 2934.
60. Kalantar, V., *Numerical simulation of cooling performance of wind tower (Baud-Geer) in hot and arid region.* Renewable Energy, 2009. **34**(1): p. 246-254.
61. Nejat, P., J.K. Calautit, M.Z.A. Majid, B.R. Hughes, I. Zeynali, and F. Jomehzadeh, *Evaluation of a two-sided windcatcher integrated with wing wall (as a new design) and comparison with a conventional windcatcher.* Energy and Buildings, 2016. **126**: p. 287-300.
62. Nejat, P., J.K. Calautit, M.Z.A. Majid, B.R. Hughes, and F. Jomehzadeh, *Anti-short-circuit device: A new solution for short-circuiting in windcatcher and improvement of natural ventilation performance.* Building and Environment, 2016. **105**: p. 24-39.
63. Soutullo, S., C. Sanjuan, and M.R. Heras, *Energy performance evaluation of an evaporative wind tower.* Solar Energy, 2012. **86**(5): p. 1396-1410.

64. Khan, M.N. and I. Janajreh, *Transevaporative cooling performance of a three-sided wind catcher.* Jordan Journal of Mechanical and Industrial Engineering, 2017. **11**(Specialissue): p. 225-233.
65. Calautit, J.K. and B.R. Hughes, *Measurement and prediction of the indoor airflow in a room ventilated with a commercial wind tower.* Energy and Buildings, 2014. **84**: p. 367-377.
66. Ghadiri, M.H., N.L.N. Ibrahim, and M. Dehnavi, *The effect of tower height in square plan wind catcher on its thermal behavior.* Australian Journal of Basic and Applied Sciences, 2011. **5**(9): p. 381-385.
67. Zaki, A., P. Richards, and R. Sharma, *The effect of onset turbulent flows on ventilation with a two-sided rooftop windcatcher.* Journal of Wind Engineering and Industrial Aerodynamics, 2022. **225**: p. 104993.
68. Zaki, A. and R. Sharma, *The effect of external airflows on ventilation with a rooftop windcatcher.* Journal of Wind Engineering and Industrial Aerodynamics, 2021. **219**: p. 104799.
69. Esfeh, M.K., A.A. Dehghan, M.D. Manshadi, and S. Mohagheghian, *Visualized flow structure around and inside of one-sided wind-catchers.* Energy and Buildings, 2012. **55**: p. 545-552.
70. Gharakhani, A., E. Sediadi, M. Roshan, and H. Bagheri Sabzevar, *Experimental study on perfomance of wind catcher in tropical climate.* ARPN Journal of Engineering and Applied Sciences, 2017. **12**: p. 2551-2555.
71. Zaki, A., P. Richards, and R. Sharma, *Analysis of airflow inside a two-sided wind catcher building.* Journal of Wind Engineering and Industrial Aerodynamics, 2019. **190**: p. 71-82.
72. Pakari, A. and S. Ghani, *Airflow assessment in a naturally ventilated greenhouse equipped with wind towers: numerical simulation and wind tunnel experiments.* Energy and Buildings, 2019. **199**: p. 1-11.
73. Al Touma, A., K. Ghali, N. Ghaddar, and N. Ismail, *Solar chimney integrated with passive evaporative cooler applied on glazing surfaces.* Energy, 2016. **115**: p. 169-179.
74. Bahadori, M.N., M. Mazidi, and A.R. Dehghani, *Experimental investigation of new designs of wind towers.* Renewable Energy, 2008. **33**(10): p. 2273-2281.
75. Jomehzadeh, F., P. Nejat, J.K. Calautit, M.B.M. Yusof, S.A. Zaki, B.R. Hughes, and M.N.A.W.M. Yazid, *A review on windcatcher for passive cooling and natural ventilation in buildings, Part 1: Indoor air quality and thermal comfort assessment.* Renewable and Sustainable Energy Reviews, 2017. **70**: p. 736-756.
76. Belatrache, D., S. Bentouba, and M. Bourouis, *Numerical analysis of earth air heat exchangers at operating conditions in arid climates.* International Journal of Hydrogen Energy, 2016. **42**.
77. Long, T., N. Zhao, W. Li, S. Wei, Y. Li, J. Lu, S. Huang, and Z. Qiao, *Numerical simulation of diurnal and annual performance of coupled solar chimney with earth-to-air heat exchanger system.* Applied Thermal Engineering, 2022. **214**: p. 118851.
78. Jassim, J.A.A.W., S.A. Hassan, and B.H. Maula, *Design of wind catcher for earth air heat exchangers to rationalize energy consumption.* Journal of Advanced Research in Fluid Mechanics and Thermal Sciences, 2020. **65**(2): p. 286-294.

79. Calautit, J.K., D. O'Connor, P.W. Tien, S. Wei, C.A.J. Pantua, and B. Hughes, *Development of a natural ventilation windcatcher with passive heat recovery wheel for mild-cold climates: CFD and experimental analysis.* Renewable Energy, 2020. **160**: p. 465-482.
80. Calautit, J.K., D. O'Connor, and B.R. Hughes, *A natural ventilation wind tower with heat pipe heat recovery for cold climates.* Renewable Energy, 2016. **87**: p. 1088-1104.
81. Calautit, J., D. O'Connor, S. Shahzad, K. Calautit, and B. Hughes, *Numerical and experimental analysis of a natural ventilation windcatcher with passive heat recovery for mild-cold climates.* Energy Procedia, 2019. **158**: p. 3125-3130.
82. Barreto, G., K. Qu, Y. Wang, M. Iten, and S. Riffat, *An innovative window heat recovery (WHR) system with heat pipe technology: Analytical, CFD, experimental analysis and building retrofit performance.* Energy Reports, 2022. **8**: p. 3289-3305.
83. Anter, A.G., A.A. Sultan, A.A. Hegazi, and M.A. El Bouz, *Thermal performance and energy saving using phase change materials (PCM) integrated in building walls.* Journal of Energy Storage, 2023. **67**: p. 107568.
84. Abdo, P., B.P. Huynh, A. Braytee, and R. Taghipour, *An experimental investigation of the thermal effect due to discharging of phase change material in a room fitted with a windcatcher.* Sustainable Cities and Society, 2020. **61**.
85. Seidabadi, L., H. Ghadamian, and M. Aminy, *A novel integration of PCM with wind-catcher skin material in order to increase heat transfer rate.* International Journal of Renewable Energy Development, 2019. **8**(1): p. 1-6.
86. Li, L. and C.M. Mak, *The assessment of the performance of a windcatcher system using computational fluid dynamics.* Building and Environment, 2007. **42**(3): p. 1135-1141.
87. Li, J., J. Calautit, and C. Jimenez-Bescos, *Experiment and numerical investigation of a novel flap fin louver windcatcher for multi-directional natural ventilation and passive technology integration.* Building and Environment, 2023: p. 110429.
88. Feddema, J.J., *A Revised Thornthwaite-Type Global Climate Classification.* Physical Geography, 2005. **26**(6): p. 442-466.
89. Zhang, M. and Y. Gao, *Time of emergence in climate extremes corresponding to Köppen-Geiger classification.* Weather and Climate Extremes, 2023. **41**: p. 100593.
90. Beck, H.E., N.E. Zimmermann, T.R. McVicar, N. Vergopolan, A. Berg, and E.F. Wood, *Present and future Köppen-Geiger climate classification maps at 1-km resolution.* Scientific Data, 2018. **5**(1): p. 180214.
91. Peel, M.C., B.L. Finlayson, and T.A. McMahon, *Updated world map of the Köppen-Geiger climate classification.* Hydrol. Earth Syst. Sci., 2007. **11**(5): p. 1633-1644.
92. Oropeza-Perez, I. and P.A. Østergaard, *Active and passive cooling methods for dwellings: A review.* Renewable and Sustainable Energy Reviews, 2018. **82**: p. 531-544.
93. Ahmed, T., P. Kumar, and L. Mottet, *Natural ventilation in warm climates: The challenges of thermal comfort, heatwave resilience and indoor air quality.* Renewable and Sustainable Energy Reviews, 2021. **138**: p. 110669.
94. Suhendri, M.D. Koerniawan, and R.R. Alprianti, *Solar chimney as a natural ventilation strategy for elementary school in urban area.* AIP Conference Proceedings, 2018. **1984**(1).

95. Antaryama, I.G.N., *APPLICABILITY OF DIRECT EVAPORATIVE COOLING FOR LOWRISE RESIDENTIAL BUILDING IN SURABAYA.* Journal of Architecture and Built Environment,, 2022. **49**(July 2022): p. 65-74.
96. Zulkurnain, H., M.M. Mohd Suffian, and S. Nancy Julius, *Performance of The Direct Evaporative Cooler (DEC) Operating in A Hot and Humid Region of Sabah Malaysia.* Journal of Advanced Research in Fluid Mechanics and Thermal Sciences, 2022. **93**(2): p. 17-27.
97. Arumugam, P., V. Ramalingam, and P. Vellaichamy, *Effective PCM, insulation, natural and/or night ventilation techniques to enhance the thermal performance of buildings located in various climates – A review.* Energy and Buildings, 2022. **258**: p. 111840.
98. Schnieders, J., W. Feist, and L. Rongen, *Passive Houses for different climate zones.* Energy and Buildings, 2015. **105**: p. 71-87.
99. Zhou, J., X. Zhang, J. Xie, and J. Liu, *Effects of elevated air speed on thermal comfort in hot-humid climate and the extended summer comfort zone.* Energy and Buildings, 2023. **287**: p. 112953.
100. Hlaing, T.S. and S. Kojima, *Comparative Study on Performance of Wind-Catcher Shading Device and Other Types of Shading Device on Residential Houses in Tropics.* Planning, 2022. **17**(6): p. 1705-1712.
101. Kubota, T., T. Takahashi, A.R. Trihamdani, H. Mori, and T. Asawa. *Development of a wind catcher for high-rise apartments in the hot-humid climate of Indonesia*. 2022. IOP Publishing Ltd.
102. Shanthi Priya, R., M.C. Sundarraja, and S. Radhakrishnan, *Experimental study on the thermal performance of a traditional house with one-sided wind catcher during summer and winter.* Energy Efficiency, 2012. **5**(4): p. 483-496.
103. Drach, P.R.C., *A study on air circulation: the case of House VI of "Vila" 37 with the application of wind-catch.* Building Simulation, 2009. **2**(4): p. 307-316.
104. Sadeghi, H. and V. Kalantar, *Performance analysis of a wind tower in combination with an underground channel.* Sustainable Cities and Society, 2018. **37**: p. 427-437.
105. Benhammou, M., B. Draoui, M. Zerrouki, and Y. Marif, *Performance analysis of an earth-to-air heat exchanger assisted by a wind tower for passive cooling of buildings in arid and hot climate.* Energy Conversion and Management, 2015. **91**: p. 1-11.
106. Aït-Mesbah, S., J.-L. Dufresne, F. Cheruy, and F. Hourdin, *The role of thermal inertia in the representation of mean and diurnal range of surface temperature in semiarid and arid regions.* Geophysical Research Letters, 2015. **42**: p. 7572-7580.
107. Morady, E., M. Soltani, F.M. Kashkooli, M. Ziabasharhagh, A. Al-Haq, and J. Nathwani, *Improving Energy Efficiency by Utilizing Wetted Cellulose Pads in Passive Cooling Systems.* Energies, 2022. **15**(1).
108. Khani, S.M.R., M.N. Bahadori, A. Dehghani-Sanij, and A. Nourbakhsh, *Performance evaluation of a modular design ofwind tower withwetted surfaces.* Energies, 2017. **10**(7).
109. Bouchahm, Y., F. Bourbia, and A. Belhamri, *Performance analysis and improvement of the use of wind tower in hot dry climate.* Renewable Energy, 2011. **36**(3): p. 898-906.
110. Oropeza-Perez, I. and P.A. Østergaard, *Potential of natural ventilation in temperate countries – A case study of Denmark.* Applied Energy, 2014. **114**: p. 520-530.

111. Spentzou, E., M.J. Cook, and S. Emmitt, *Modelling natural ventilation for summer thermal comfort in Mediterranean dwellings.* International Journal of Ventilation, 2019. **18**(1): p. 28-45.
112. Spentzou, E., M.J. Cook, and S. Emmitt, *Low-energy cooling and ventilation refurbishments for buildings in a Mediterranean climate.* Architectural Engineering and Design Management, 2022. **18**(4): p. 473-494.
113. Schiano-Phan, R., *The Development of Passive Downdraught Evaporative Cooling Systems Using Porous Ceramic Evaporators and their application in residential buildings.* 2004.
114. Persson, J. and M. Westermark, *Phase change material cool storage for a Swedish Passive House.* Energy and Buildings, 2012. **54**: p. 490-495.
115. Makaka, G., E.L. Meyer, and M. McPherson, *Thermal behaviour and ventilation efficiency of a low-cost passive solar energy efficient house.* Renewable Energy, 2008. **33**(9): p. 1959-1973.
116. Carreto-Hernandez, L.G., S.L. Moya, C.A. Varela-Boydo, and A. Francisco-Hernandez, *Studies of ventilation and thermal comfort in different wind tower-room configurations considering humidification for a warm climate of Mexico.* Journal of Building Engineering, 2022. **46**.
117. Liu, S., R. Song, and T. Zhang, *Residential building ventilation in situations with outdoor PM2.5 pollution.* Building and Environment, 2021. **202**: p. 108040.
118. Feng, Y. and S. Du, *CLIMATE CHANGES AND LANDSCAPE RESPONSES OF CHINA DURING THE PAST 40 YEARS (1979–2018) UNDER KÖPPEN-GEIGER CLIMATE CLASSIFICATION*. Vol. V-3-2020. 2020. 731-737.
119. *Some Basic Principles of Wind Tunnel Design*. 2012 [cited 2022 16th Jun]; Available from: https://www.qats.com/cms/2012/07/17/some-basic-principles-of-wind-tunnel-design/.
120. Cattafesta, L., C. Bahr, and J. Mathew, *Fundamentals of Wind-Tunnel Design*. 2010.
121. Kirk, S. and M. Kolokotroni, *Windcatchers in Modern UK Buildings: Experimental Study.* International Journal of Ventilation, 2004. **3**(1): p. 67-78.
122. Charlesworth, P.S., *Air Exchange Rate and Airtightness Measurement Techniques - An Application Guide*. 1988, Coventry: Air Infiltration and Ventilation Centre.
123. Khan, N., Y. Su, S.B. Riffat, and C. Biggs, *Performance testing and comparison of turbine ventilators.* Renewable Energy, 2008. **33**(11): p. 2441-2447.
124. Adekoya, L.O., *Wind energy end-use: The performance characteristics of a rotating suction cowl.* Renewable Energy, 1992. **2**(4): p. 385-389.
125. Huber, P.J. and H. Rieder. *Robust statistics, data analysis, and computer intensive methods : in honor of Peter Huber's 60th birthday*. 1996.
126. Ronchetti, E., *Robust inference.* International encyclopedia of statistical science, 2011: p. 1240-1242.
127. Blocken, B., T. van Hooff, L. Aanen, and B. Bronsema, *Computational analysis of the performance of a venturi-shaped roof for natural ventilation: Venturi-effect versus wind-blocking effect.* Computers & Fluids, 2011. **48**(1): p. 202-213.
128. Kobayashi, T., M. Sandberg, T. Fujita, E. Lim, and N. Umemiya, *Numerical analysis of wind-induced natural ventilation for an isolated cubic room with two openings under*

*small mean wind pressure difference.* Building and Environment, 2022: p. 109694.
129. Hughes, B.R., J.K. Calautit, and S.A. Ghani, *The development of commercial wind towers for natural ventilation: A review.* Applied Energy, 2012. **92**: p. 606-627.
130. Li, J., J. Calautit, C. Jimenez-Bescos, and S. Riffat, *Experimental and numerical evaluation of a novel dual-channel windcatcher with a rotary scoop for energy-saving technology integration.* Building and Environment, 2023. **230**: p. 110018.
131. Hosseini, S.H., E. Shokry, A.J. Ahmadian Hosseini, G. Ahmadi, and J.K. Calautit, *Evaluation of airflow and thermal comfort in buildings ventilated with wind catchers: Simulation of conditions in Yazd City, Iran.* Energy for Sustainable Development, 2016. **35**: p. 7-24.
132. Ghadiri, M. and M. Dehnavi, *THE EFFECT OF PLAN SIZE IN WIND CATCHER ON ITS VENTILATION RATE*. 2014.
133. Zmrhal, V. and J. Boháč, *Pressure loss of flexible ventilation ducts for residential ventilation: Absolute roughness and compression effect.* Journal of Building Engineering, 2021. **44**: p. 103320.
134. Colebrook, C.F., C.M. White, and G.I. Taylor, *Experiments with fluid friction in roughened pipes.* Proceedings of the Royal Society of London. Series A - Mathematical and Physical Sciences, 1937. **161**(906): p. 367-381.
135. Taitel, Y. and A.E. Dukler, *A model for predicting flow regime transitions in horizontal and near horizontal gas-liquid flow.* AIChE Journal, 1976. **22**(1): p. 47-55.
136. Mak, C.M., J.L. Niu, C.T. Lee, and K.F. Chan, *A numerical simulation of wing walls using computational fluid dynamics.* Energy and Buildings, 2007. **39**(9): p. 995-1002.
137. Elmualim, A.A. and H.B. Awbi, *Wind Tunnel and CFD Investigation of the Performance of "Windcatcher" Ventilation Systems.* International Journal of Ventilation, 2002. **1**(1): p. 53-64.
138. Esfeh, M.K., A. Sohankar, A.R. Shahsavari, M.R. Rastan, M. Ghodrat, and M. Nili, *Experimental and numerical evaluation of wind-driven natural ventilation of a curved roof for various wind angles.* Building and Environment, 2021. **205**: p. 108275.
139. Bahadori, M.N. and F. Haghighat, *Passive cooling in hot, arid regions in developing countries by employing domed roofs and reducing the temperature of internal surfaces.* Building and Environment, 1985. **20**(2): p. 103-113.
140. Nejat, P., Y. Fekri, M. Sheikhshahrokhdehkordi, F. Jomehzadeh, H. Alsaad, and C. Voelker, *The Windcatcher: A Renewable-Energy-Powered Device for Natural Ventilation—The Impact of Upper Wing Walls.* Energies, 2024. **17**(3): p. 611.
141. Chen, X., S. Riffat, H. Bai, X. Zheng, and D. Reay, *Recent progress in liquid desiccant dehumidification and air-conditioning: A review.* Energy and Built Environment, 2020. **1**(1): p. 106-130.
142. Kheirkhah, P. and N. Nasrollahi, *Windcatchers and their applications in contemporary architecture.* Energy and Built Environment, 2020. **3**.
143. Fan, Y., Y. Li, J. Hang, and K. Wang, *Diurnal variation of natural convective wall flows and the resulting air change rate in a homogeneous urban canopy layer.* Energy and Buildings, 2017. **153**: p. 201-208.
144. Fan, Y., Y. Li, J. Hang, K. Wang, and X. Yang, *Natural convection flows along a 16-storey high-rise building.* Building and Environment, 2016. **107**: p. 215-225.

145. Lee, H., A. Ozaki, M. Lee, and W. Cho, *A fundamental study of intelligent building envelope systems capable of passive dehumidification and solar heat collection utilizing renewable energy.* Energy and Buildings, 2019. **195**: p. 139-148.
146. Calautit, J.K. and B.R. Hughes, *Wind tunnel and CFD study of the natural ventilation performance of a commercial multi-directional wind tower.* Building and Environment, 2014. **80**: p. 71-83.